(NASA-CR-141235) DEVELOPMENT OF ULTRASONIC METHODS FOR HEMODYNAMIC MEASUREMENTS Progress Report (Colorado State Univ.) 115 p HC $5.25 CSCL 06D G3/52

N75-17084

Unclas 10233

DEVELOPMENT OF ULTRASONIC METHODS FOR HEMODYNAMIC MEASUREMENTS

by

M. B. HISTAND* C. W. MILLER*

M. K. WELLS F. D. MCLEOD

E. R. GREENE D. WINTER

From the Departments of

Mechanical Engineering and Physiology and Biophysics

COLORADO STATE UNIVERSITY

FORT COLLINS, COLORADO 80523

A Semi-annual Progress Report Prepared for the

National Aeronautics and Space Administration

Under NASA GRANT NSG-2009

February 1, 1975

*Principal Investigators

TABLE OF CONTENTS

I. Introduction

This progress report summarizes the results of our research in diagnostic ultrasound conducted during August 1974 - January 1975. The major items to which the report will be addressed are:

A. Based on state of the art Doppler ultrasound instrumentation, a transcutaneous method to measure instantaneous mean blood flow in peripheral arteries of man is defined. Problems toward which further research will be directed prior to construction of the final instrumentation package are discussed.

B. A detailed evaluation of transcutaneous and implanted cuff ultrasound velocity measurements was completed. Using our conventional narrow gate scan with the PUDVM the accuracies of velocity, flow, and diameter measurements were assessed for steady flow in rigid tubes, bovine carotid segments, dialysis tubing, and for pulsatile flow, in anesthetized dogs.

C. The analysis of the backscattered power was undertaken to determine the accuracy of transmural diameter measurements by the half power method.

D. The wide gate-full illumination method of measuring instantaneous mean velocity was assessed in steady flow for the dialysis tube and for pulsatile flow in the dog.

E. The performance criteria of the PUDVM were described. A spectrum analyzer and FFT digital program were used to examine the spectral characteristics of the Doppler signals as a function of Reynold's number.

F. The performance of the NASA-PUDVM was assessed.

G. A standard transducer test system was designed and evaluated.

H. Ultrasound dosimetry procedures were investigated.

I. Spectral analysis of the PUDVM signals was performed using a sonogram.

II. Volume Flow Measurement Technique

The primary objective of this research project is the definition and preliminary evaluation of a transcutaneous method for the measurement of instantaneous mean flow in the peripheral arteries of an animal or human. The effort is directed toward the eventual development of ultrasound instrumentation that can be easily applied for the quantitative measurement of flow in a subcutaneous vessel. State of the art instrumentation is used. With an emphasis for the method based on ease of application and accuracy, we have examined the various possibilities using state of the art Doppler instrumentation to accomplish this goal. The theoretical analysis of resolution, methodology, and three methods for volume flow measurement were described in the progress report submitted in July, 1974. Based upon this report and further developmental studies both in simulated blood flow systems (steady flow in dialysis tubes) and in special animal preparations (chronic implantation of flow cuffs), we have defined a method based upon current state of the art instrumentation for the measurement of mean flow.

A. Uniform illumination method

Mean instanteous flow will be computed from the product of the mean instantaneous velocity obtained from the first moment of the Doppler power spectrum from a wide gate encompassing the entire vessel diameter and the cross-sectional area obtained from a half power diameter measurement. The method will combine the measurement of instantaneous mean velocity using a piezoelectric crystal larger than the vessel diameter which will uniformly illuminate the cross-section of the vessel at a specific location with a PUDVM gate opened to enclose the near wall and far wall. Coupled with this measurement the geometry

of the vessel will be obtained from a small crystal, narrow gate PUDVM scan to obtain the half power points and thus the vessel diameter. We ultimately envision a digital display of the computed flow.

An important facet of the method is the design of a transducer which can be easily positioned on the skin for Doppler angle determination and velocity measurement. Our preliminary design is shown in Figure 1. Rectangular piezoelectric crystals will be placed at (1), (2), (3), (4), (5) permitting angle determinations at a variety of depths (shown). By rotating the transducer about its axis and using e.g. crystal (1) as a transmitter and crystal (2) as a receiver the returned signal can be nulled and thus the normal to the flow axis determined. In the dialysis flow system the accuracy is ± .5°. The design of the holder will be based upon the movable protractor designs we have developed for transcutaneous narrow gate scans. The transducer will be positioned by audio recognition of the signal.

We have carefully examined the wide gate method for determining mean velocity and are convinced the accuracy is high for Reynolds numbers above 1500. Further study of flow in the laminar region (parabolic profiles) is to be conducted. See Section IV. In addition, the power scan method (Section III) has proven to be an effective means for measuring diameter on the dialysis tube although we have problems resolving the far wall in the animal. Since some discrepancies exist in measuring diameter by the half power method we will devote a major effort to perfect this method. Low pass filtering will be tried as an alternative to locate the walls.

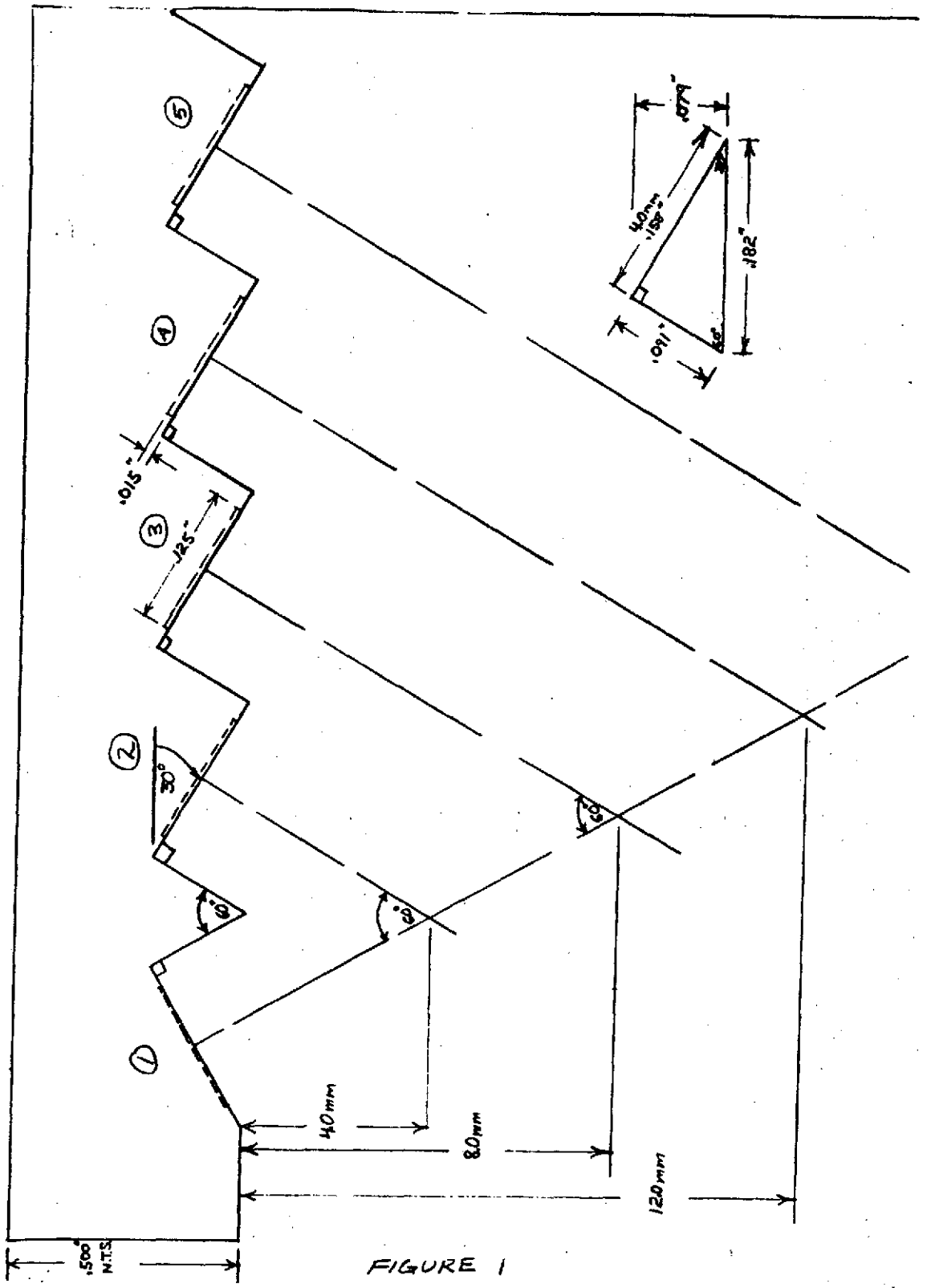
5
4
3
2
1
.015"
.125"
30°
40mm
80mm
120mm
.500" N.T.S.
.079"
40mm
.158"
.182"
.091"
60°

FIGURE 1

III. Implant and Transcutaneous Velocity and Flow Comparisons

Detailed tests have been conducted on dialysis, rigid tube, and bovine carotid arterial simulation systems. In these systems the conventional narrow gate scan method that has been utilized in our laboratory for the last two years was carefully evaluated. Although errors exist in volume flow calculation by the narrow gate method, this method can serve as a means of evaluating the correlation between transcutaneous flow measurements and those made with a cuff implanted on the vessel. Since we are seeking an accurate and simple method to measure mean flow, we have not assessed corrections for boundary errors and truncation as discussed in the previous report. We plan to look at these errors during 1975.

A. Narrow gate fluid system experiments

Narrow gate scan flow measurements were taken in three types of vessels: rigid tube, bovine graft, and dialysis tubing. Data presented in Tables 1 and 2 were taken only under the following instrument settings and experimental procedures.

Instrument	Setting
PUDVM	#2
PW	8 cycles
PR	2 (nominally 20 kc)
Gate	1 μsec
Transducer	#116 2.8 mm crystal

All data was recorded on magnetic tape, digitized and processed by the digital computer. Since the flow system was steady (nonpulsatile), the peak and average values were similar. The average values were compared to collection measurements for the rigid tube and bovine graft systems.

TABLE 1

Flowrate Measured (Q_m) vs. Flowrate PUDVM (Q_{PD})

Type Vessel	Dimensions	Re	Qm cc/sec	Qpdcc/sec	Avg.	% Error
Rigid Tube Plexiglas	11.0mm ID	740	6.50	3.51		− 45
	13.0mm OD	800	7.00	3.88		− 44
crystal/ID ratio .255		1030	9.00	5.71		− 37
		1150	10.00	6.80		− 32
		1320	11.50	7.42 8.68 7.84 8.42	8.09	− 30
		1490	13.00	11.85		− 8
		1600	14.65	13.47 12.65	13.06	− 10
		1830	16.00	12.79 17.92	15.36	− 4
		2290	20.00	19.05		− 5
		2600	22.70	25.68 22.99	24.34	+ 7
		2860	25.00	23.14		− 7
		3040	26.20	25.62 24.52	25.07	− 4
		3600	31.40	33.56		+ 7
		5200	45.80	41.67 44.09	42.88	− 6
		7500	65.40	82.23 79.46	80.84	+ 27
Bovine Graft	7.7mm ID	2500	15.00	14.77 14.88	14.82	− 1
	10.0mm OD					
crystal/ID ratio .365		5000	30.00	32.55 33.31 33.05 30.63	32.38	+ 8
		5800	35.00	29.95 31.37	30.66	− 12

TABLE 2

Type Vessel	Dimensions	Re	Qm cc/sec	Qpp cc/sec	Avg.	%
Dialysis Tubing	6.3 mm ID	1000	4.73	3.38 3.68	3.53	- 34
crystal/ID ratio .455		1500	7.10	4.68 4.56	4.62	- 35
		2000	9.46	7.08 7.66	7.32	- 23
		2500	11.83	8.52 9.02	8.77	- 25
		3000	14.19	13.32 14.00	13.66	- 4
		3500	16.56	13.77 15.26	14.52	- 12
		4000	18.92	14.82 16.10	15.46	- 18
		4500	21.30	16.91 17.86	17.39	- 16
		5000	23.60	17.16 19.55	18.36	- 22
	7.2 mm ID	1000	5.65	3.42 3.72	3.57	- 37
crystal/ID ratio .390		1500	8.48	6.12 5.48	6.16	- 27
			8.48	6.30 6.37		
			8.48	6.14 6.53		
		2000	11.30	7.82 8.33	8.07	- 28
		2500	14.13	10.05 12.15	11.10	- 21
		3000	16.80	15.76 15.98	16.14	- 4
			16.80	16.02 16.80		
		3500	19.80	18.00 18.70	18.35	- 7
		4000	22.60	20.95 20.98	20.97	- 7
		4500	25.40	22.34 22.88	22.51	- 11
		5000	28.35	23.34 24.25	23.80	- 16

A rotometer (± 5% calibration to collection) was used as a standard during the dialysis tube study. The comparisons would help determine the ability of the narrow gate scan and developed velocity profile integration technique for flow rate determination.

Results from the tables suggest the following:

a. Standard and Doppler flow rates compare optimally only within certain observed Reynolds number values for each vessel type.

Re 1500-5000	rigid tube
Re 3000-4500	7.2 dialysis tubing
Re 3000-4500	6.3 dialysis tubing
Re 2500-5000	Bovine graft

b. As the tubing diameter increases (crystal diameter/ID ratio decreases) flow rates obtained from the PUDVM approach the standard values; within 10%.

c. Flow rates determined by the PUDVM for flow regimes of relatively low Re value (<2000) greatly differ from collection or rotometer values.

B. Narrow gate comparisons of velocity and flow in the dog

We have conducted extensive tests to compare the measured velocity and flow parameters obtained on subcutaneous arteries using implanted Doppler ultrasonic cuffs and transcutaneous probes. The dog was surgically implanted with ultrasonic cuffs on the right and left femoral arteries, the abdominal aorta, and the carotid artery. The carotid artery was surgically exteriorized for ease of transcutaneous recording. Post mortum exam will indicate whether the artery under these circumstances is straight and uniform. Generally, we find that the transcutaneous and cuff narrow gate velocity and flow scans compare favorably when the Doppler angle is obtained accurately. Table 3 summarizes the

TABLE 3

Narrow gate measurements of diameter, flow and velocity

transcutaneous and cuff

NASA DOG 15689

XCUT vs. CUFF

Right Carotid

	TYPE	NUMBER OF SAMPLES	DIA mm	
Diameter (mm)	Xcut	N=7	4.18±.03	All H.R.
	Cuff	N=11	4.20±.10	
Average Flow (cm^3s^{-1})	Xcut	N=4	2.62±.02	102<HR<128
	Cuff	N=5	2.58±.10	
	Cuff	N=5	2.96±.09	128<HR<137
	Xcut	N=2	2.37±.00	141<HR<143
PEAK V_G (cms^{-1})	Xcut	N=4	112.5±10.1	102<HR<128
	Cuff	N=5	107.8± 7.2	
	Cuff	N=6	75.1±22.3	128<HR<137
	Xcut	N=5	91.1±10.7	141<HR<143

Notes:

PD #2	Cuff ID 5.0 mm crystal 2.5 mm
PW 8	Xcut Xducer crystal 2.8 mm
PRF 2,3	All data taken during anesthetic
Gate 1 μsec	RMS reading 0.15 V

For delays of 1 μsec or .5 μsec the data is similar

results of the experiments with the animal. We will concentrate on measurements from the right carotid artery although recordings from the abdominal and femoral arteries confirm what we have found on this particular artery. For heart rates in the range of 100 to 130 the centerline peak velocity measured with the PUDVM for the transcutaneous and the implanted cuff compares within the first standard deviation. Normally, the centerline peak velocities are approximately 100 cm/sec and we see for averages of approximately 5 experiments that the transcutaneous value was 112 and the value measured with the implanted cuff at a location 1cm proximal to the transcutaneous measurements location was 107 cm/second. As the heart rate increases there is greater variability both in the waveforms and the resulting velocity values for cuff and the transcutaneous method. By integrating the velocity profiles, one can obtain the average flow, and again for a heart rate of 100 to 130 per second the average flow for the transcutaneous was 2.62 and for the cuff 2.58 cm^3/sec showing good agreement between the two methods. For higher heart rates there is more divergence in the measurements made with the two methods. Finally, the diameters calculated from velocity profiles show very close agreement for the transcutaneous and the implanted cuff. Diameters at the specific locations were approximately 4.2 mm.

The purpose of these experiments was to compare the two methods. We are not implying that the narrow gate method is the most accurate means of measuring diameter, flow or centerline peak velocity, However, these studies do demonstrate the high degree of correlation between transcutaneous measurements and implanted cuff measurements; necessary criteria for supporting our contention that transcutaneous measurements

of velocity and flow can be obtained with a high degree of accuracy.

Figures 2, 3, 4, show the velocity waveforms, velocity profiles, and average flow waveforms from the implanted cuff on the carotid artery. Figures 5, 6, 7 show comparable data obtained with a 2.8 mm transcutaneous probe positioned 1 cm distal to the cuff.

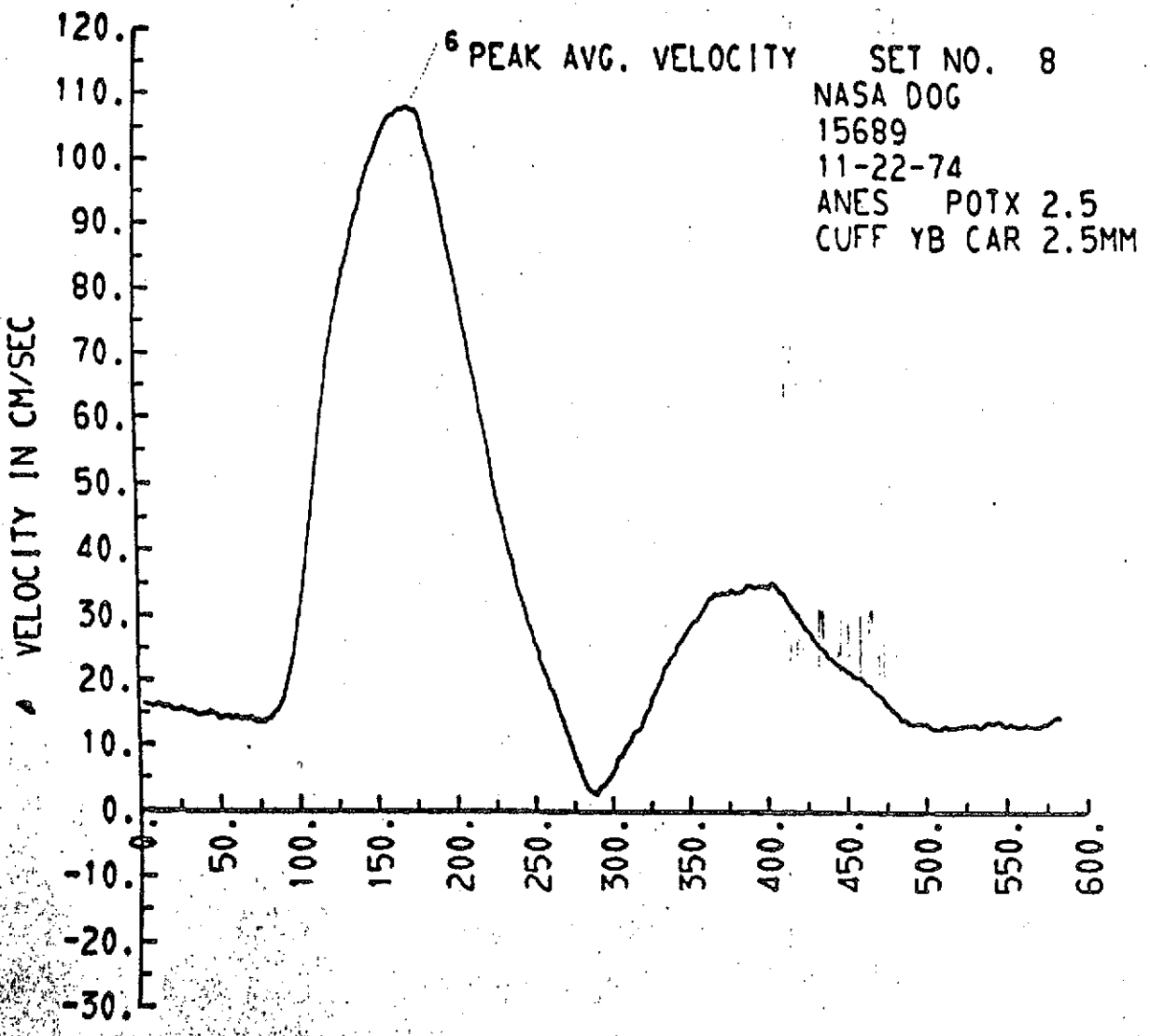

FIGURE 2. CENTERLINE PEAK VELOCITY RECORDED FROM THE IMPLANTED CUFF.

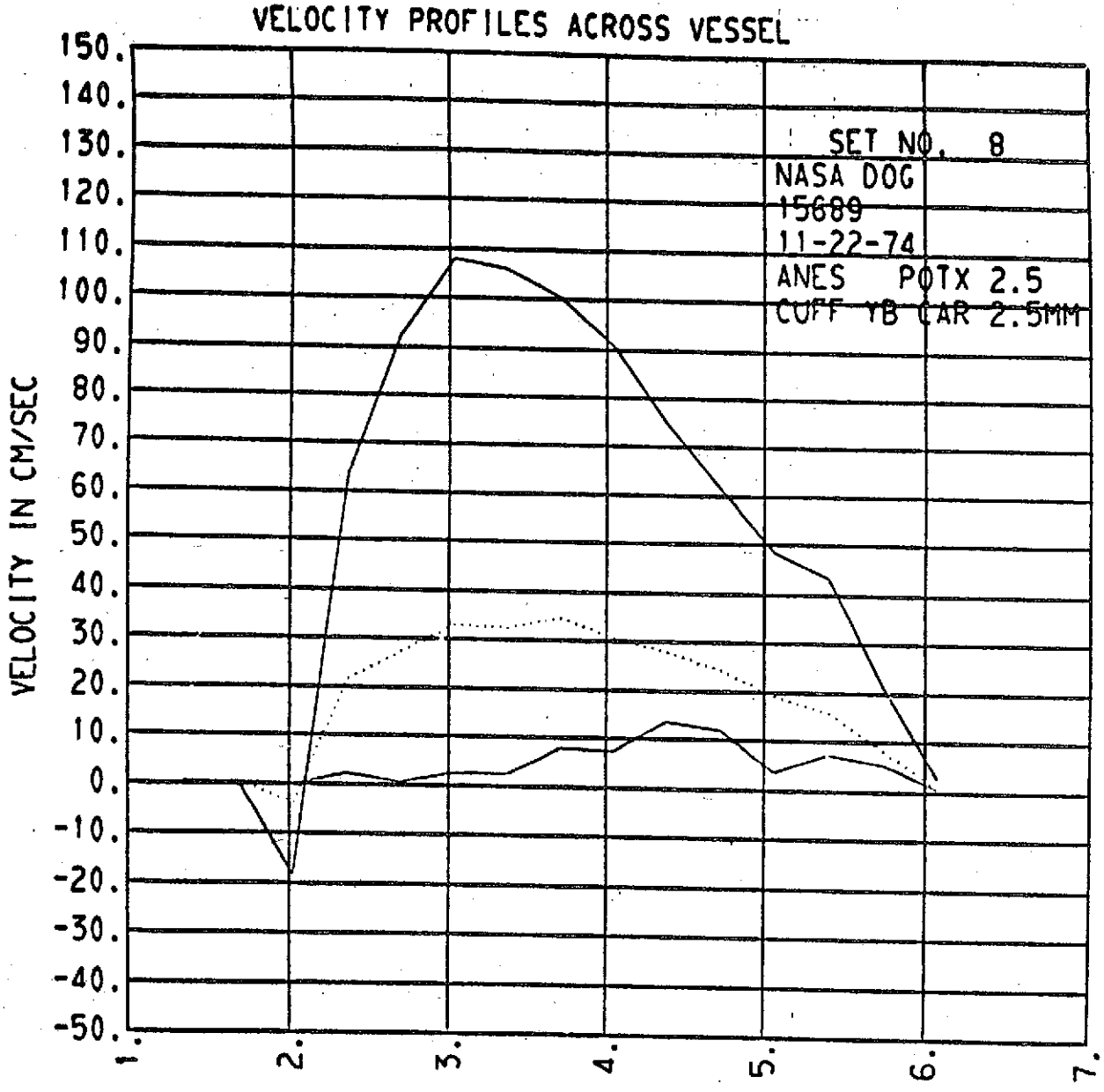

FIGURE 3. PEAK FORWARD, AVERAGE AND PEAK REVERSE PROFILES RECORDED FROM THE CUFF.

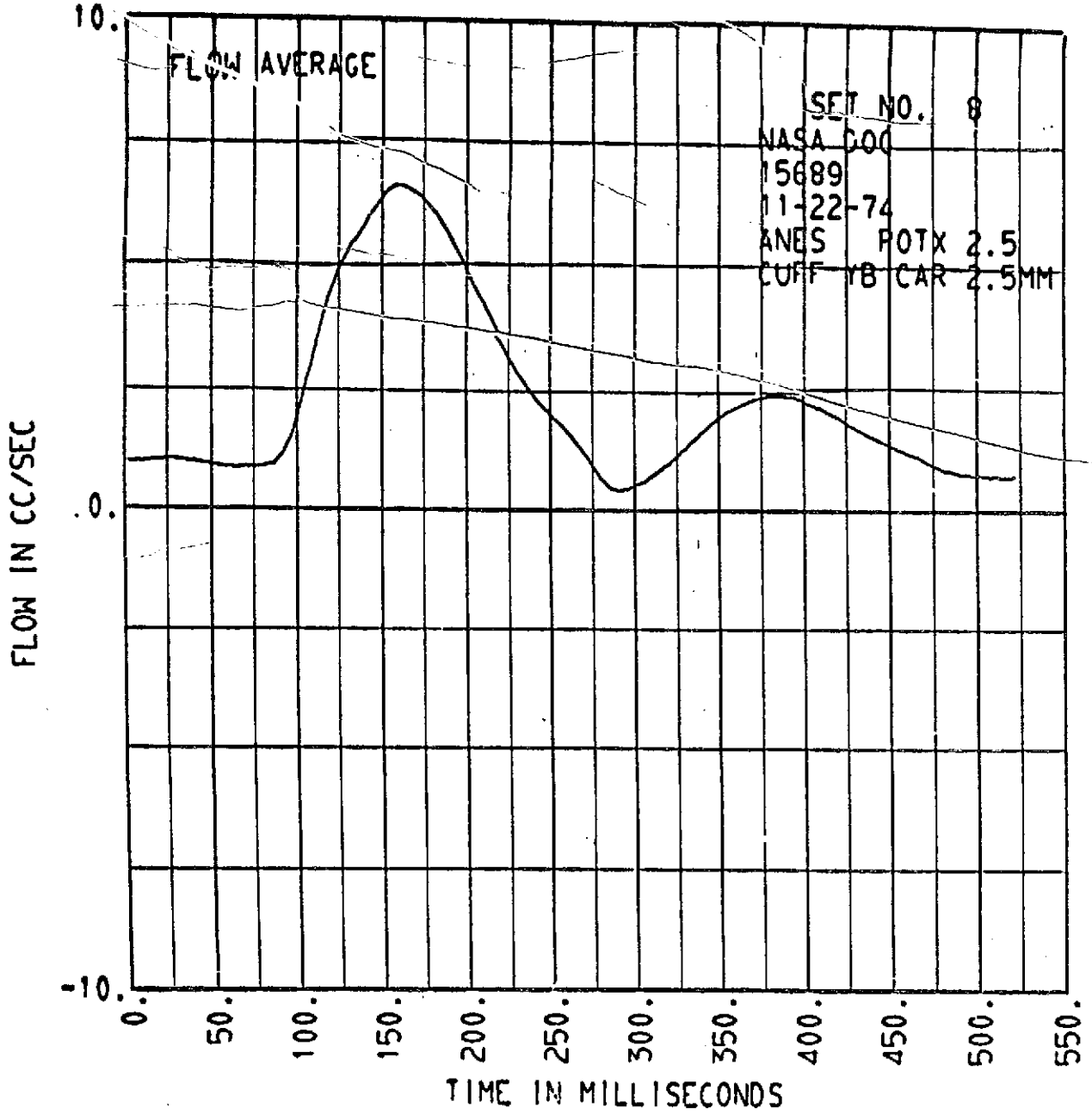

FIGURE 4. AVERAGE FLOW RECORDED WITH THE CUFF.

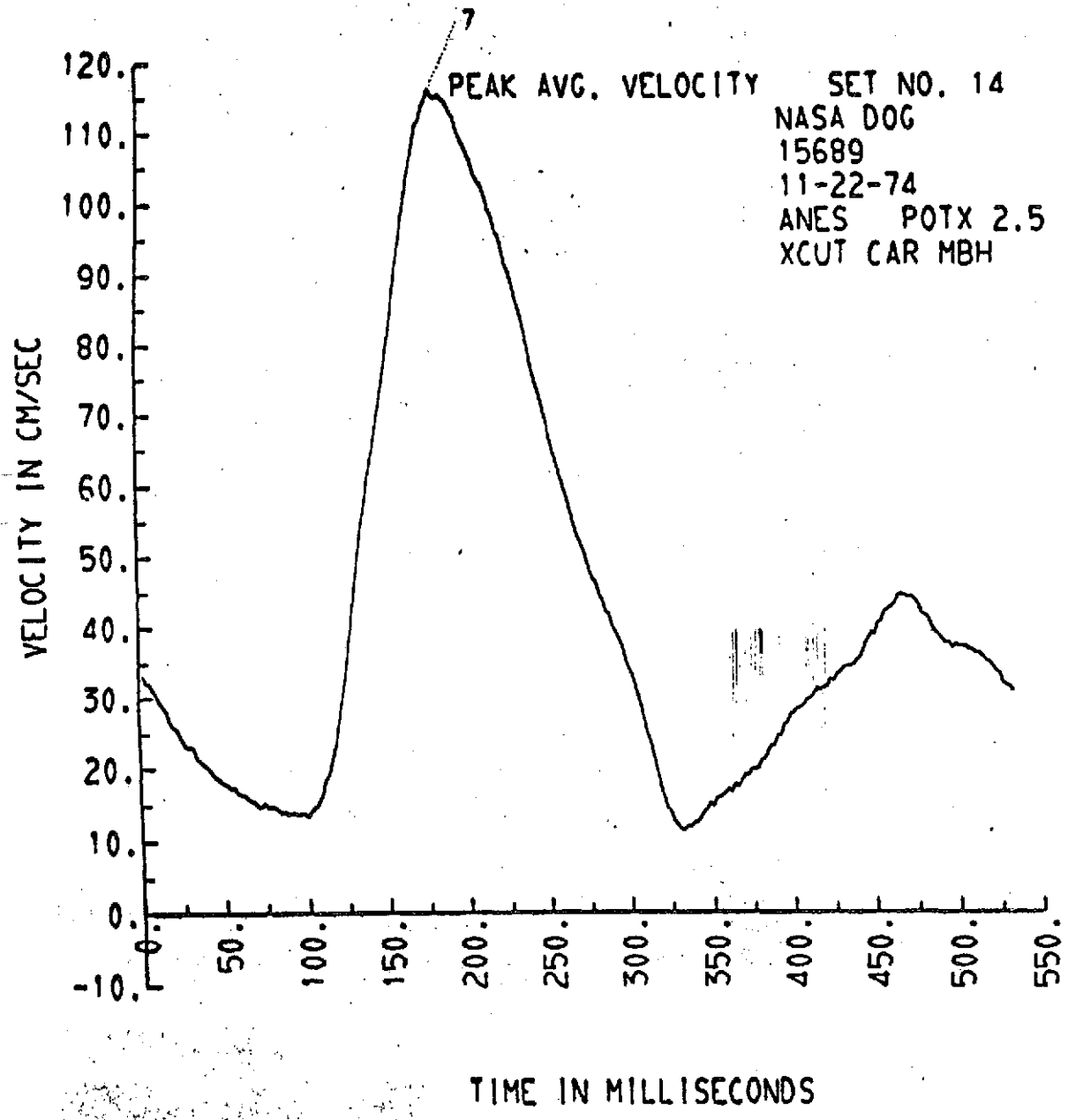

FIGURE 5. SAME DATA AS SHOWN IN FIGURE 2 EXCEPT RECORDED TRANSCUTANEOUSLY. NOTE HIGH DEGREE OF CORRELATION WITH FIGURE 2.

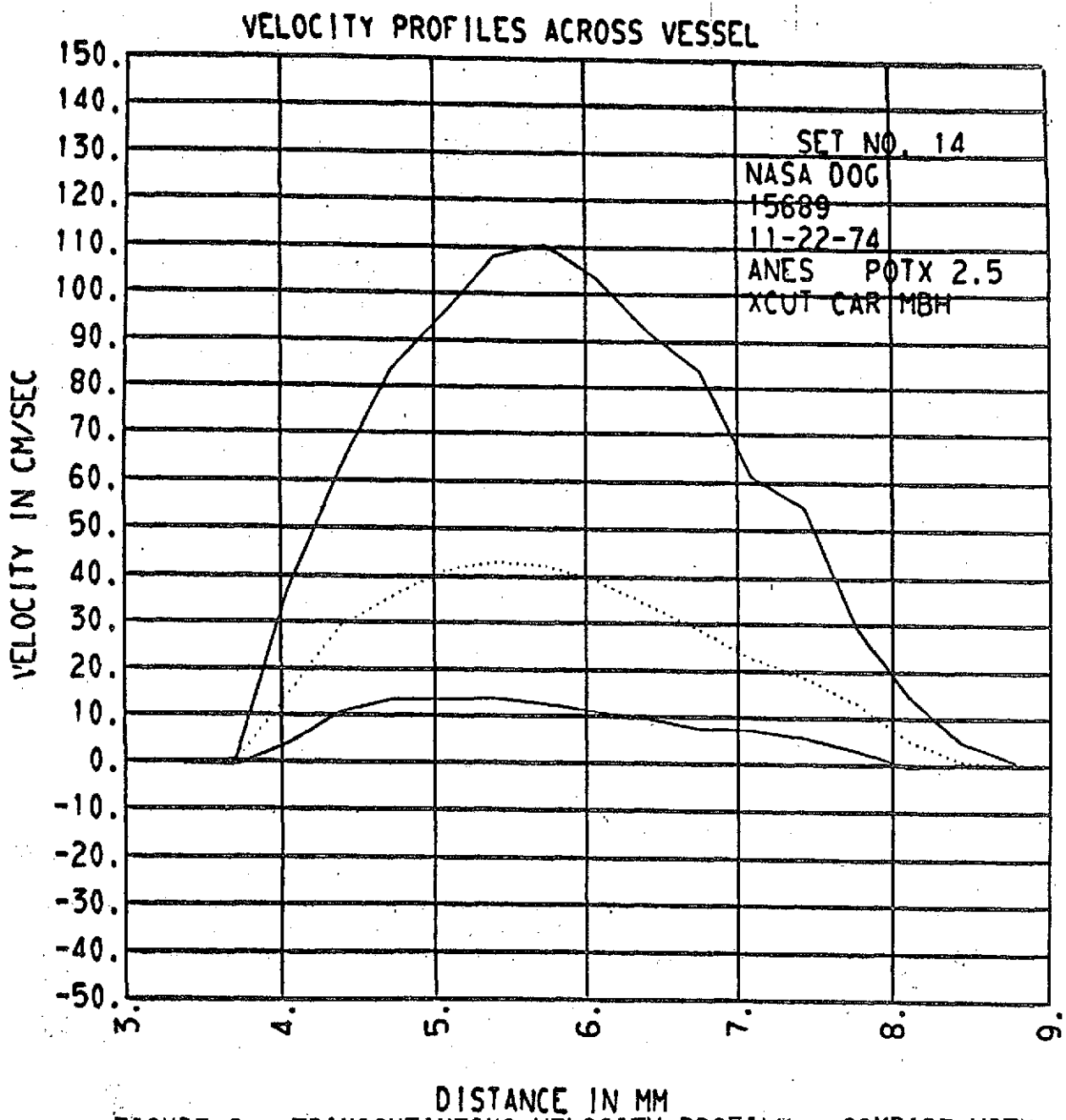

FIGURE 6. TRANSCUTANEOUS VELOCITY PROFILE. COMPARE WITH FIGURE 3.

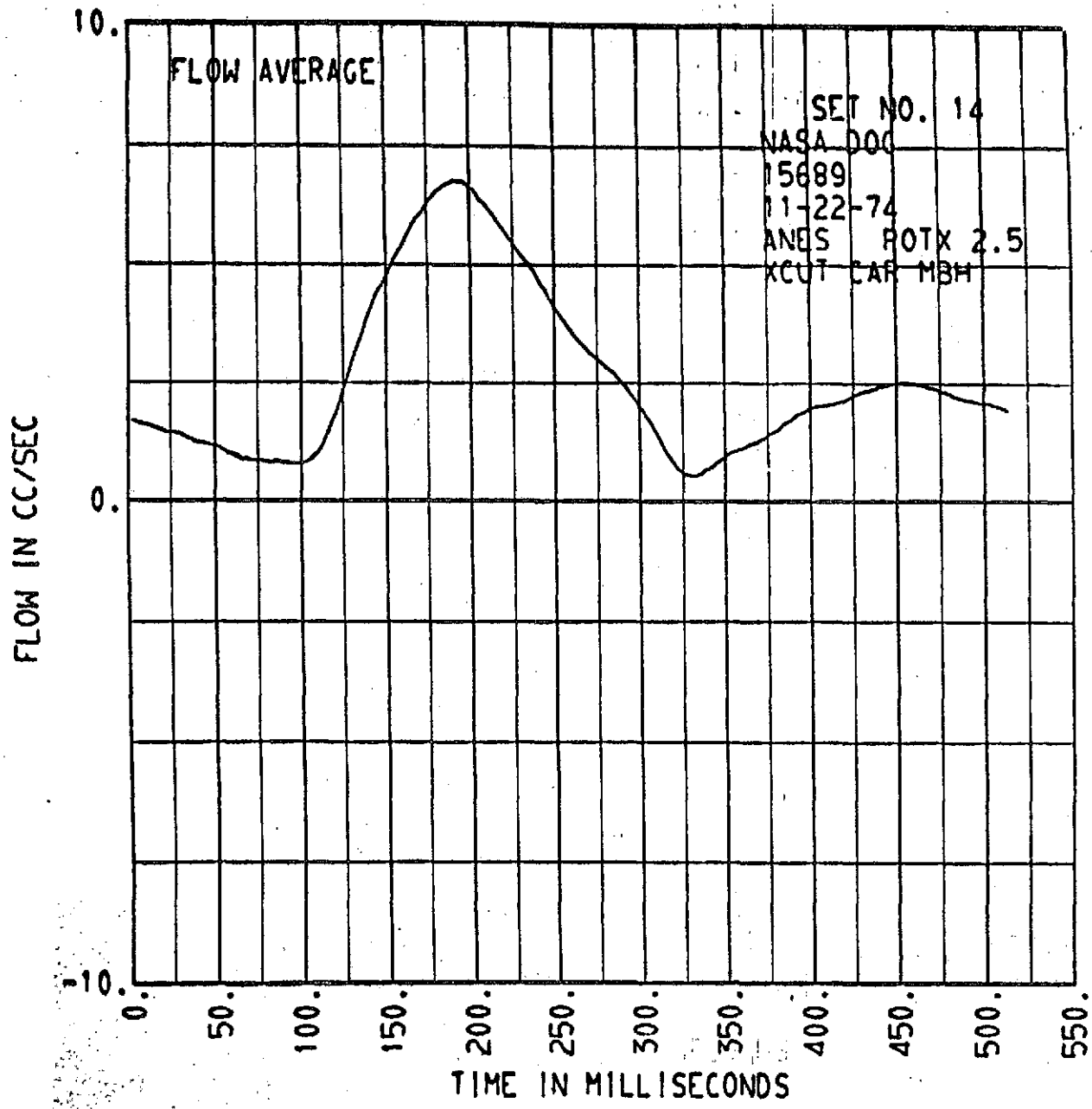

FIGURE 7. TRANSCUTANEOUS MEAN FLOW. COMPARE WITH FIGURE 4.

IV. Half Power Diameter Measurements

We propose that the geometry (diameter) of the blood vessel can be accurately measured by a power scan with a small >.50R transducer. The first approach to the assessment of this method involves half power measurements of diameter on dialysis tubes of known diameter. Results are summarized in Table 4.

A. Dialysis Tube Results

For a 7.7 mm tube measured diameters were ~ 7.5 mm with a 2.8 mm crystal ($\frac{Dcrystal}{Dtube}$ = .36) and 7.65 with a 5.5 mm crystal ($\frac{Dcrystal}{Dtube}$ = .71). These errors would reduce the true volume flow measurement by ~ 10%. Figure 8 displays a power scan of the dialysis tube. For vessels of ~ 4 mm diameter or less problems arise: the half power diameters are approximately 25% too small presumedly due to the curvature of the vessel and the large crystal. This is inconsistent with the half power measurements made with 5-8 mm crystals which result in a 10% over estimate of diameter in a 7 mm tube. We are currently trying to resolve this problem by considering low pass filtering of the audio spectrum. Therefore, a more detailed and systematic approach will be taken. Our conclusion is that the half power method is the simplest and most accurate method for transcutaneous diameter determination for vessels whose diameter is > 7 mm.

B. Reiteration of errors in half power measurements

Ambiguity in finding the half power points is limited by four factors:

1) Ambient Noise. The quality of the power scan is affected by the Doppler signal to noise ratio (S/N). Both base line shifts and signal variance are present with poor S/N. In practice this is not

a problem, however, when S/N ratios on the order of 20 to 50 dB are obtained.

2) Wall motion and wall motion "noise." Wall motion tends to "blur" the wall location during the power scan, thus a mean diameter is obtained. While the "blurring" is reduced by multichannel operation it is not completely eliminated because of the finite integration time required to measure the signal power (Rayleigh signal statistics and fading must be integrated out). Large amplitude low frequency echoes from the wall are another wall motion problem. These echoes tend to distort the sample function near the wall and make it appear compressed. This problem is reduced by high pass filtering to eliminate the echoes. Alternately, low pass filtering can be used to select or enhance the wall echo and provide an impulse response at the wall. We plan to examine the latter to determine its accuracy in the diameter estimation.

3) Range attenuation. The Doppler signal power falls off as a function of range, tending to obscure the step function endpoint. This difficulty can be eliminated either by range gain compensation, proper transducer design, or graphical correction of the power scan record. See actual data from dog experiments.

4) A fourth and perhaps minor limitation is vessel curvature at the wall. The step function concept was developed for a plane or nearly flat surface, however, a vessel wall is a curved surface. This curvature Δ, is easily shown to be

$$\Delta = r - \sqrt{r^2 - \left(\frac{a}{2}\right)^2}$$

where a is the transducer beam diameter and r is the vessel radius. Evaluation of this for a transducer diameter of .25r leads to a

curvature of less than 1%.

Combination of the above limitations leads to an experimental wall location error on the order of 1/4 sample function length and a diameter error on the order of $\frac{\sqrt{2}}{4}$ times the sample function length. In practical terms the sample function length is on the order of 1 mm, thus vessel diameter measurement is on the order of ± .44 mm. Although seemingly precise, this is still a 10% error on a 4 mm vessel.

C. Half Power measurements on blood vessels

Using implanted cuffs and transcutaneous probes we have recorded rms power scans on the abdominal aorta and carotid arteries. Consistent with our findings in the dialysis tube, the abdominal aorta values are accurate but the carotid diameters appear ~ 25% too small. Figure 9 exhibits power scans for the abdominal aorta. Note the range attenuation which necessitates interpolating a half power point at the far wall. Transcutaneous measurements produce significant power fluctuations at the far wall (wall motion) which may obscure the half power points. Low pass filtering may alleviate this problem. Figure 10 exhibits power scans for the carotid artery producing diameters of ~ 3.45 mm which we believe to be too small. Our previous measurements of carotid inside diameters by surgical exposure result in values of ~ 4 mm. Therefore, we must be cautious in using the half power method of diameter determination in vessels less than 7 mm in diameter.

Table 5 exhibits data on half power diameters for the carotid and abdominal aorta. The diameters for the carotid should be ~ 4 mm. The diameter for the abdominal aorta is quite close to the expected value.

TABLE 4

Half Power Diameter Measurement

Dialysis Tube

TRANSDUCER	DIAMETERS(MM)			RATIO OF CRYSTAL DIAMETER TO VESSEL DIAMETER
#116-EC65 2.8 mm	7.47	7.55	7.47	.36
LTZ 5 5.5 mm	7.55	7.71		.71
LTZ 5 8.0 mm	8.20	8.61 (7.88(Rel500))	8.60	1.03
EC65 5.5 mm	8.69	8.70		.71
EC65 8.0 mm	8.69	8.53	8.93	1.03

Notes:

PD #2
PW8
PRF 2
Gate 1 μsec

Tubing OD 7.8 mm
Tubing ID 7.7 mm
Re 3000

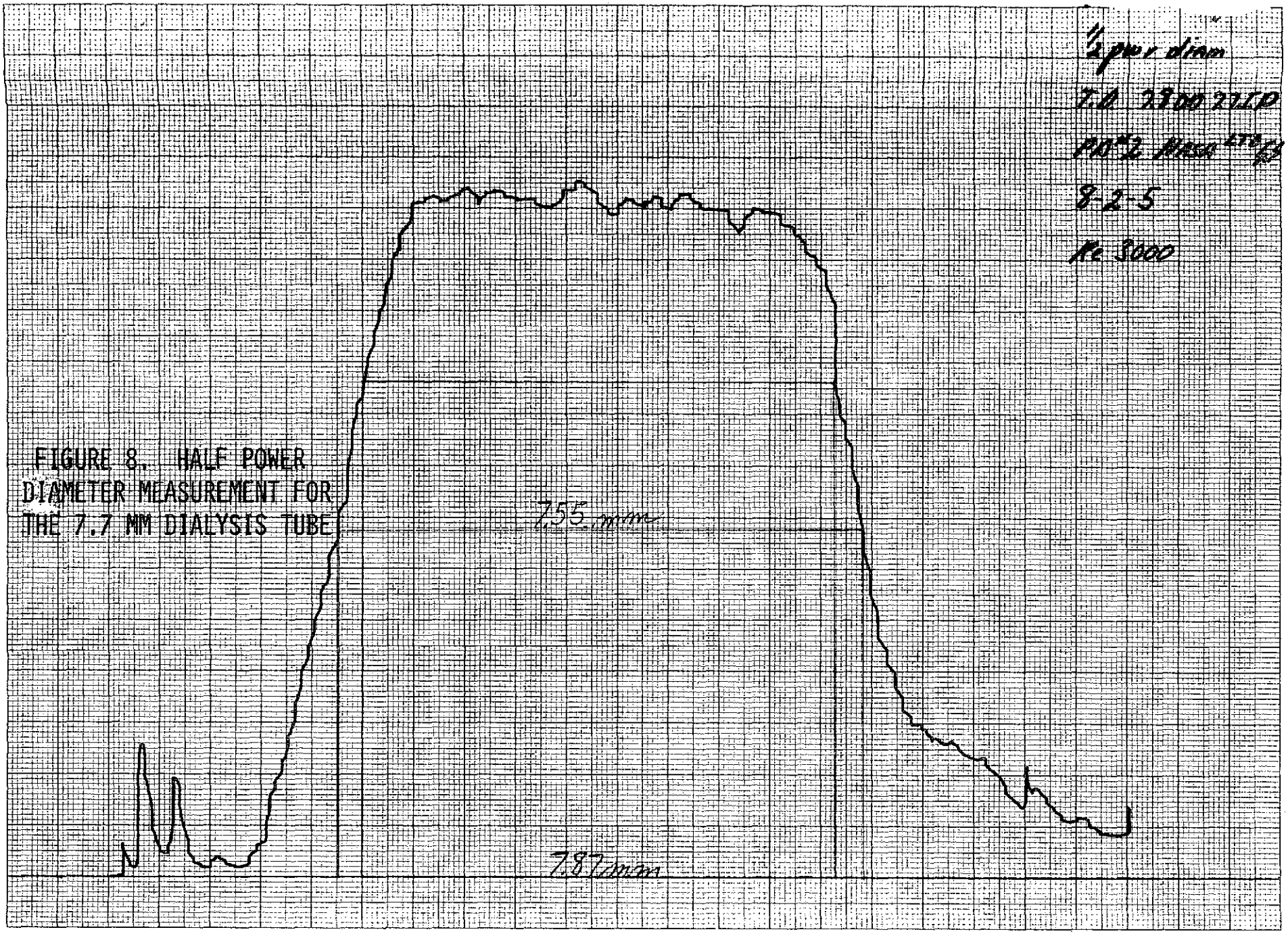

FIGURE 8. HALF POWER DIAMETER MEASUREMENT FOR THE 7.7 MM DIALYSIS TUBE

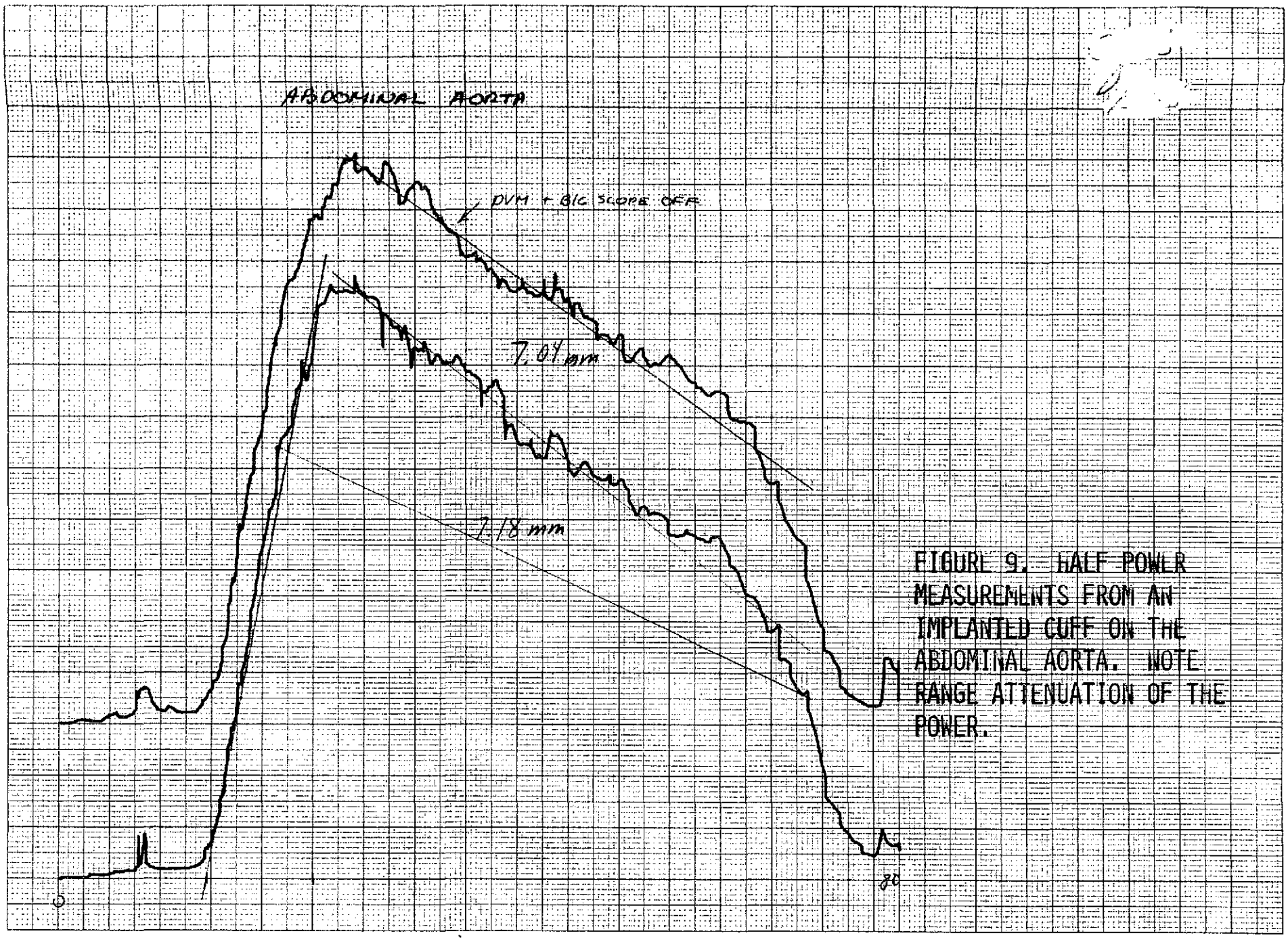

FIGURE 9. HALF POWER MEASUREMENTS FROM AN IMPLANTED CUFF ON THE ABDOMINAL AORTA. NOTE RANGE ATTENUATION OF THE POWER.

.69

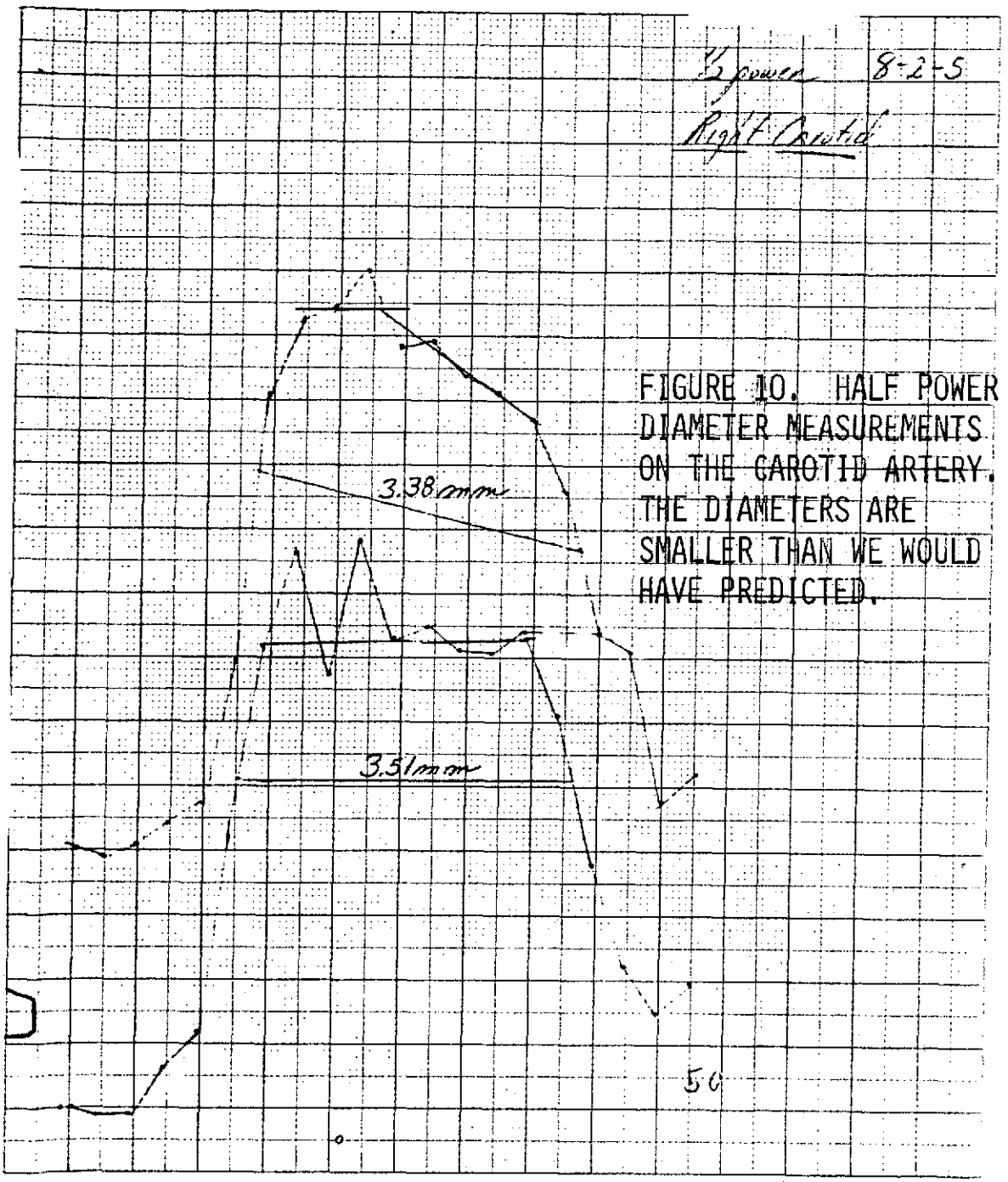

FIGURE 10. HALF POWER DIAMETER MEASUREMENTS ON THE CAROTID ARTERY. THE DIAMETERS ARE SMALLER THAN WE WOULD HAVE PREDICTED.

TABLE 5

1/2 Power Diameters

NASA DOG 15689

	TRANSDUCER	RATIO OF CRYSTAL DIAMETER TO VESSEL DIAMETER	TECHNIQUE	DIAMETERS
RT CAR	#116	.73	Xcut	2.40
RT CAR	NASA LTZ 5.5	1.44	Xcut	2.65
RT CAR	NASA LTZ 7.0	1.84	Xcut	2.00 2.40
RT CAR	R. C. Cuff YB 2.5	.65	Potx 5.0 Cuff	2.60
RT CAR	R. C. Cuff YB 2.5	.65	Potx 2.5 Cuff	2.70 2.70 2.65

Notes:

PD#2
PW8
PRF 2.3
Gate 1 μsec

RMS .15 V
Delay Δt 1/2 μsec, 1 μsec

C=1.5x105 cm/sec

Vessel Diam Assumed 3.8 mm ID

V. Wide Gate Full Vessel Illumination

A rectangular 2 mm by 10 mm transducer was fabricated from LTZ 2 to assess to accuracy of the wide gate full illumination method to measure mean velocity in a vessel. Presently, the zero crosser has been used for signal processing although we calculate an error as great as 15% may occur in determining the first moment of the power spectrum. Our preliminary findings in the dialysis tube steady flow system are quite encouraging. As shown in Table 6, we have obtained results with large circular crystals and two different large rectangular crystals, one of LTZ 5 and one of LTZ 2. By far the best results are obtained with the LTZ 2 indicating errors in measurement of the mean velocity in the range of Reynolds number from 2000 to 5000 are less than 7%. At the very low Reynolds numbers larger errors occur which merit further investigation. We cannot adequately explain the reason that larger errors occur with certain piezoelectric materials, and further investigation is going to be conducted in transducer design and fabrication in order to optimize the results. Figures 11, 12, and 13 exhibit the power spectra obtained with the LTZ 2 wide gate transducer. For a wide gate measurement one would expect a nearly rectangular power spectrum and we are obtaining very close approximations to that under these circumstances. We find also that the zero crosser is a much better than expected signal processor for signals using these spectra implying that more sophisticated signal processing may not be necessary. However, we plan to further investigate the use of first moment and zero crosser offset processing of these signals to see if the accuracy can be further improved.

TABLE 6

COMPARISON $\overline{V}_{PD}$ vs. $\overline{V}m$ fn(Re)

TRANSDUCER NASA LTZ 8.0 mm
NASA EC65 8.0 mm
NASA LTZ 5

Re	$\overline{V}_{PD}$ (cm/sec)				$\overline{V}m$ (cm/sec)		% difference from standard		
	(1)	(2)	(3)	(4)	(2)	(1)	(1)	(2)	(3)
1000	15.72	17.3	18.6	18.5	13.42	13.16	19	28.9	38.6
1500	22.26	25.1	28.2	26.0	20.14	19.74	13	24.6	40.0
2000	28.16	30.9	36.7	31.1	26.83	26.32	7	15.2	36.8
2500	33.31	36.9	42.2	34.5	33.55	32.90	1	10.0	25.8
3000	40.22	42.7	47.7	40.5	40.25	39.48	1	6.1	18.5
3500	45.75	48.5	55.1	45.5	46.97	46.06	-1	3.2	17.3
4000	51.48	53.9	61.2	50.0	53.69	52.64	-2	0.4	13.9
4500	56.45	60.0	67.3	57.1	60.40	59.22	-5	0.7	11.4
5000	61.58	65.8	73.4	61.7	67.10	65.80	-7	1.9	09.4

Full Vessel Illum
PW8
PD2
PR2
GN1.0
Gate 18.0 µsec
Power .15V
Delay 8 µsec
7.5 mm dialysis

(1) NASA LTZ 2 rectangle (2 mm X 10 mm)
(2) NASA LTZ 8.00 mm 21 Jan (circular)
(3) NASA EC65 8.00 mm 23 Jan (circular)
(4) NASA LTZ 5 rectangle (2 mm X 10 mm)

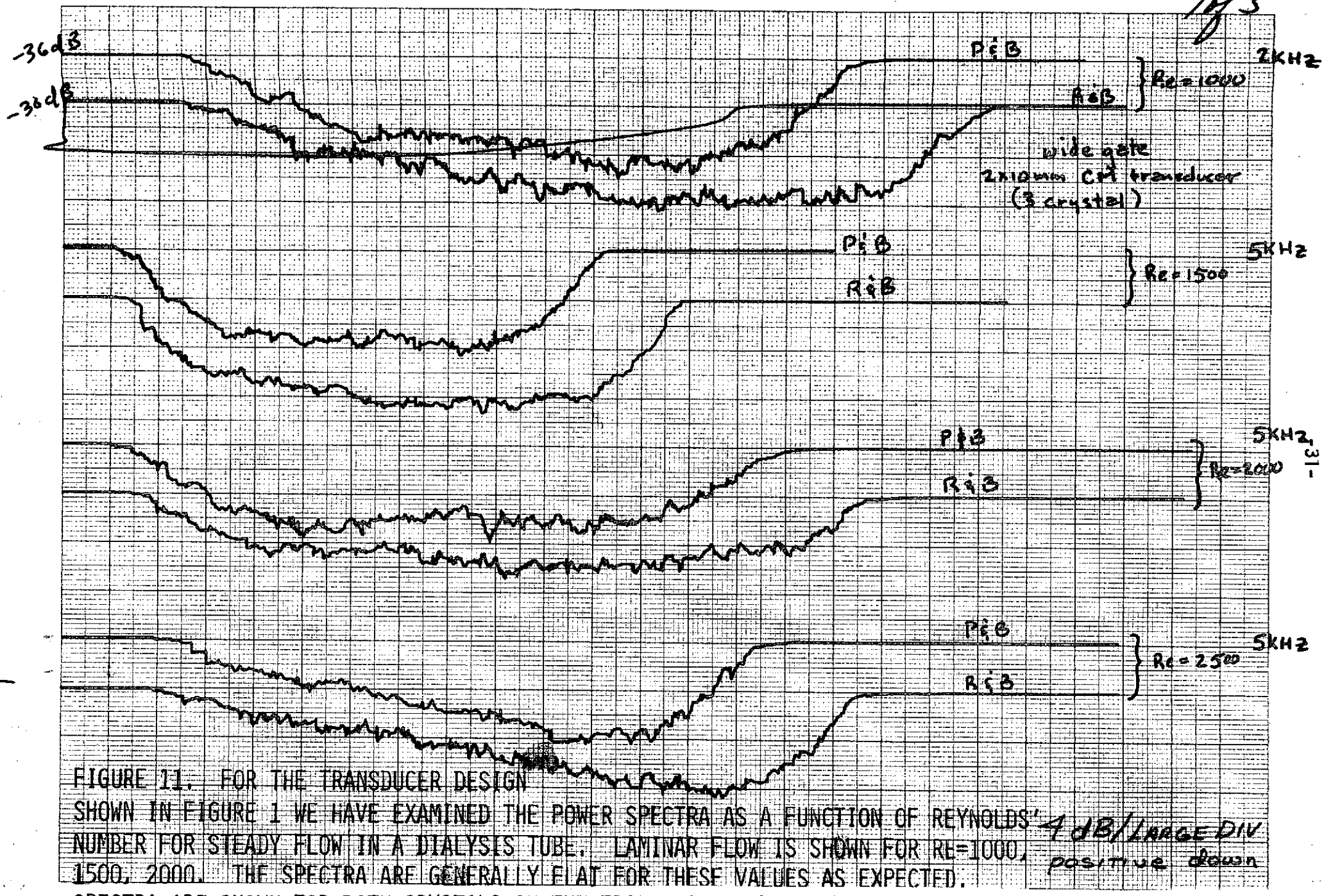

FIGURE 11. FOR THE TRANSDUCER DESIGN SHOWN IN FIGURE 1 WE HAVE EXAMINED THE POWER SPECTRA AS A FUNCTION OF REYNOLDS' NUMBER FOR STEADY FLOW IN A DIALYSIS TUBE. LAMINAR FLOW IS SHOWN FOR RE=1000, 1500, 2000. THE SPECTRA ARE GENERALLY FLAT FOR THESE VALUES AS EXPECTED. SPECTRA ARE SHOWN FOR BOTH CRYSTALS ON THE TRANSDUCER. FOR REYNOLDS' NUMBERS ABOVE 2000 (TRANSITION TO TURBULENCE) THE SPECTRA ARE MORE SKEWED TO THE HIGH FREQUENCIES.

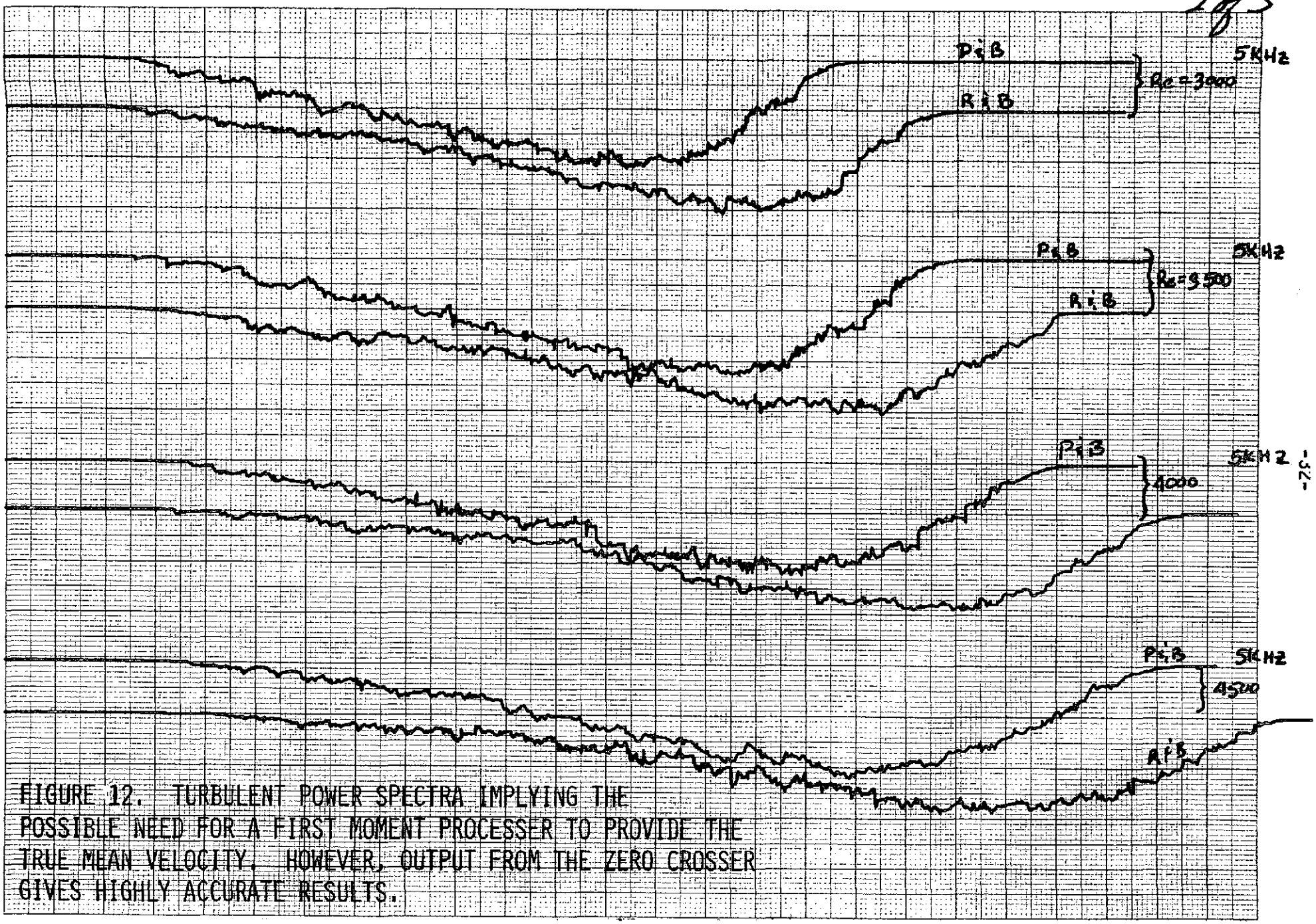

FIGURE 12. TURBULENT POWER SPECTRA IMPLYING THE POSSIBLE NEED FOR A FIRST MOMENT PROCESSER TO PROVIDE THE TRUE MEAN VELOCITY. HOWEVER, OUTPUT FROM THE ZERO CROSSER GIVES HIGHLY ACCURATE RESULTS.

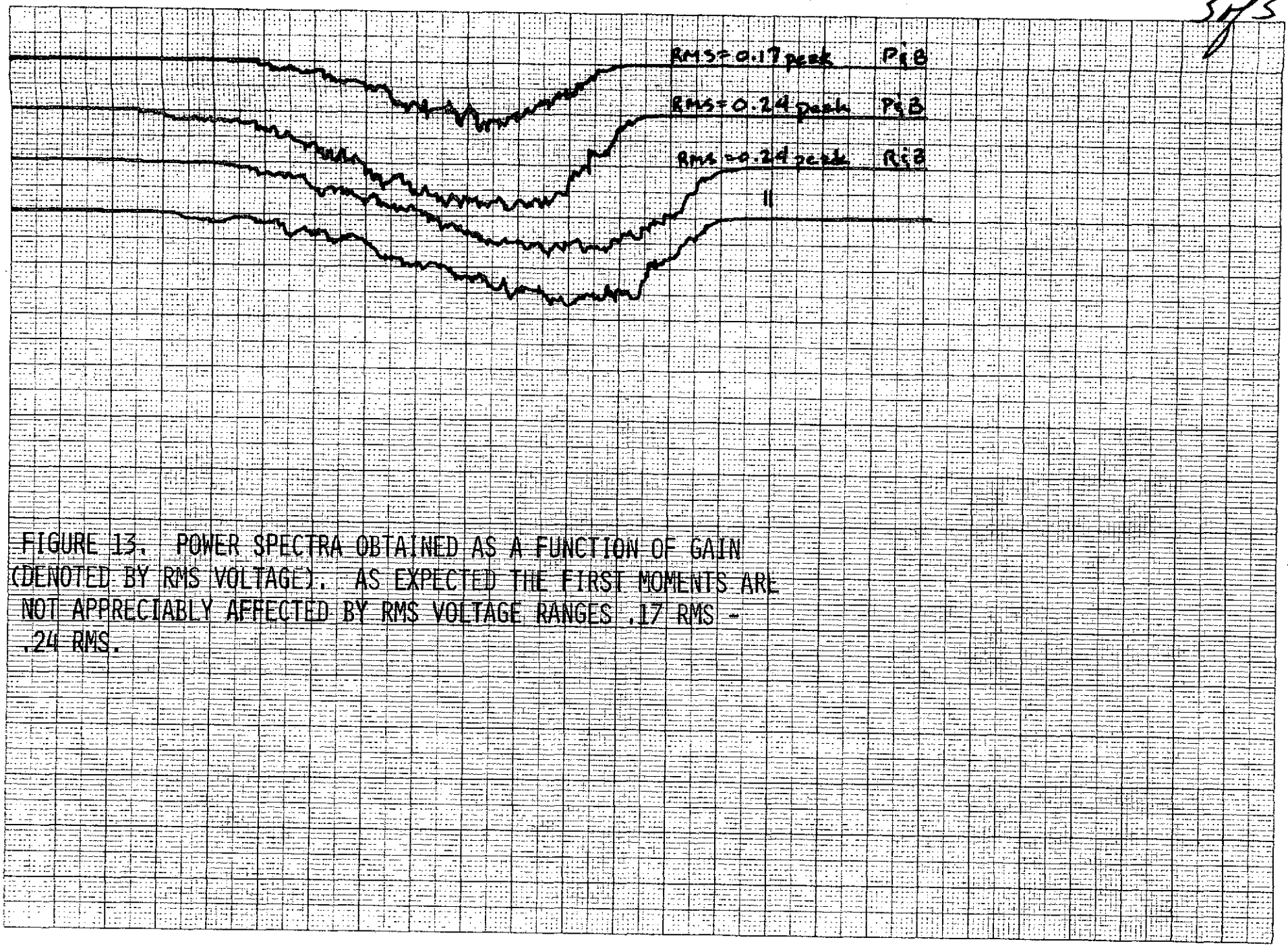

FIGURE 13. POWER SPECTRA OBTAINED AS A FUNCTION OF GAIN (DENOTED BY RMS VOLTAGE). AS EXPECTED THE FIRST MOMENTS ARE NOT APPRECIABLY AFFECTED BY RMS VOLTAGE RANGES .17 RMS - .24 RMS.

VI. Ultrasound Dosimetry

Preliminary efforts have been made to document the power levels emitted by the pulsed ultrasonic Doppler velocity detector. The first experiment was conducted at the Colorado Medical Center in Dr. Paul Carson's laboratory (February 14, 1975). The setup consisted of determining the force exerted by the emitted pulse upon a highly absorbable buffer plate (SOAB). This force was determined using an electro-balance (Cahn). The initial results indicate that the pulse Doppler when operated at the highest pulse repetition rate (40kc) and longest pulse width (16 cycles) emits a sound beam which averages a power level of 296 MW/CM^2. In these studies a 2.8 mm circular transducer was employed. If a 25% insertion factor is assumed for tissue, the result is a power level of approximately 75 MW/CM^2. Peak intensity equals 4.9 W/CM^2. More work is planned in the future to document the power levels emitted by such devices as the pulsed ultrasonic Doppler velocity detector. We feel that intelligent use of ultrasonic flowmeters demands that continual knowledge of the ultrasound dosage be at hand.

VII. Spectral Analysis of Pulse Doppler Signals Using Sonograms

In an attempt to find the best method for determining the average blood flow rate in an artery, we have performed analyses of the Doppler shifted signal using sonograms. The data display consists of the time varying audio signal displayed at varying levels of amplitude (each different intensity of the contour represents a 6 db change). This technique permits display of the spectral patterns of the signal and from the graph, the various velocity components within the return Doppler shifted signal are easily viewed.

This report will present the initial results using this technique and will suggest future directions. Sonograms were made for the Doppler shifted signals from an implanted flow cuff around the abdominal aorta of a dog (2.8 mm transducer). Two types of sonograms were made from the Doppler shifted signal at locations across the flow stream by approximate range gating and by using a wide gate which encompassed the entire flow stream. These results will be compared with the zero crosser output (wide gate, scan, and computer calculated).

Figure 13A depicts a sonogram showing the Doppler shifted information received with a wide gate. The peak velocity recorded across the flow stream is approximately 101 cm/sec if the lowest amplitude signal is used. By selecting velocity components of higher contour intensities (continuous contours) values of 94 and 91 cm/sec result. The entire velocity data for all combinations are shown in Table 7.

TABLE 7

Blood velocity values (cm/sec) measured using wide and narrow gate pulse Doppler options on the abdominal aorta of a dog.

Wide Gate

Zero Crosser		Sonogram	
$\overline{V}$ Peak	$\overline{V}$	$\overline{V}$ Peak	$\overline{V}$
73	19.8	101,94,91	37.4

Narrow Gate

Zero Crosser	Sonogram	Computer Calculated from profiles	
$\overline{V}$ Peak at $\mathcal{C}_L$	@centerline $\overline{V}$ peak	$\overline{V}$ peak	$\overline{V}$
81	95	42	12.2

The table shows for the wide gate the average velocity at peak systole as claculated from the zero crosser and sonogram outputs. The average velocity is similarly listed. The narrow gate measurements for the peak velocity at the flow stream centerline are also depicted for both the sonogram and zero crosser and finally, the standard method of profile integration produces the average peak velocity and the mean velocity. These data show that by using a narrow sound beam that obviously a large portion of the velocity information which exists towards to vessel walls will not be detected using the zero crosser and wide gate. The result is a higher than actual recorded blood velocity when using the zero crosser. The sonogram whether using a wide gate or narrow gate produces approximately the same velocity and is close to the peak velocity measured with a narrow gate zero crosser method. The reason the wide gate zero crosser and sonogram methods produce

a higher mean velocity than actual is obviously due to the narrow sound beam. The discrepancy between the zero crosser and sonogram is due to the faulty method of obtaining the mean velocity by integrating the sonogram. No weighting of the various amplitudes of the signal were attempted.

We believe that an alternative method for computing the mean velocity of blood in a superficial vessel may involve the use of a large transducer and a wide gate pulsed Doppler or even continuous wave Doppler coupled with sonogram analysis. A possible valuable approach to attempt would be to compare this approach to the actual blood velocity. Account must be taken of the varying signal amplitudes (1st moment analysis) but the sonograms offer that possibility. Sonogram analysis also offers an alternative method to the zero crosser for detecting the local velocities across a flow stream. Figure 13B, for example, shows a sonogram for the velocity signal recorded at the centerline. It is interesting to note that a relatively narrow band signal occurs during systole in contrast to the situation using a wide gate where a wide range of spectra exist. Similarly, at the vessel walls, this narrow amplitude band disappears (Figure 13C). Presumably the vessel wall is a major influence in the pattern - both due to its influence upon flow and the fact that the vessel wall moves in and out of the sample volume.

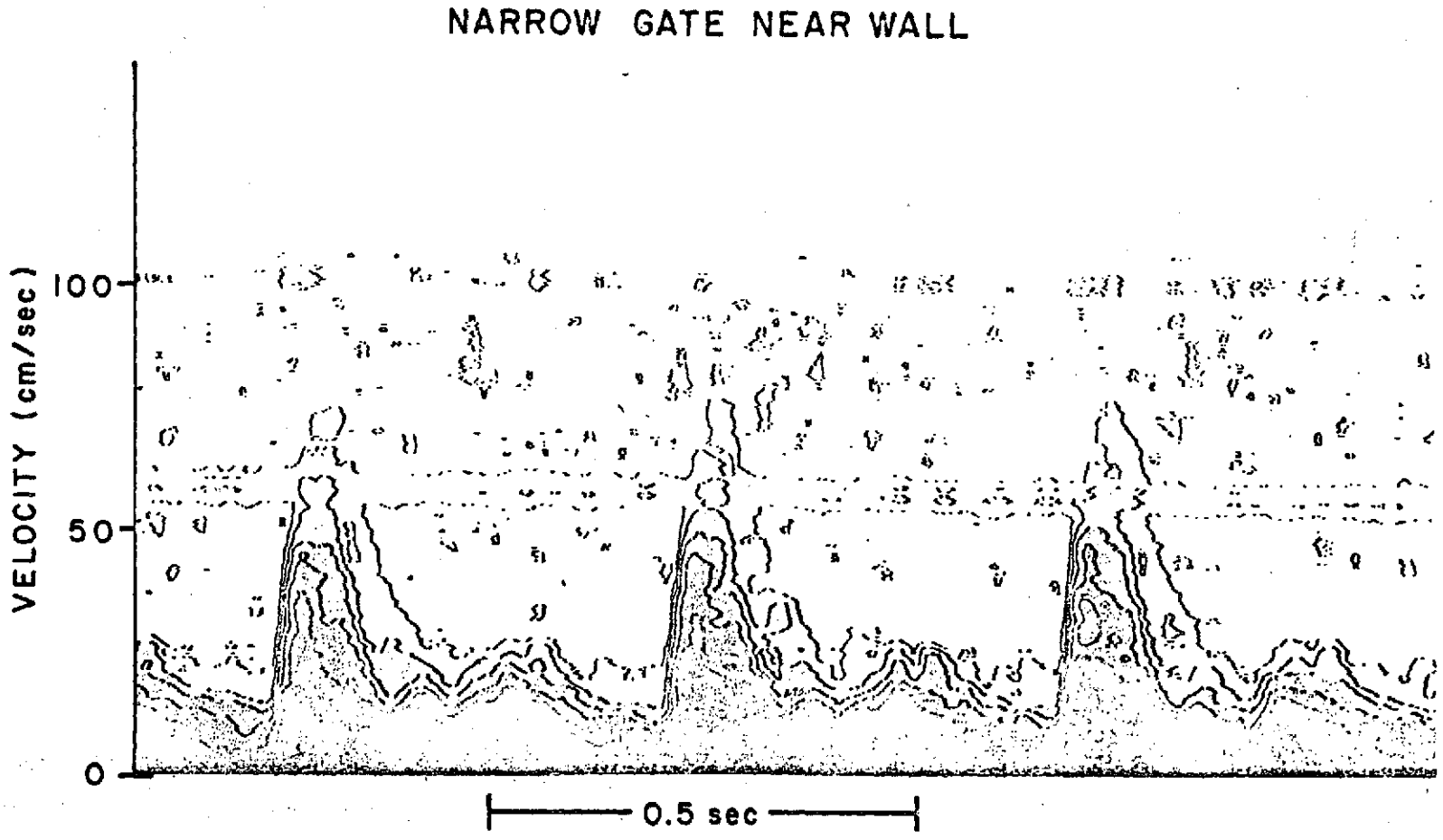

FIGURE 13A. SONOGRAM PRODUCED WITH THE PULSE DOPPLER IN THE WIDE GATE MODE FROM A FLOW CUFF ON THE ABDOMINAL AORTA OF A DOG.

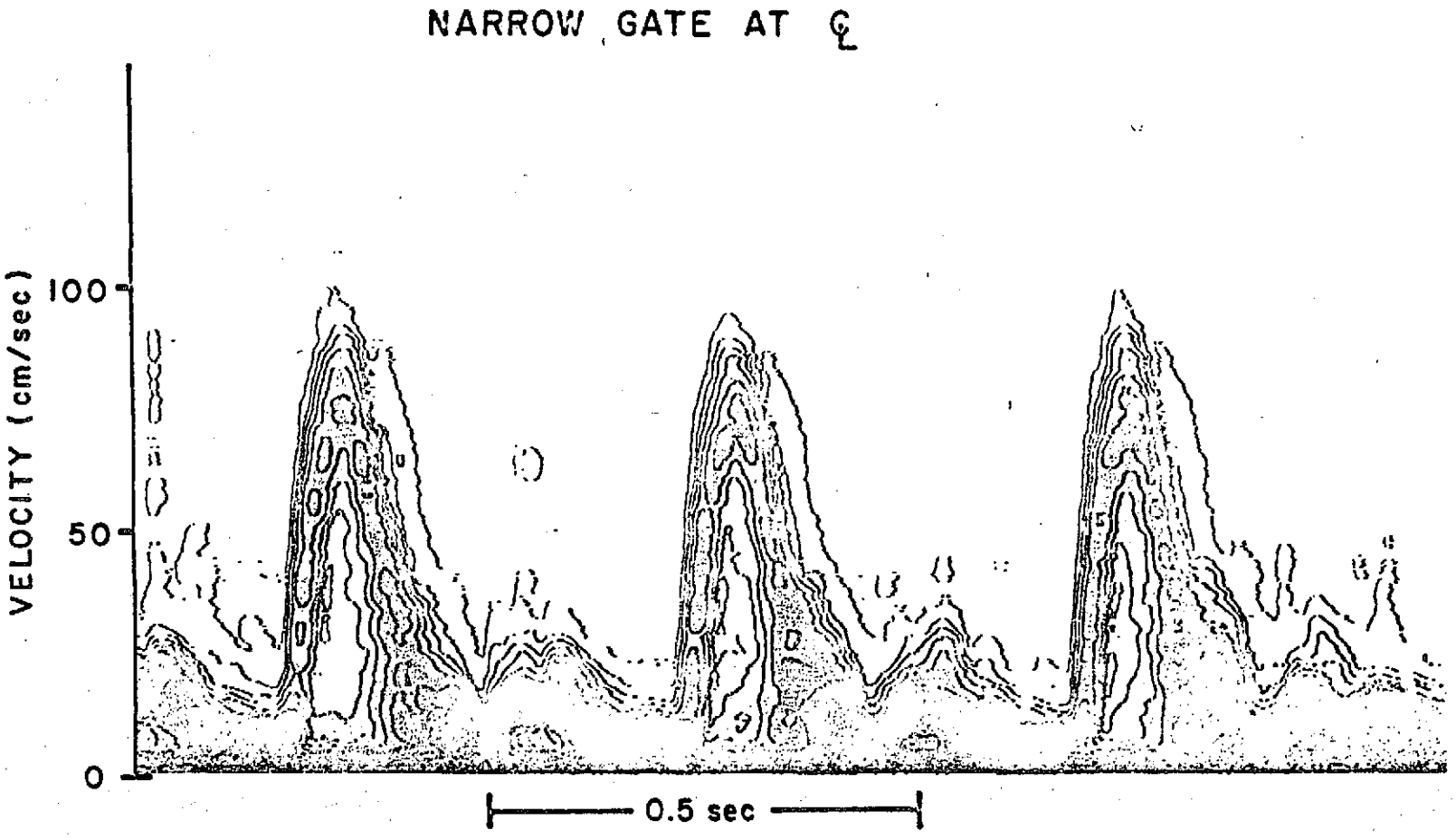

FIGURE 13B. SONOGRAM PRODUCED WITH A NARROW GATE FROM THE CENTERLINE OF THE FLOW STREAM IN A DOG IMPLANTED WITH A FLOW CUFF ON THE ABDOMINAL AORTA.

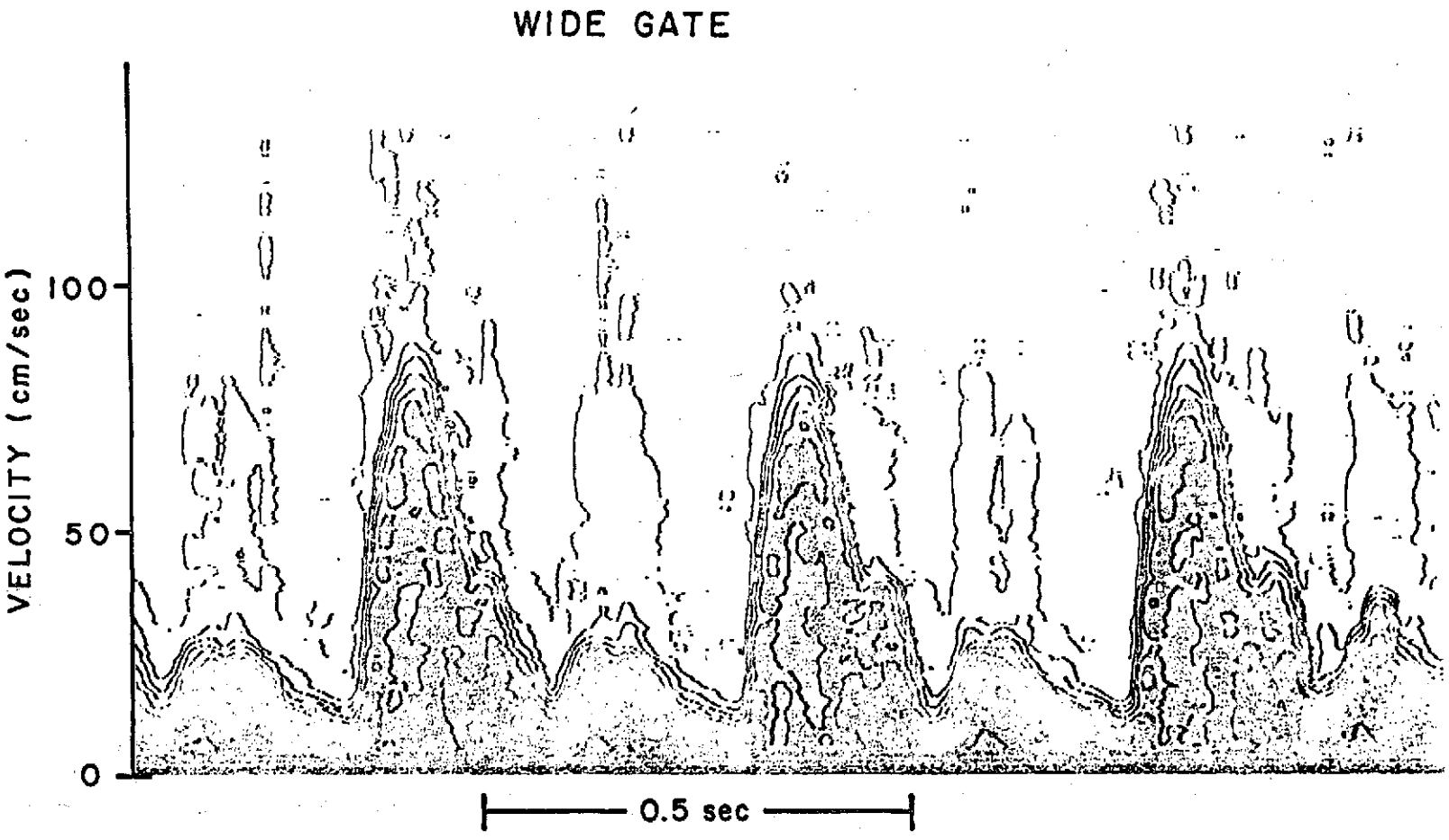

FIGURE 13c. SONOGRAM PRODUCED WITH A NARROW GATE FROM A PORTION OF THE FLOW STREAM NEAR THE WALL OF THE ABDOMINAL AORTA IN A DOG IMPLANTED WITH A FLOW CUFF ON THE ABDOMINAL AORTA.

VIII. Performance of the Pulsed Doppler Velocity Meter

A. Objectives

The objective of this phase of the research program was an evaluation of the PUDVM for laminar and turbulent flow measurements. Previous studies from this laboratory (1) reported on the effects of emission pulse length, transducer and ultrasound receiver bandwidth, and sample gate duration on the length of the PUDVM sample function. The effects of these individual parameters on the measured velocity profiles were not considered here since it was our purpose to determine whether a PUDVM system with given operating characteristics could adequately describe the nature of the various velocity profiles.

Velocity information from the PUDVM is contained in a frequency modulated audio signal that is obtained by mixing the backscattered (or Doppler shifted) ultrasound signal with an ultrasound signal at the transmitted frequency. The frequency difference between these two signals, the Doppler frequency, is directly proportional to the velocity of the moving scatterers in the sample region and is given by the Doppler equation

$$\Delta f = f_D = \frac{2 f_o V \cos \theta}{C} \qquad (1)$$

where f_o is the frequency of the emitted ultrasound, V the velocity of the scatterers, θ the angle between the ultrasound beam and the velocity vector and C the speed of sound in the medium. Since the PUDVM sample region is of finite size, a spectrum of Doppler frequencies will be measured in any flow field where velocity gradients exist such as in a contained flow.

The purpose of the experiments reported here was to compare different methods of determining the average frequency shift of the Doppler spectrum

or, equivalently, the average speed of the moving scatterers within the region of flow sampled by the PUDVM. Three techniques were used to estimate the average frequency of the Doppler signal: (1) direct frequency to voltage conversion using a zero crossing detector; (2) calculation of the first moment of the Doppler spectrum obtained with the aid of a spectrum analyzer; and (3) computer-aided estimation of the first moment of the Doppler spectrum using Fast Fourier Transform (FFT) techniques. Average velocities in the sample volume were calculated from the average frequencies using the Doppler equation and the resulting profiles were compared to the theoretically predicted velocity distributions.

B. Methods

The experiments were conducted in a specially designed test system which is shown schematically in Figure 14. The flow system produces steady fully developed laminar or turbulent flow in dialysis tubes ranging in size from 6 to 20 mm diameter. The test section consists of a long length of circular dialysis tubing supported and submerged in a water bath. Measurements were made at positions located several hundred tube diameters downstream from the entrance to the dialysis tubing to ensure that the flow was fully developed. Flowrates were monitored with a rotometer and could be adjusted with an inlet valve. The performance of the rotometer was verified by timed collection and found to be accurate to within 5% of the manufacturer's calibration values. The working fluid in the test system was water seeded with cornstarch or cellulose particles to act as scatterers of the ultrasound. Concentration of the scatterers was typically 5% by volume.

An ultrasound transducer was positioned over the dialysis tube in the vertical plane determined by the tube axis and with the ultrasound

beam axis at an angle of 60° to the direction of flow. The transducer consisted of a 2.8 mm diameter lead titanate zirconate crystal with epoxy backing.

Velocity and frequency data were obtained with the PUDVM for flow Reynolds numbers ranging from 950 to 5000. All measurements reported here were monitored in the flow system in a dialysis tube of nominal diameter 7 mm. The tube diameter varied with flow rate from 7.2 to 7.6 mm and this variation was considered in the calculation of the Reynolds numbers. For these tests, the PUDVM emission frequency ranged from 7.25 MHz to 7.5 MHz. Other operating parameters included an emission pulse length of 8 cycles (about 1 μsec) gate of 1 μsec and pulse repetition frequency of about 20 KHz.

For each Reynolds number the velocity profile as measured from the output of the zero-crossing detector was recorded on graph paper using an X-Y plotter. The RMS voltage of the audio signal was monitored with a B and K RMS voltmeter. Peak RMS audio amplitude was maintained between 0.15 and 0.25 volts RMS and the signal to noise ratio of the audio signal was at least 40 volts/volt. The velocity signals were scanned continuously across the tube for each Reynolds number. A spectrum analyzer (Hewlett-Packard model 8552/56) was used to determine the frequency spectra of audio signals measured at several range locations in the tube. The relative amplitudes of the frequencies present in the signal were recorded as a function of frequency on the X-Y plotter. The recorded spectra were subsequently used to determine the first moment of the Doppler signal. In addition, audio signals from these same range locations were recorded on magnetic tape for computer analysis using FFT techniques.

C. Results

Typical recordings of a velocity profile and frequency spectra for laminar flow (Re=1430) are shown in Figures 15 and 16. A tracing of the continuous velocity profile is plotted in Figure 15 as a function of the distance from the centerline of the tube. The measured profile is shown here compared to the theoretically predicted profile. The measured profile is spread at the far wall and the obvious hump on the velocity profile between the near wall and the center of the tube is apparently due to the PUDVM boundary error (1). In this example, the PUDVM underestimates velocities close to the near wall and overestimates velocities at the far wall. The measured centerline velocity is within 3% of the predicted value.

The frequency spectra at six locations in the tube are shown in Figure 15. The spectra were measured at range increments of 1 μsec across the tube however for clarity the data presented in Figure 3 are for increments of 2 μsec. For each spectrum the baseline was set approximately 8-10 db below the peak signal level. The baseline levels (in db) are referenced to a sinusoidal input signal of 1.0 V RMS. The noise baseline for zero flow was -70 db or less. The first moment of the Doppler spectrum was determined from these data and the average velocity within the sample region calculated using the Doppler equation.

A comparison of the theoretical velocity profile, the measured profile (using analog output of PUDVM) and the profile calculated from the first moment of the Doppler spectra are shown in Figure 17. The solid line is the predicted profile, dashed line the measured profile and the points correspond to the calculated profile. Agreement between the predicted profile and either the measured or calculated profile is

excellent within the central core of the flow and the measured and calculated distributions are within 10% of each other except near the walls of the tube. For distances from the wall less than 1/4 the tube radius both the zero-crossing counter and first moment calculation lead to substantial errors in the velocity estimate for this example.

Similar comparisons can be made for the case of fully developed turbulent flow. Figures 18 and 19 illustrate the measured velocity profile and Doppler frequency spectra respectively for a flow with Reynolds number 3860. The measured profile is compared to the theoretically predicted mean velocity distribution given by Schlichting (2) as

$$\frac{u}{\bar{u}} = k\left(\frac{r}{R}\right)^{1/n}$$

where u = axial velcoity, $\bar{u}$ = average axial velocity, and n and k depend upon the Reynolds number. For Reynolds numbers from 2000 to 5000 k and n remain approximately constant and have values of .791 and 6.0 respectively.

Over the central 80% of the tube cross section the PUDVM consistantly overestimates the mean velocity by 5 to 10%. The shape of the measured profile is again somewhat smoothed and especially distorted near the tube walls.

The Doppler frequency spectra for this example of turbulent flow are shown in Figure 19. They are considerably more broad than the spectra observed in laminar flow because of the random distribution of turbulent velocity fluctuations that are superimposed on the mean flow. The spectra remain relatively symmetric however. Figure 20 shows the profile calculated from the first moment of the Doppler frequency spectra along

with the measured and theoretical profiles. The profile based on the first moment agrees well with the measured profile except in the neighborhood of the walls.

Comparisons among measured, calculated and theoretical profiles for seven different Reynolds numbers are summarized in Figures 21-27. Theoretical profiles are shown in solid line, measured in dashed, and the dots represent velocities calculated from frequency spectra.

Computer aided estimates of the velocity profiles were obtained using Fast Fourier Transform (FFT) techniques to calculate the first moment of the Doppler spectra. Operation of the FFT program used for this analysis is described in Appendix I. Typical results of the FFT analysis are shown in Figures 28-34. The FFT estimated profiles are compared to theoretical profiles for Reynolds numbers ranging from 950 to 4800. The FFT consistantly overestimates velocities for both laminar and turbulent profiles. For laminar flow the estimated profiles have the characteristic parabolic shape of the velocity distribution in a circular pipe, however, the peak (centerline) velocities are overestimated by 15 to 20%. The shapes of the calculated turbulent profiles are not in obvious agreement with theoretical predictions.

D. Observations

1. In laminar flow, the velocities in the central core of the tube (±0.6 radius from the tube center) as measured by the zero-crosser and first moments from the wave analyzer spectra agree within 5% with the expected theoretical velocities.

2. In turbulent flow, estimates of velocities within the central core of the tube by the zero-crosser and first moment from the wave

analyzer agree with each other within 2-3%, but both peak velocity estimates are 6-17% higher than the expected theoretical velocities, the error decreasing with increasing Reynolds number. This over-estimation of velocities was consistantly found in repeated experiments.

3. Velocities estimated from the audio spectra using FFT and computer techniques are from 10% (in laminar flow) to 22% (in turbulent flow) higher than the expected theoretical values.

4. In flow near the walls, the velocities estimated by spectral analysis, both with the wave analyzer and FFT, are many times the expected theoretical values. This is most likely due to the low power of the signals near the wall. In the case of the wave analyzer, spectra obtained near the wall often had a baseline level only 10 db above the noise level. Inclusion of white noise into the spectra would tend to shift the first moment of the spectra toward higher velocities.

5. Overall, the zero crossing counter provides a velocity estimate that is at least as good as the velocity calculated from the first moment of the Doppler spectrum. Near the walls, the zero crosser gives a better indication of the true velocity than the frequency spectrum.

E. Conclusions

1. Central core velocities as estimated by the zero crosser and the first moment from the wave analyzer spectra agree well with each other, but are only estimates of the true velocity in laminar flow.

2. The velocities estimated by the first moment of the FFT analyzed audio signal are not accurate estimates of the true velocity.

3. Since the zero crosser is more reliable near the walls, it

gives a more accurate estimation of the velocity profiles than does the first moment of the audio spectra from the wave analyzer. However, since the baseline level of the audio signal near the wall was not held constant and, in fact, often approached noise levels, an electronic first moment processor might prove as accurate as the zero crosser near the walls.

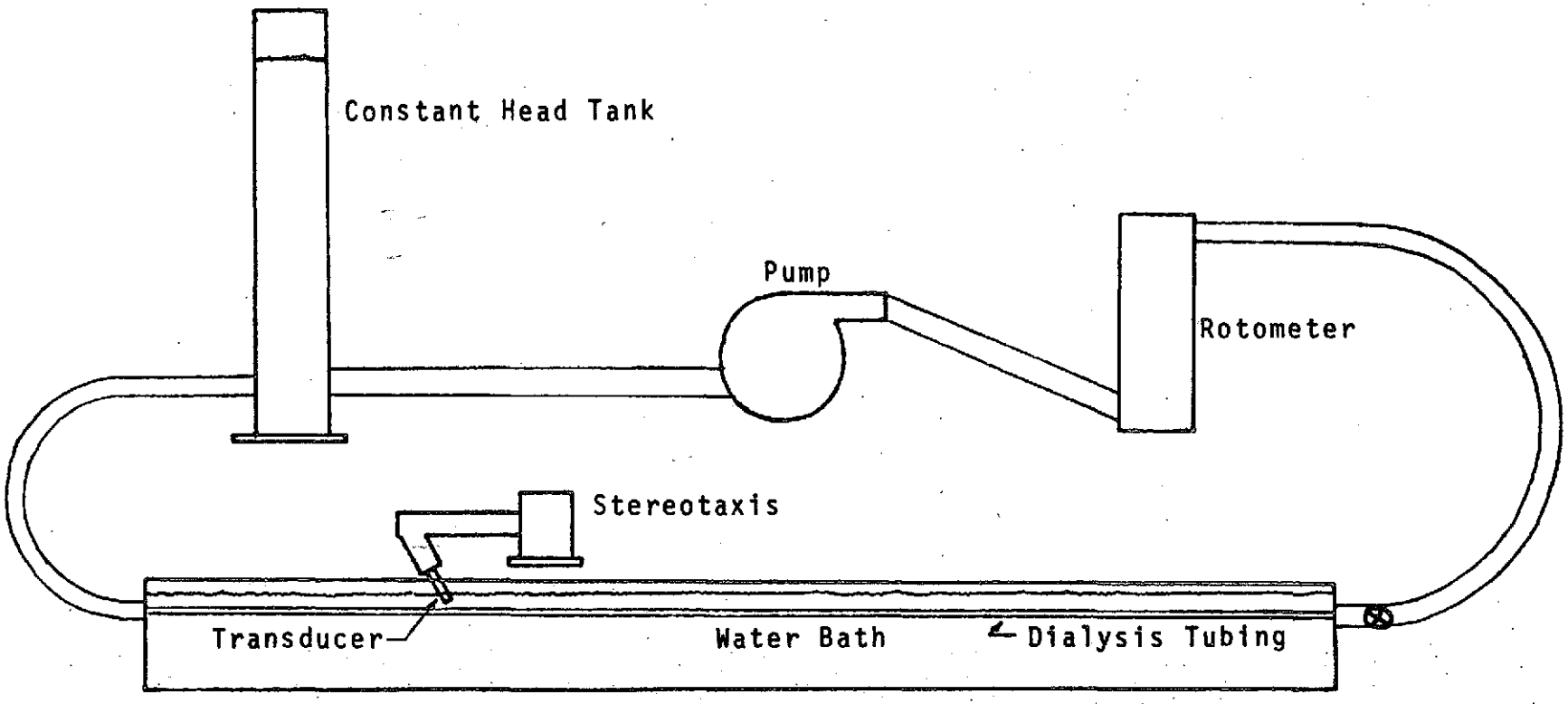

Figure 14 Schematic Drawing of Test Tank Used to Produce Fully Developed Laminar and Turbulent Pipe Flow

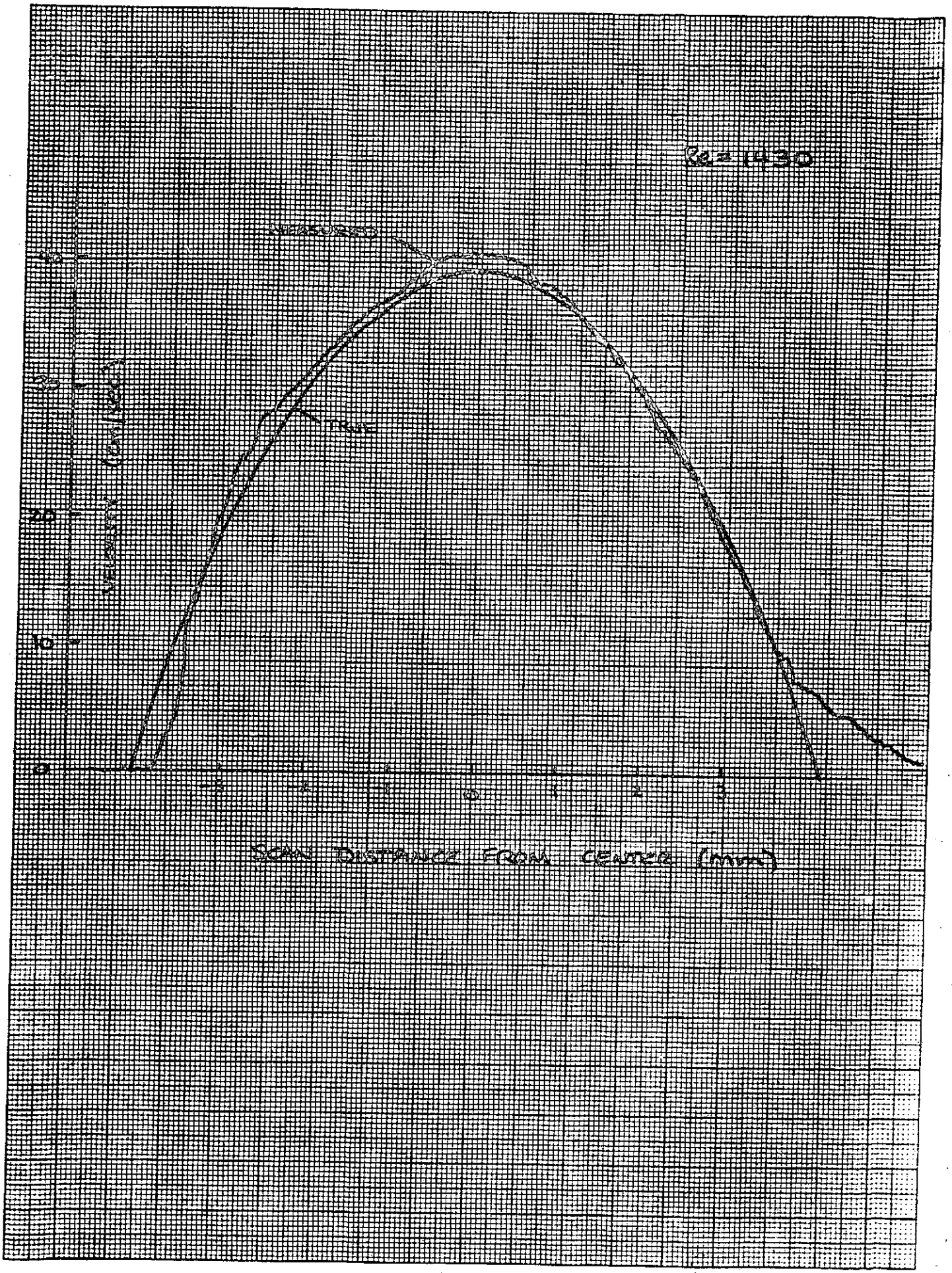

FIGURE 15

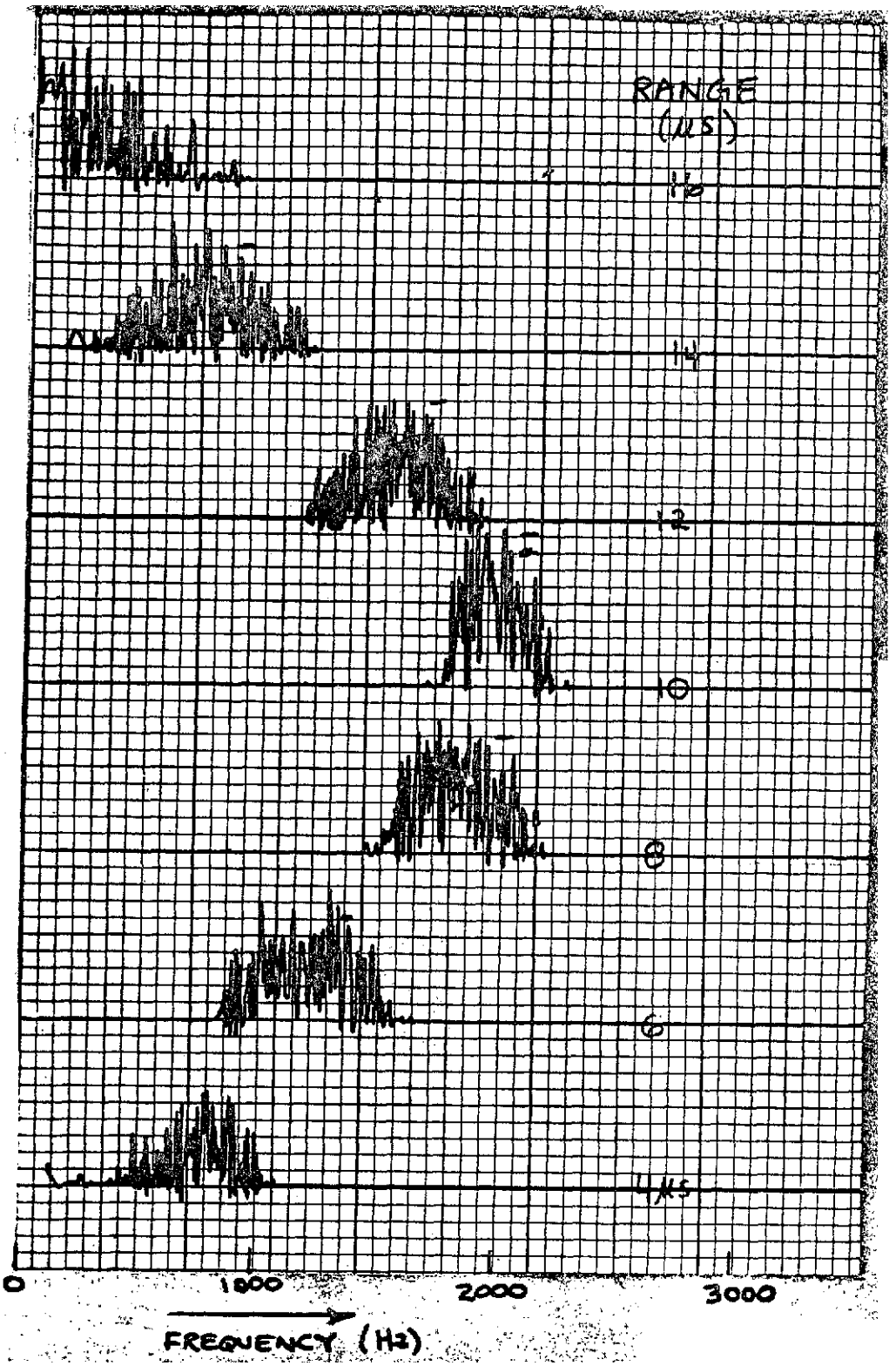

FIGURE 16

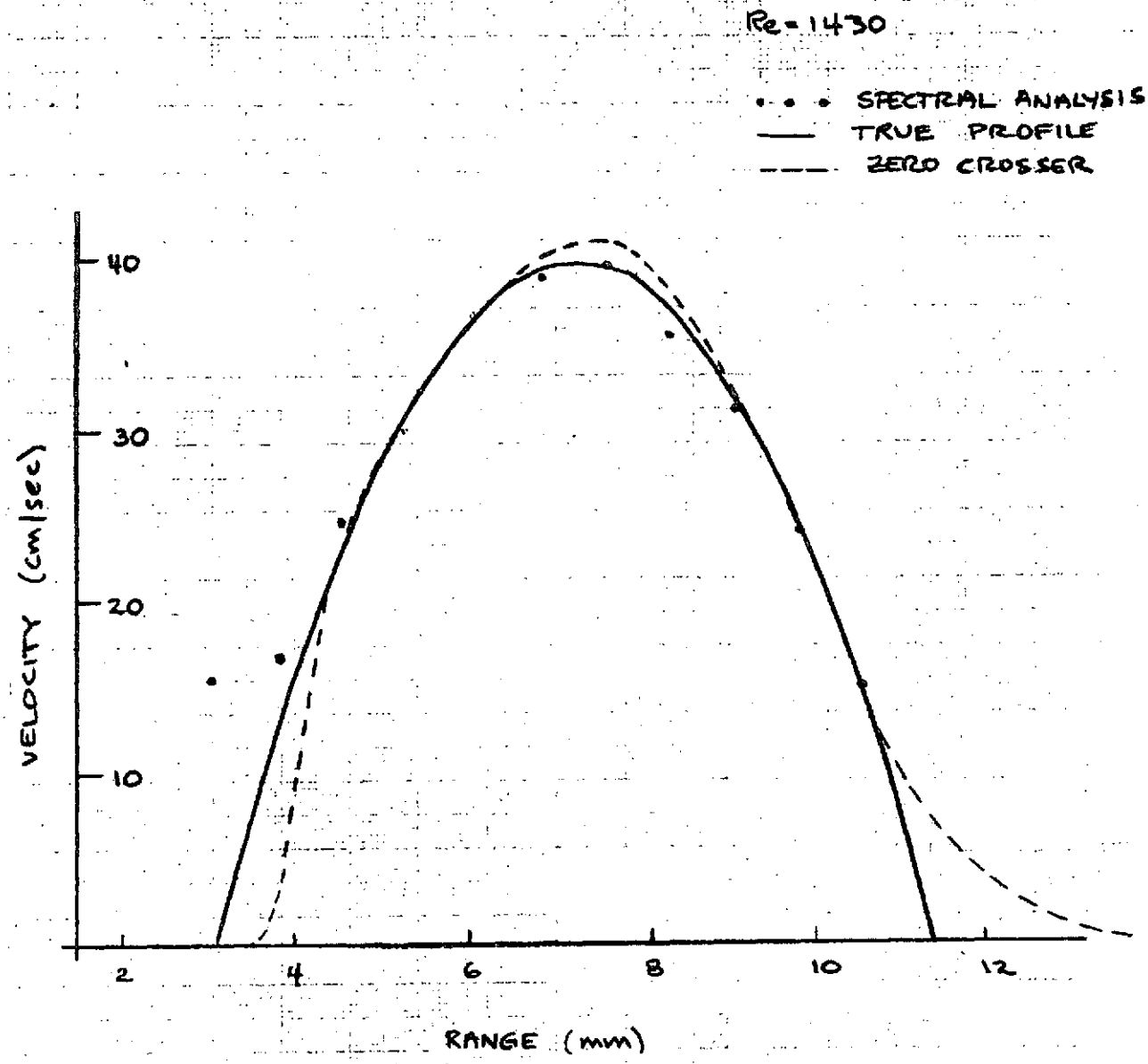
Re = 1430
• • • SPECTRAL ANALYSIS
—— TRUE PROFILE
– – – ZERO CROSSER
VELOCITY (cm/sec)
40
30
20
10
2
4
6
8
10
12
RANGE (mm)

FIGURE 17

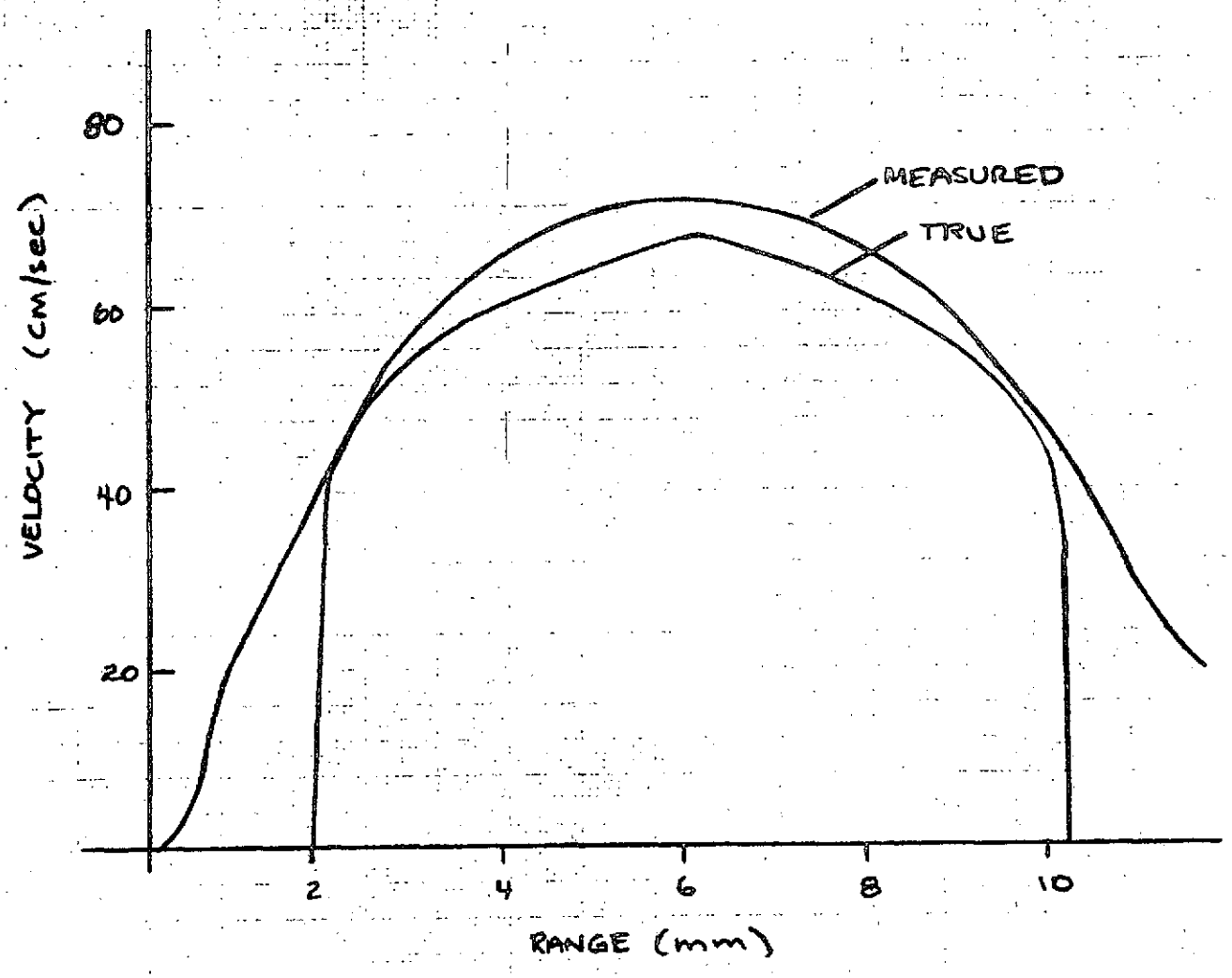
Re= 3860
VELOCITY (cm/sec)
80
60
40
20
MEASURED
TRUE
2
4
6
8
10
RANGE (mm)

FIGURE 18

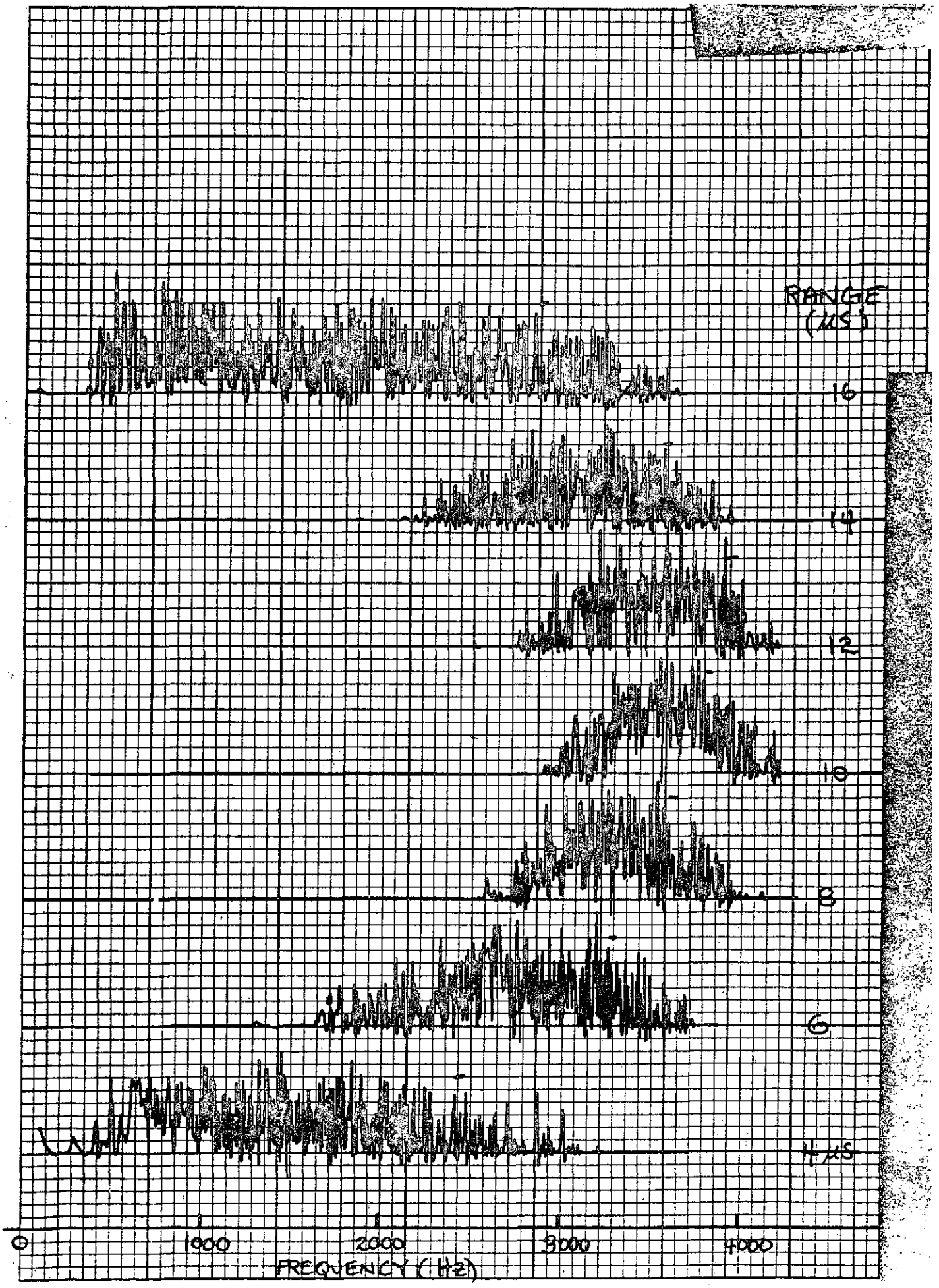

FIGURE 19

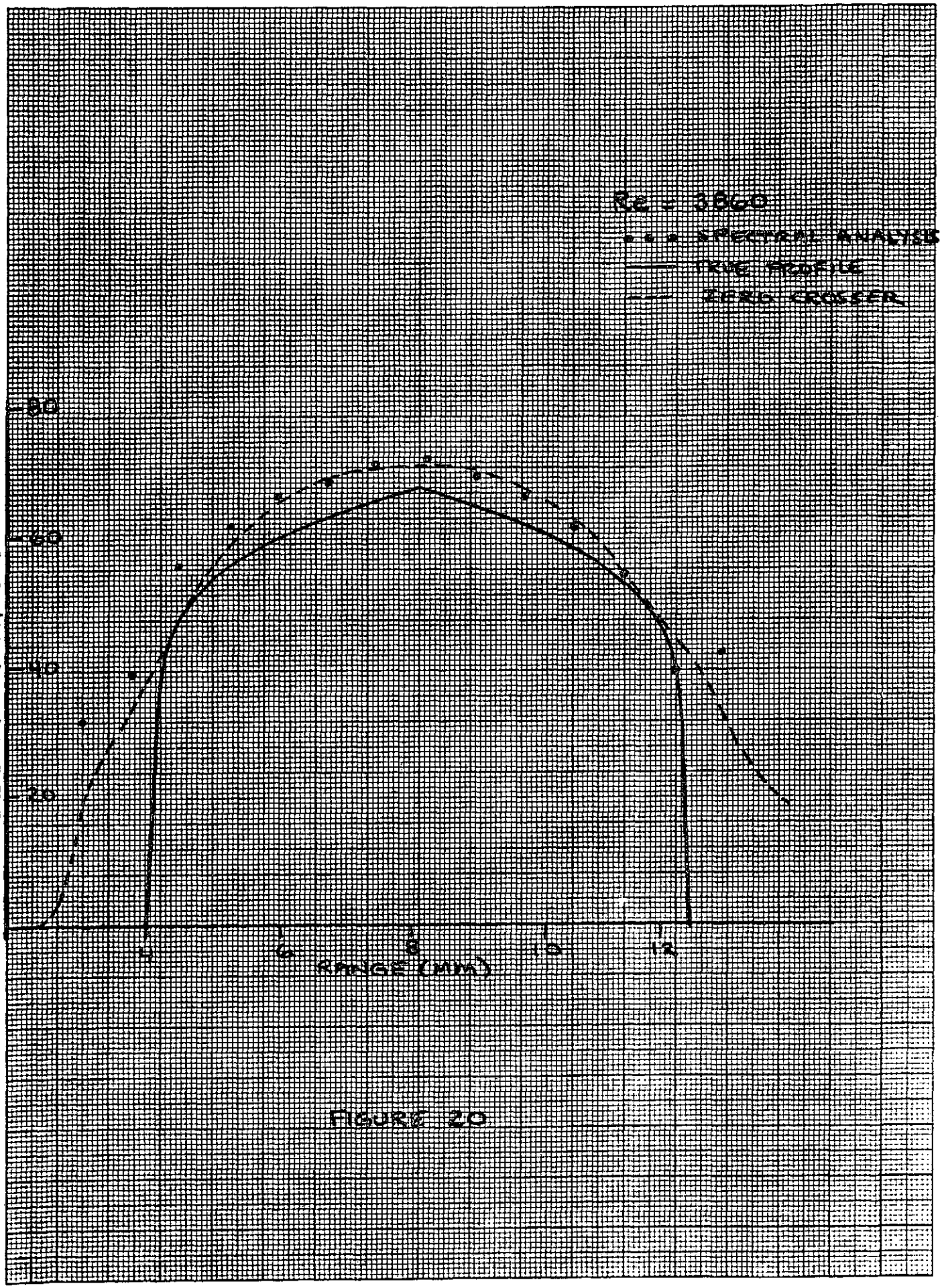

FIGURE 20

Tank Study 6/20/74 tube dia. = 7.2 mm

redrawn 1-8-75

Re = 948

.... spectral analysis

——— theoretical profile

- - - - - zero-crosser output

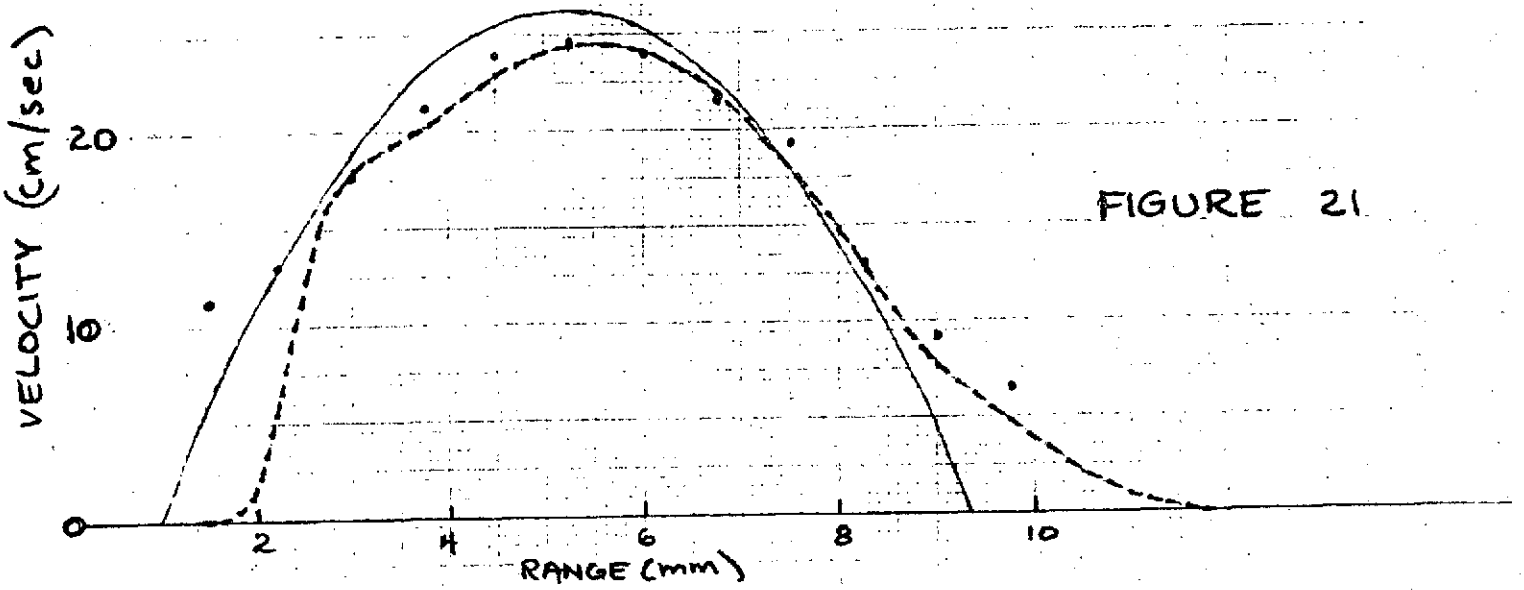

FIGURE 21

Re 1430

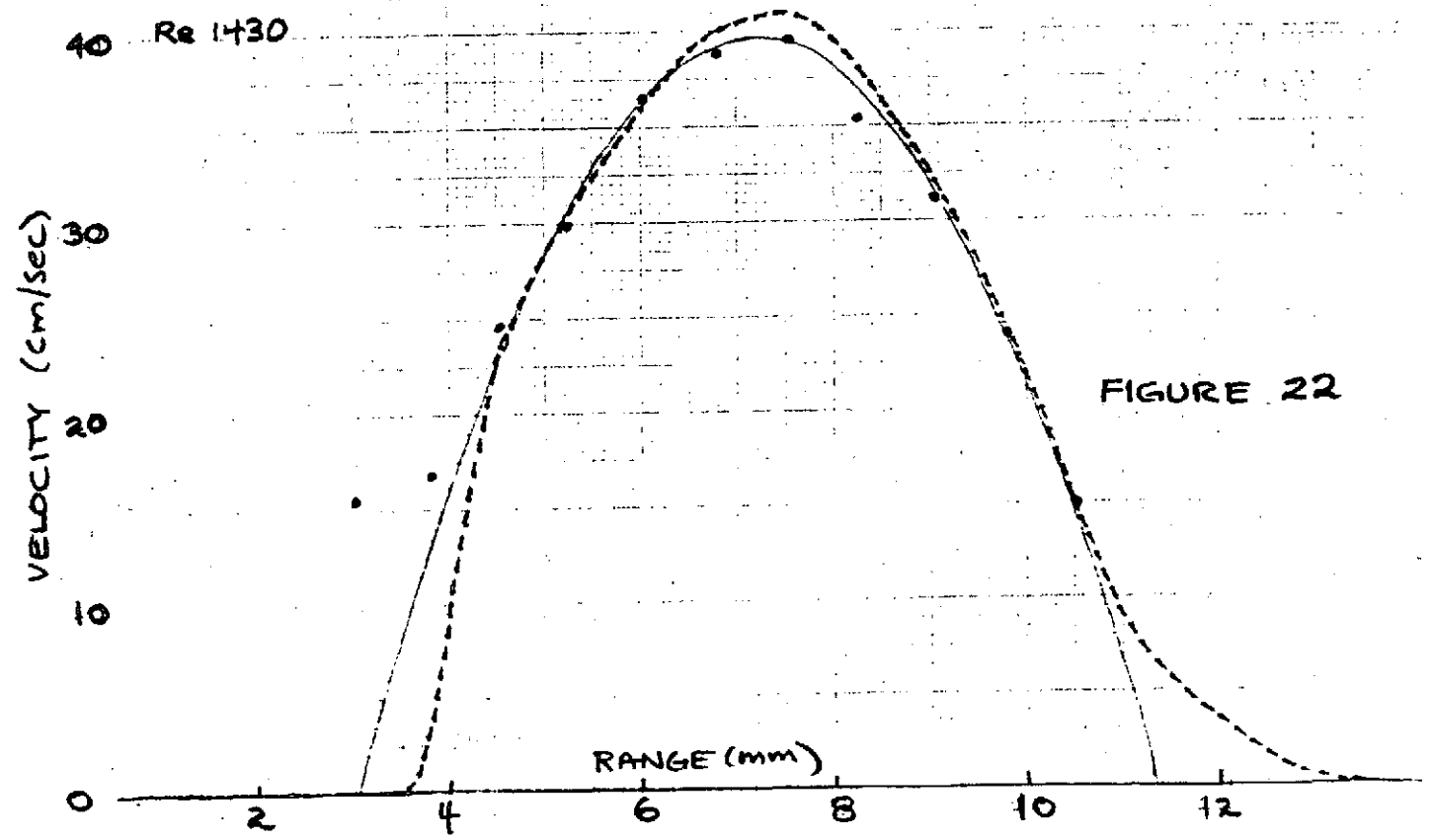

FIGURE 22

Tank Study 6/20/74 tube dia = 7.2mm

redrawn 1-8-75

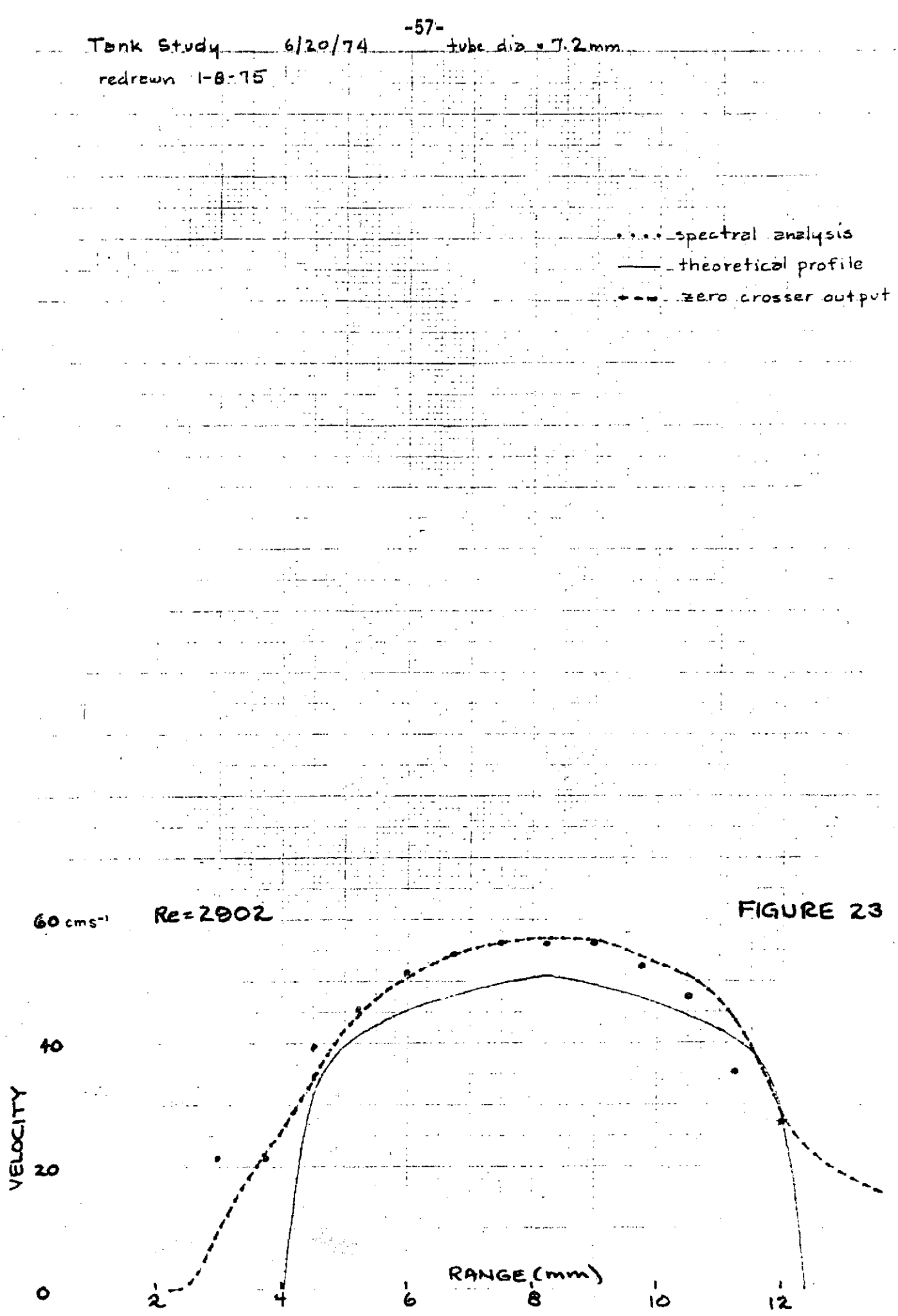

FIGURE 23

Tank Study 6/20/74 tube dia = 7.2 mm

redrawn 1-8-75

.... spectral analysis

—— theoretical profile

- - - zero crosser output

Re=3376

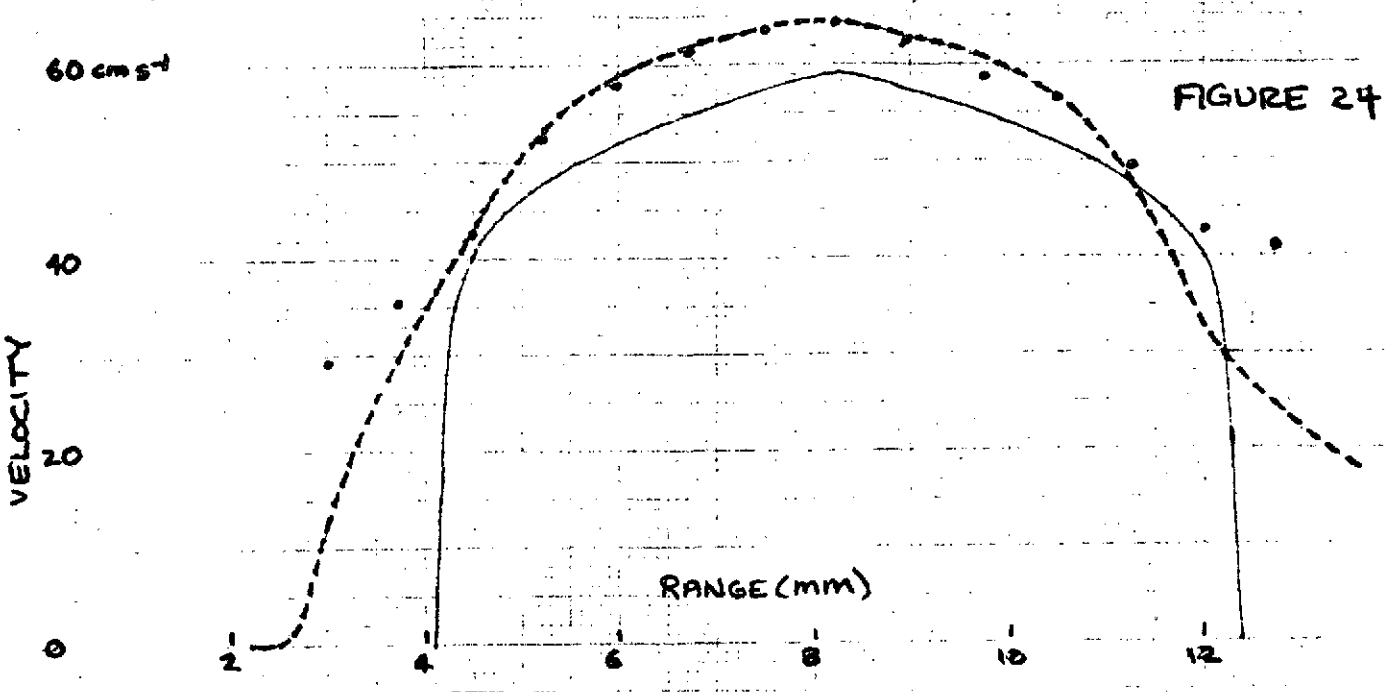

FIGURE 24

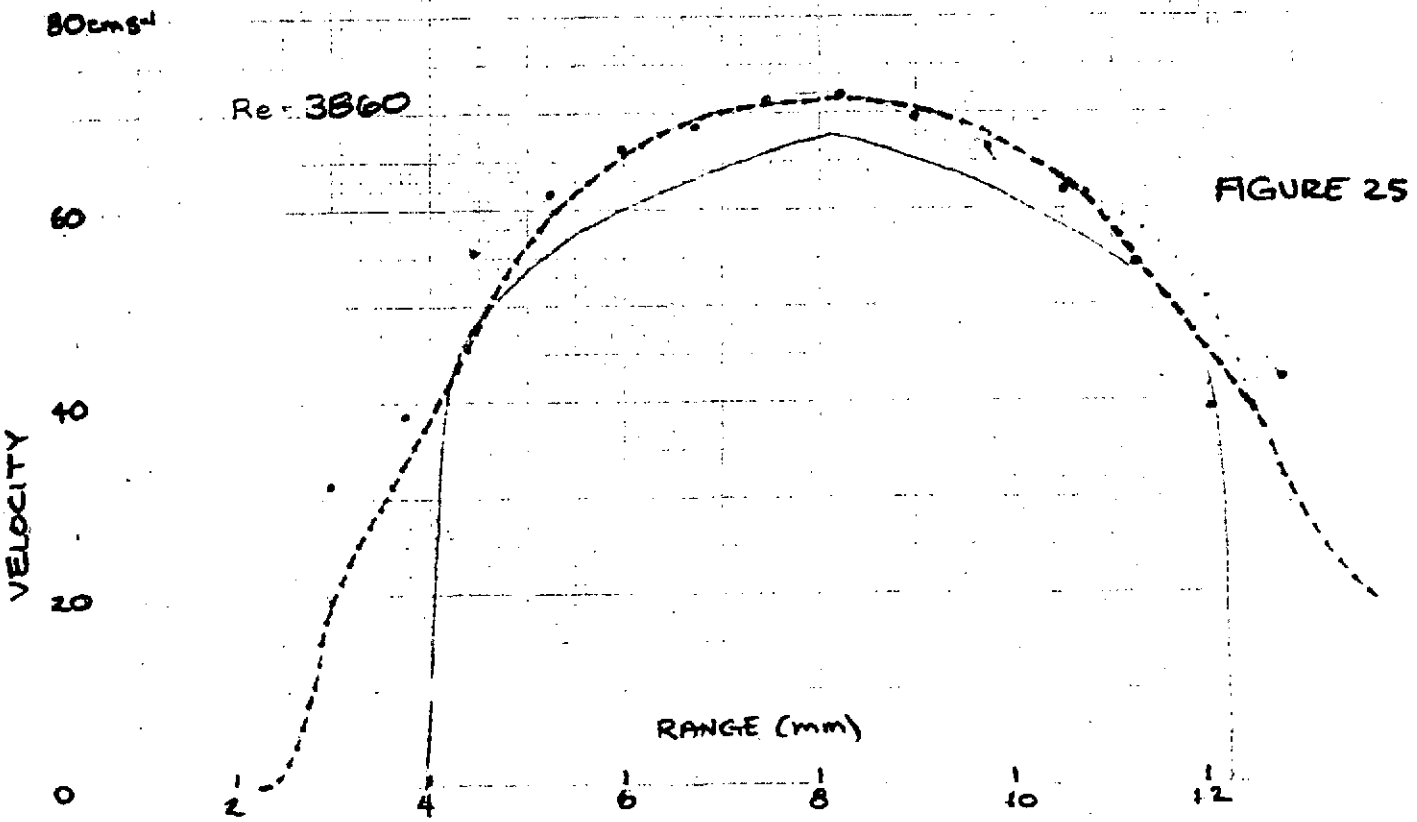

FIGURE 25

Tank Study 6/20/74 tube dia = 7.2 cm

redrawn 1-8-75

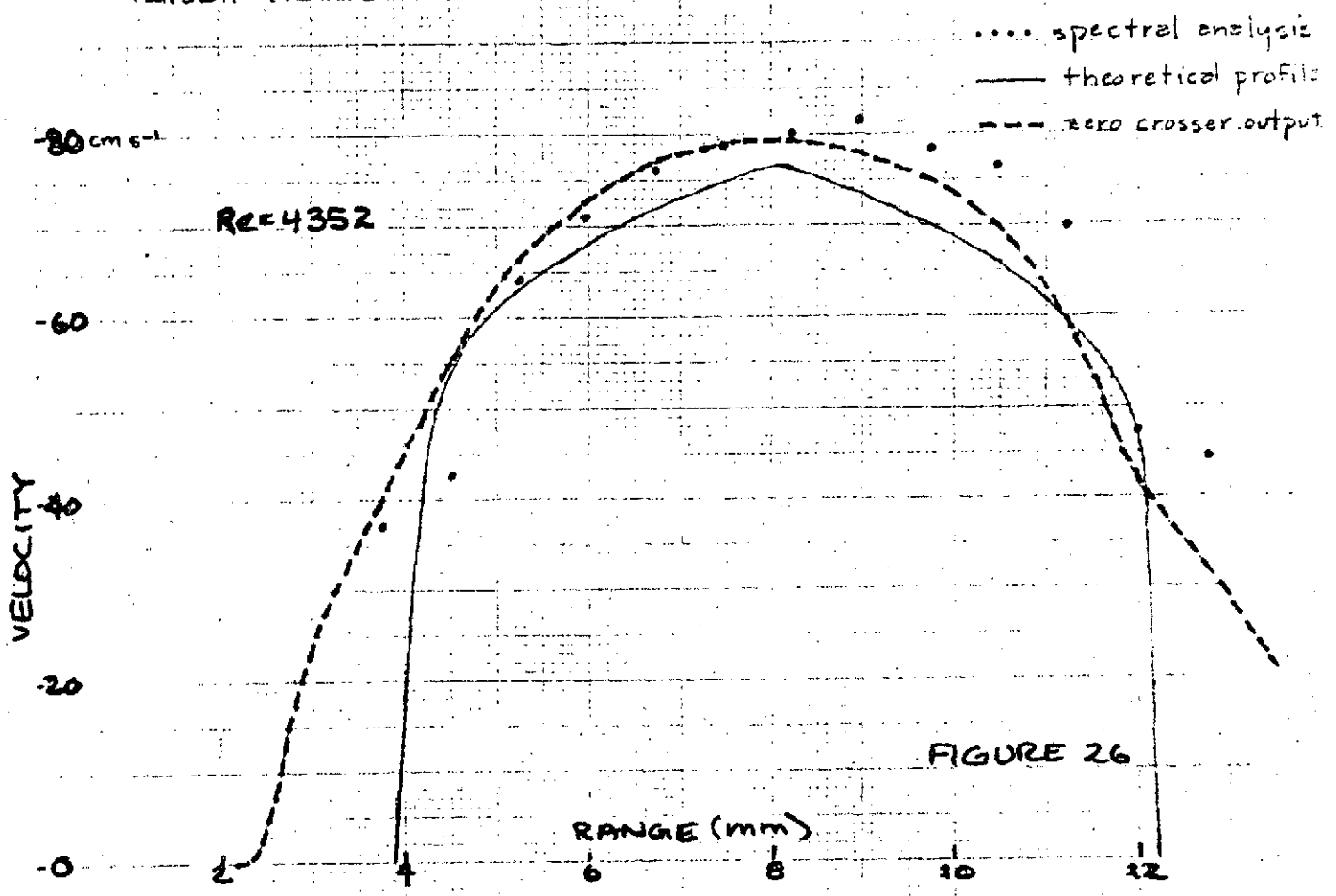

FIGURE 26

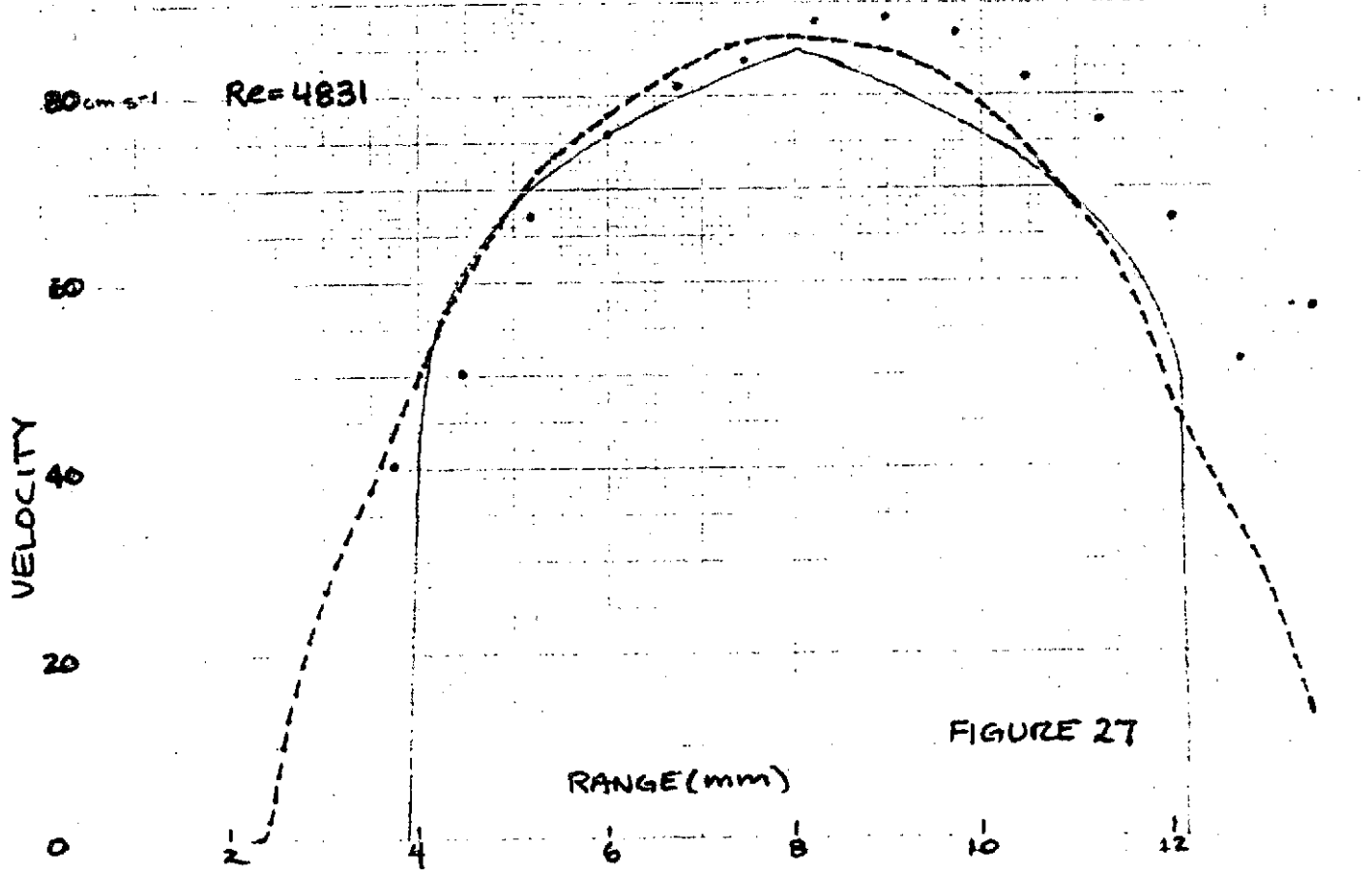

FIGURE 27

Tank_study 11/13/74 tube d.i.a = 7.2mm

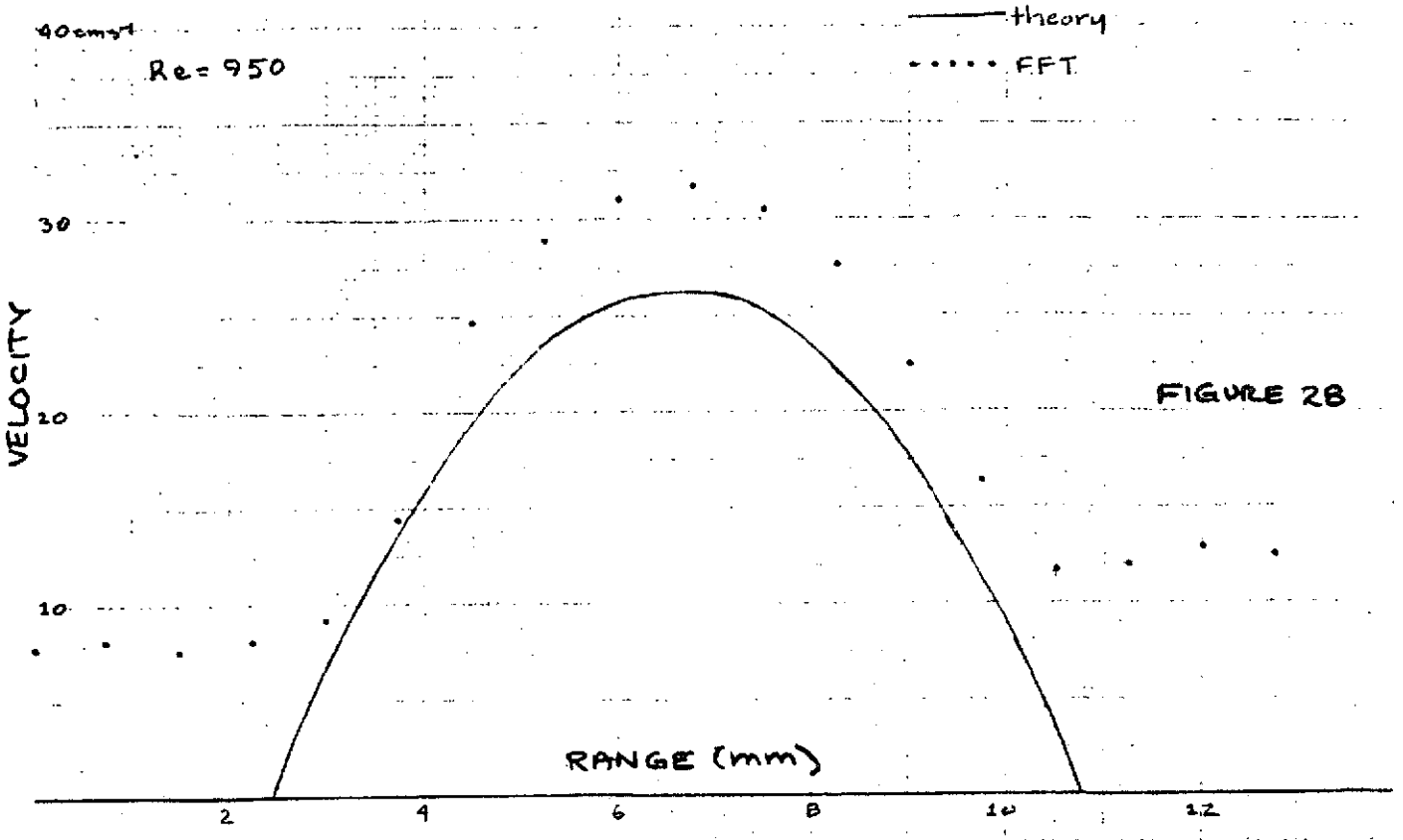

FIGURE 28

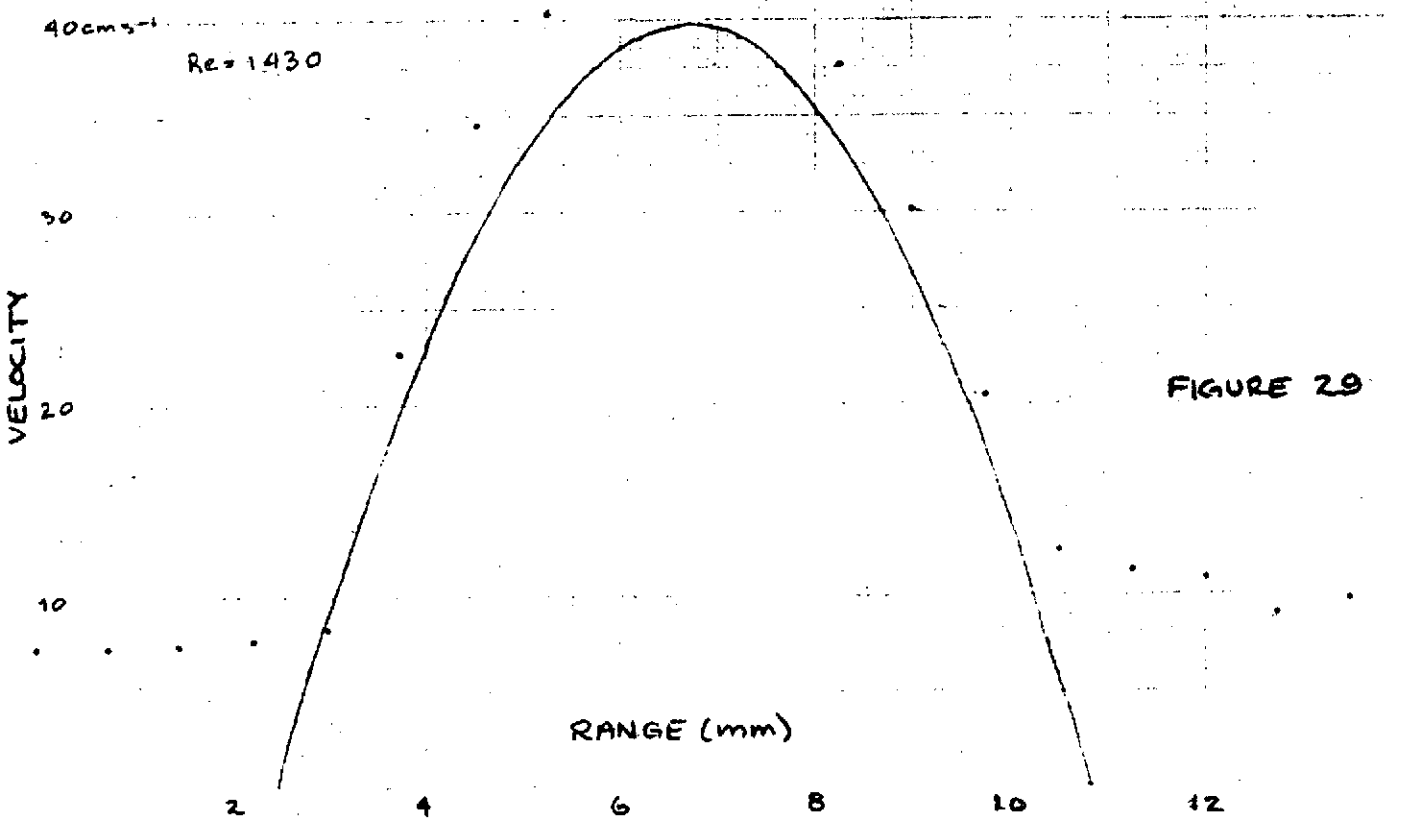

FIGURE 29

Tank study 11/13/74 tube dia = 7.2mm

FIGURE 30

Tank Study 11/13/74 tube dia = 7.2 mm

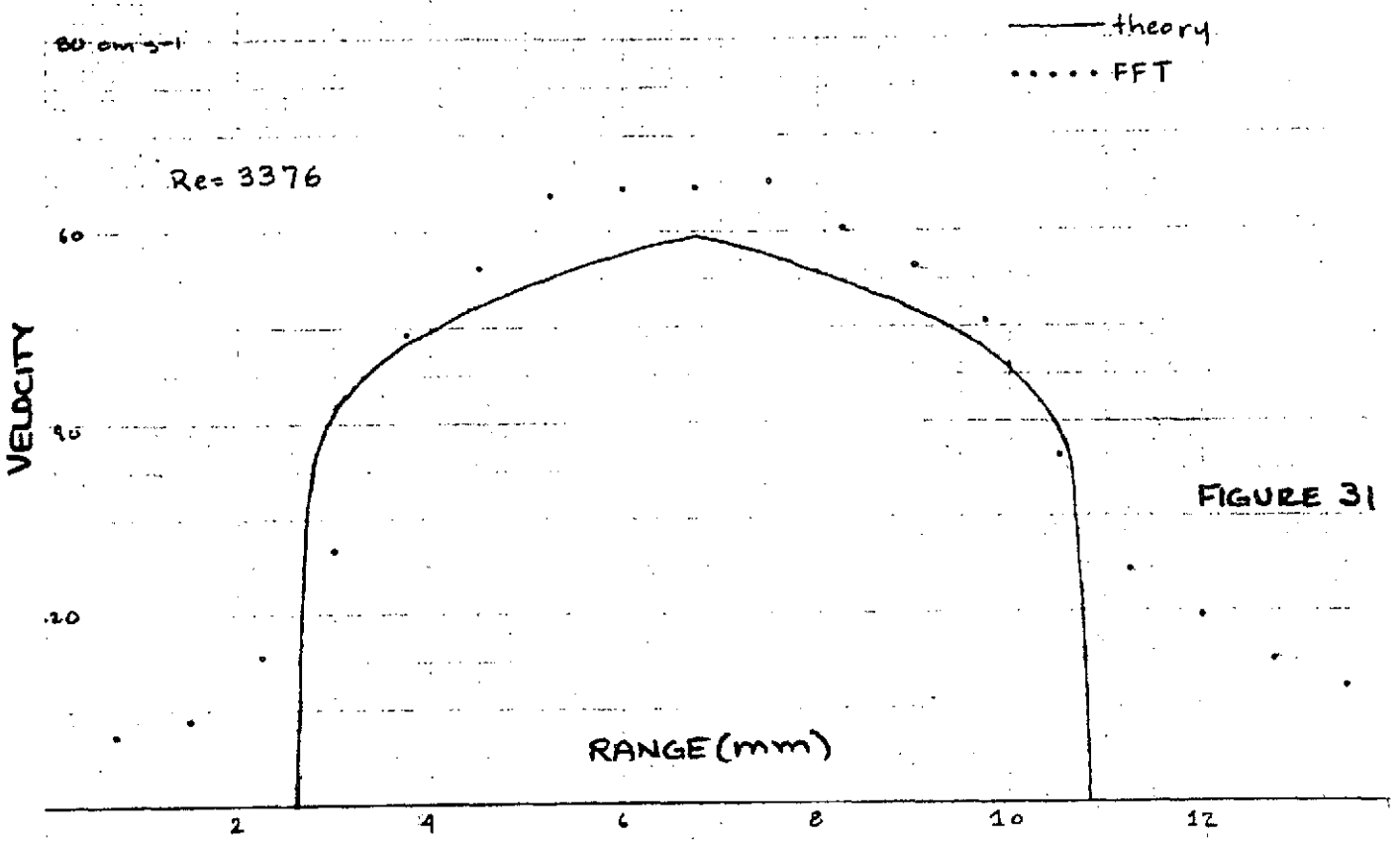

FIGURE 31

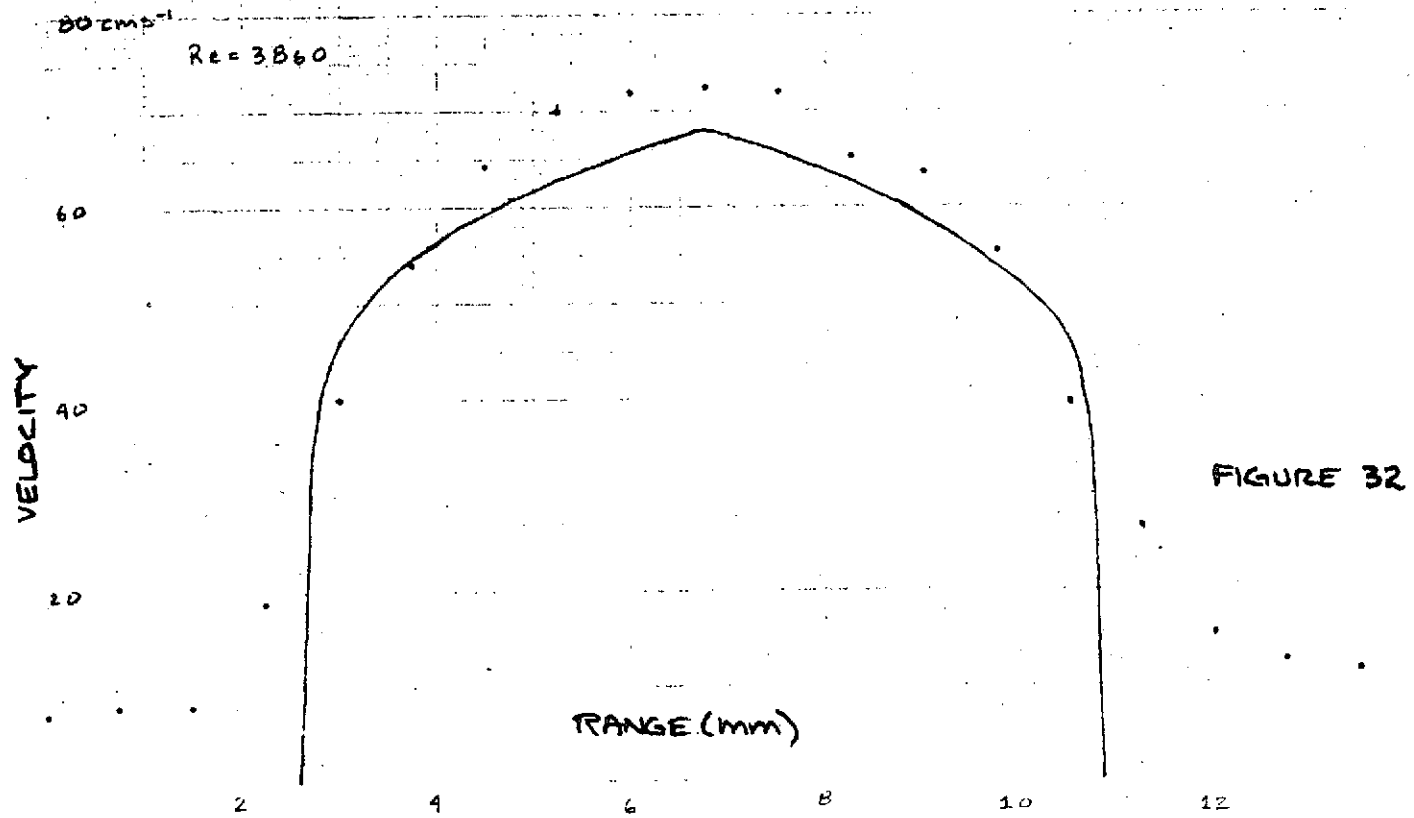

FIGURE 32

Tank Study 11/13/74 tube dia = 7.2 mm

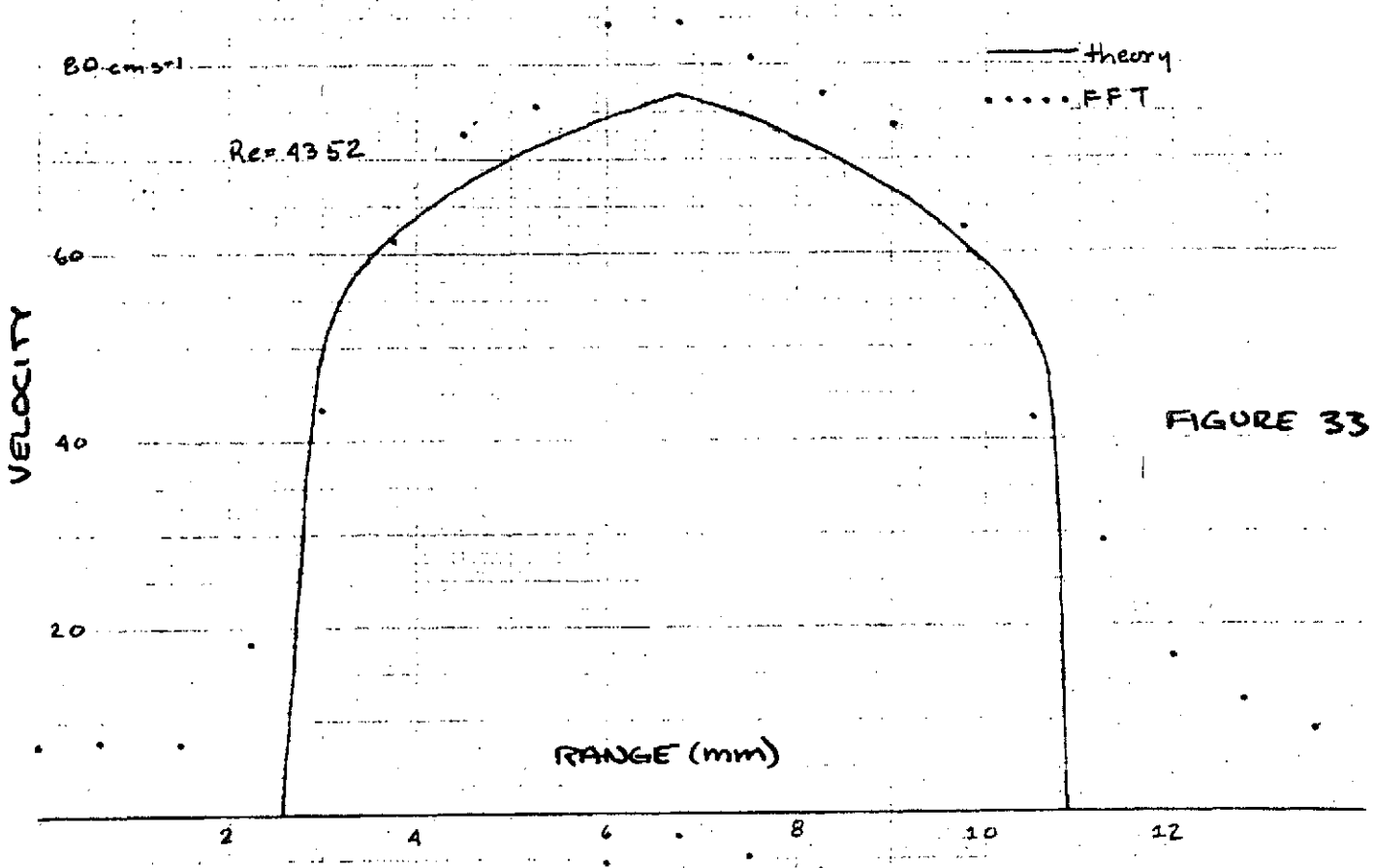

FIGURE 33

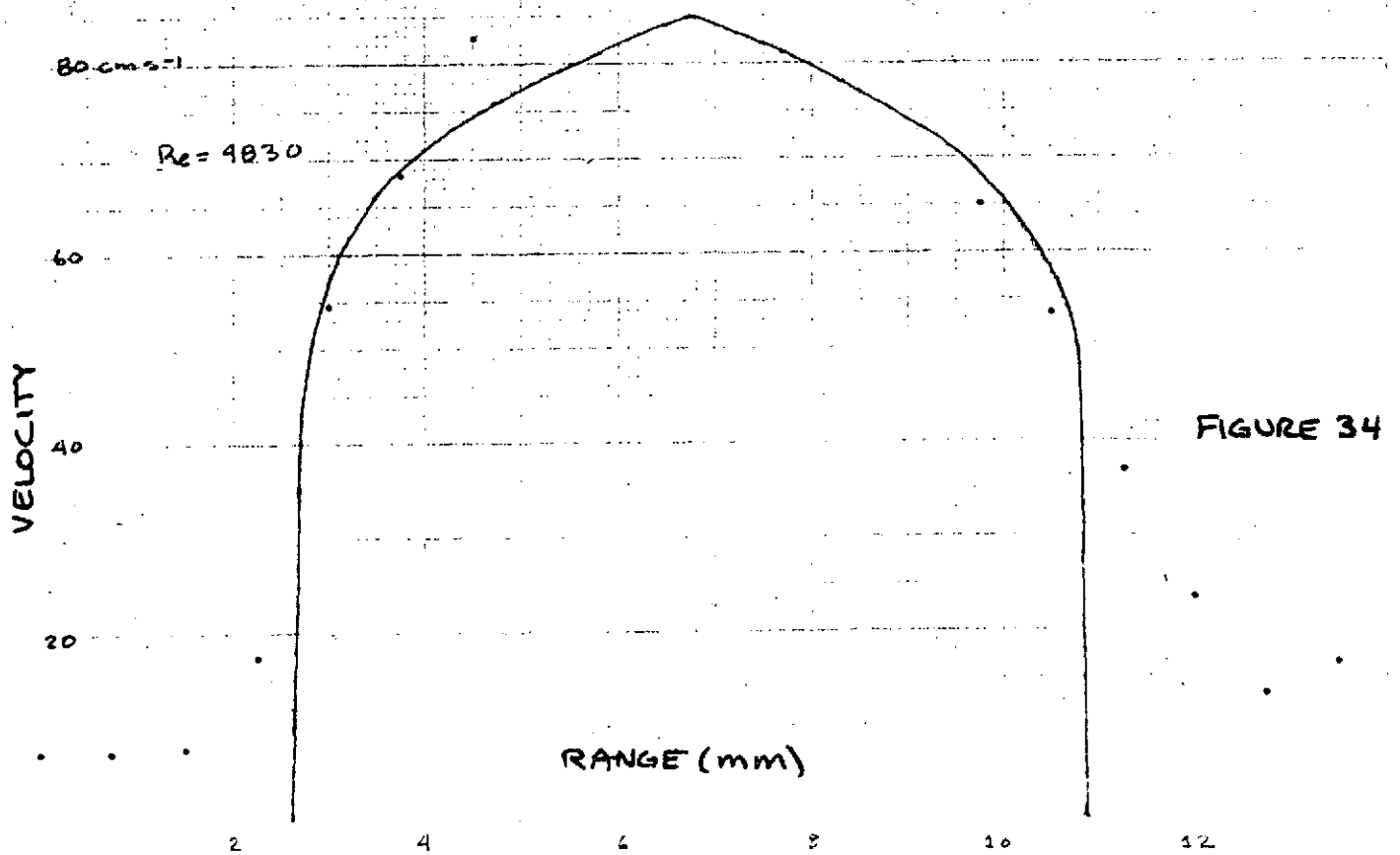

FIGURE 34

IX. Performance of the NASA-PUDVM

A. Objectives and Methods

The PUDVM designed and built by the NASA Ames Research Center was loaned to our laboratory for use in animal experiments and for testing and comparison with other pulsed Doppler velocity meters. The NASA instrument was used for studies on coronary blood flow in horses and the pertinent physiological and biomechanical results have been summarized in the report "Hemodynamic Patterns in Coronary Arteries" by Wells et. al. This report is included here as Appendix II.

The performance of the PUDVM was determined from tests carried out on the flow system described above in Section V. In general the performance of the NASA-PUDVM in the tank facility was inferior to the performance of the McLeod instrument. This was attributed to the low signal to noise ratio and the low sensitivity of the NASA-PUDVM. It was decided that any detailed evaluation of the PUDVM capabilities and subsequent definition of techniques for the transcutaneous measurement of flow should be based on tests with the McLeod PUDVM. These results are described above in Section V.

The effect of emission pulse length, gate length and pulse repetition frequency on the performance of the NASA-PUDVM was determined by comparing the velocity profiles measured for steady laminar flow in the test system. In addition, the accuracy of the flowmeter was measured for different input gains.

B. Results

An important factor that strongly affects the accuracy of the PUDVM is the signal to noise ratio S/N. The number of scatterers

directly influences the strength of the backscattered Doppler signal and it was found that in tank studies with the NASA-PUDVM the test fluid had to contain a 10 to 15% concentration of scatterers to bring the signal to an acceptable level. However, with a high concentration of scatterers a proportionally larger number of particles would settle to the bottom of the tube and distort the profile from the desired parabolic shape. It was not found practical to run the test system for more than a minute or two with particle concentrations greater than about 10% by volume. Even at this concentration, however, the two input amplifiers had to be operating at their maximum effective gain in order for the PUDVM to properly estimate velocity. To determine the sensitivity of the PUDVM to input gain, the following experiment was performed: The PUDVM sample region was centered on the tube axis and flow maintained at a constant rate. The output of the PUDVM was measured for various settings of the "gain" and "range" amplifiers and compared to the expected output which was determined from the calibration signal. The results are given in Figure 35 which shows curves of output vs. gain for five values of range gain. Notice that only for range gains of 95 and 100% of full scale was the PUDVM output within 5% of the expected value. Furthermore in order to achieve this adequate output the gain was in excess of 70% of its full scale value. For gains above about 75% the audio signal became distorted and the output would decrease slightly. Hence to measure velocities accurately in the tank system the range gain had to be set between 95 and 100% and the gain between 70 and 75%. The optimum operating point was easily found by maximizing the output of the PUDVM with the two gain controls. However, there was not guarantee that the maximum output would agree with the expected output. This difficulty was particularly acute

when attempting to use the PUDVM to measure velocities at distances more than a few millimeters from the transducer. For this reason, the NASA-PUDVM is not suited for transcutaneous measurements of hemodynamic patterns. On the other hand, when measuring blood flow in animals with transducers positioned directly on the vessel, the NASA-PUDVM estimates the time varying velocity as well as the McLeod PUDVM. This fact was confirmed by direct comparison of the NASA flowmeter with the McLeod detector. It appears that when the ultrasound pulse is scattered from cells in whole blood (45% concentration of scatterers) the power in the received echo is sufficient to produce an acceptable signal to noise ratio within the PUDVM. The output of the zero crosser then provides an accurate measure of the velocity.

The NASA-PUDVM operates with an emission pulse of 4, 8, or 16 cycles and at a pulse repetition frequency of 13, 26, or 52 KHz. To obtain sufficient S/N ratios in the tank studies the PUDVM generally had to be operated with the maximum burst length and at 26 or 52 KHz PRF.

Velcoity profiles within the dialysis tubing were obtained by slowly scanning the PUDVM sample volume across the tube and plotting the velocity estimate as a function of delay time (range). Figure 36 illustrates two measured profiles and compares them to the predicted parabolic profile. The measurements were made with an emitted pulse of 16 cycles, a gate of 1 μsec and at PRFs of 26 and 52 KHz. The shapes of the measured profiles agree well with the true profile and there is no significant effect of PRF on the estimated profile. The measured centerline velocity differs by less than 5% from the predicted value and this difference is well within the anticipated experimental error.

The distortion of the measured profiles at the near wall appears to be less than near wall distortion observed in the flow system using other pulsed Dopplers. This might be due to the low sensitivity of the NASA-PUDVM, for if the detector is sampling only the peak of the Doppler spectrum, the effective sample region would be reduced. In addition, the power of the received signal would be diminished leading to an underestimation of the true velocity. This effect is evident in Figure 36. The fact that increasing the sample gate from 1 μsec to 5 μsec does not markedly affect the measured profile and lends some support to this interpretation.

Figure 37 shows the effect of sample gate on the measured profile. Again distortion or spreading of the measured profile is not apparent at the near wall. As the sample gate is increased, the profile is spread, however, not to the degree that one would expect if the effective sample region increased at the same rate. That is, increasing the gate tends to increase the power in the received signal more than it tends to distort the profile. The increase in signal power leads to an improved estimate in velocity. Between the near wall and centerline of the tube, the velocities measured using a 5 μsec gate are in excellent agreement with the true values.

Figure 38 shows the effect of burst length on profiles measured with the NASA-PUDVM. The power of the backscattered signal varies as the length of the emitted pulse. Since this detector is extremely sensitive to signal strength, we expect inferior performance when using shorter pulse emission times. This prediction is borne out by the curves in Figure 38, especially for emitted bursts of 4 cycles. The same response is expected for decreased pulse repetition frequencies.

Figure 39 illustrates the effect of halving the PRF when using an emitted pulse of 8 cycles. For a PRF of 25 kHz the measured peak velocity is more than 20% in error.

C. Discussion and Recommendations

It was not possible to fully evaluate or calibrate the NASA-PUDVM under the test conditions described above. The major problems were the low gain of the detector and the low S/N ratio. Backscattered power could be increased by using more or larger scatterers or scatterers having a greater scattering cross-section. However, additional problems such as particle settling, profile distortion and non-specular scattering are encountered. The NASA-PUDVM appears to operate satisfactorily when measuring in blood, however it was not practical to use blood in the test system. Improved signal amplification techniques should markedly improve the performance of the NASA-PUDVM and allow for a more extensive evaluation of the instrument.

The following suggestions are made to improve the utility of the NASA-PUDVM. To optimize the instrument performance for use with different transducer material and transducer configurations, provision should be made for easily adjusting the emission frequency. At present, in order to change the ultrasound frequency it is necessary to tune both the master oscillator and the receiver amplifier circuit. These adjustments are inconvenient to make and time consuming. When using the flowmeter for measurements in animals, it is virtually impossible to readjust the PUDVM as different transducers are used. Operating an ultrasound transducer at a non resonant frequency markedly reduces its sensitivity.

Calibration of the NASA-PUDVM could be simplified if the calibration signal was a frequency of a fixed percentage of the oscillator frequency.

As designed, the device provides a calibration voltage proportional to a specific Doppler frequency shift. To calculate the corresponding velocity it is necessary to know both the speed of sound in the test fluid and the PUDVM center frequency. By using a known percentage of the center frequency, only the speed of sound would have to be known to determine the calibration velocity.

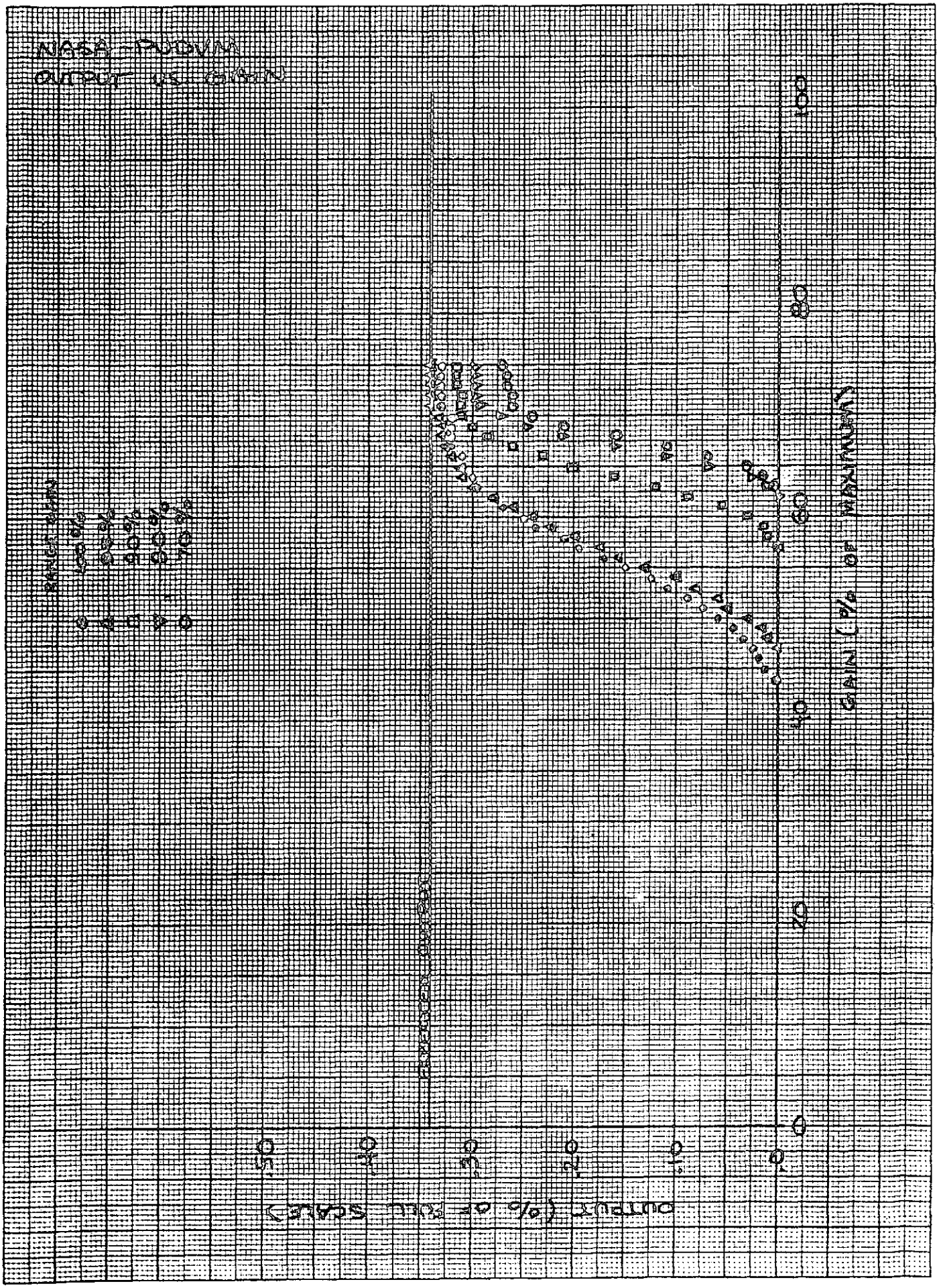

FIGURE 35

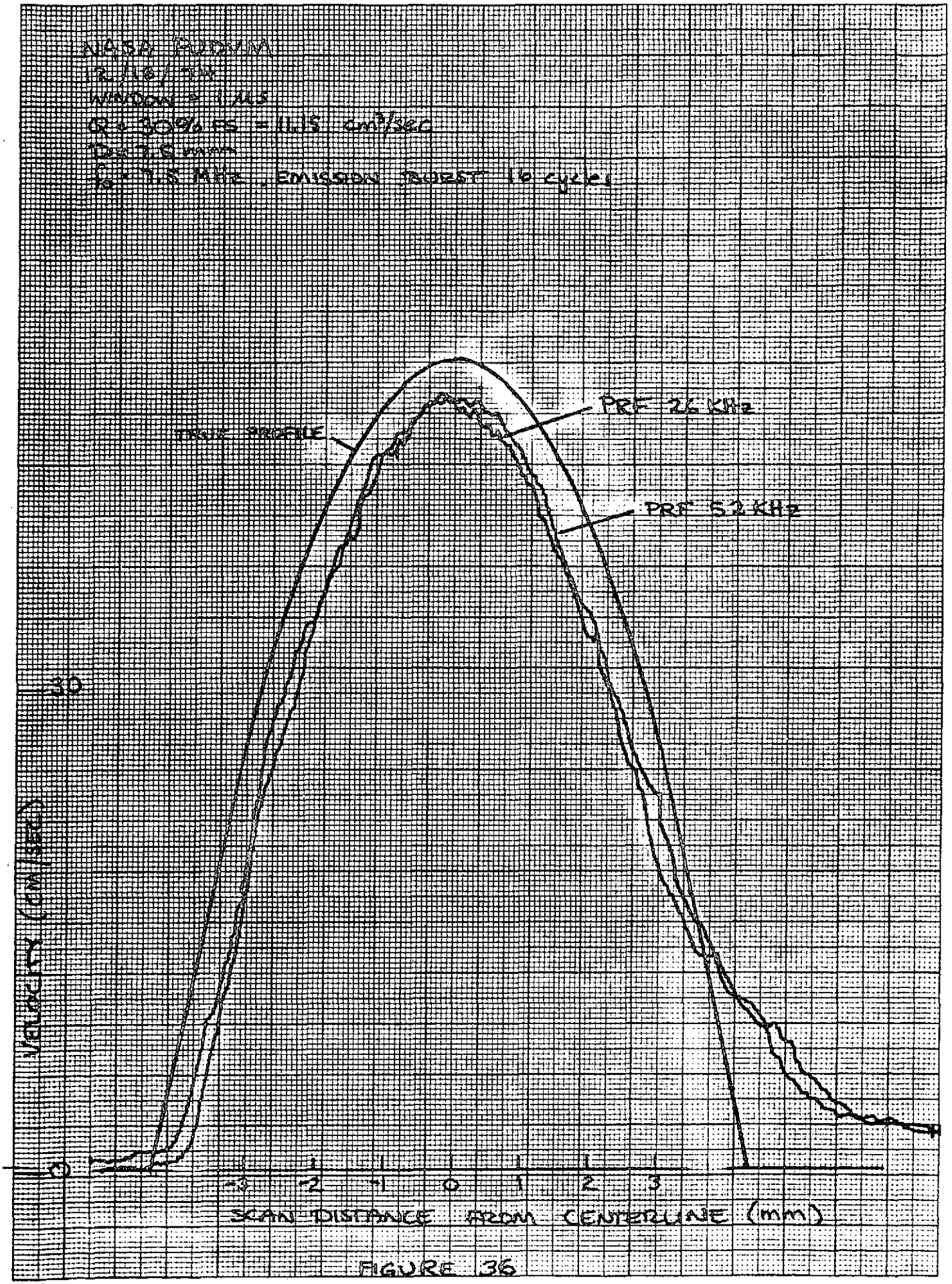

FIGURE 36

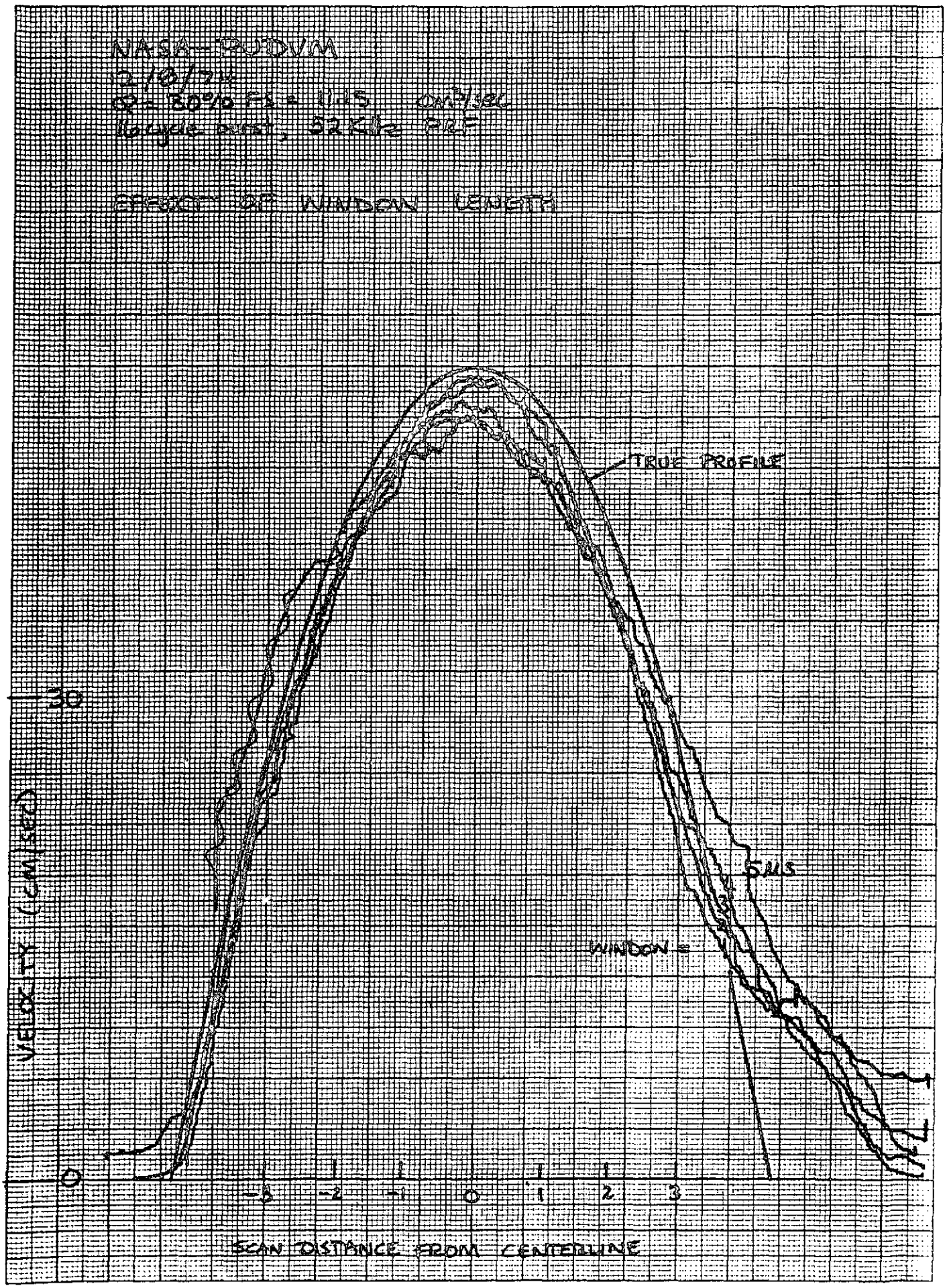

FIGURE 37

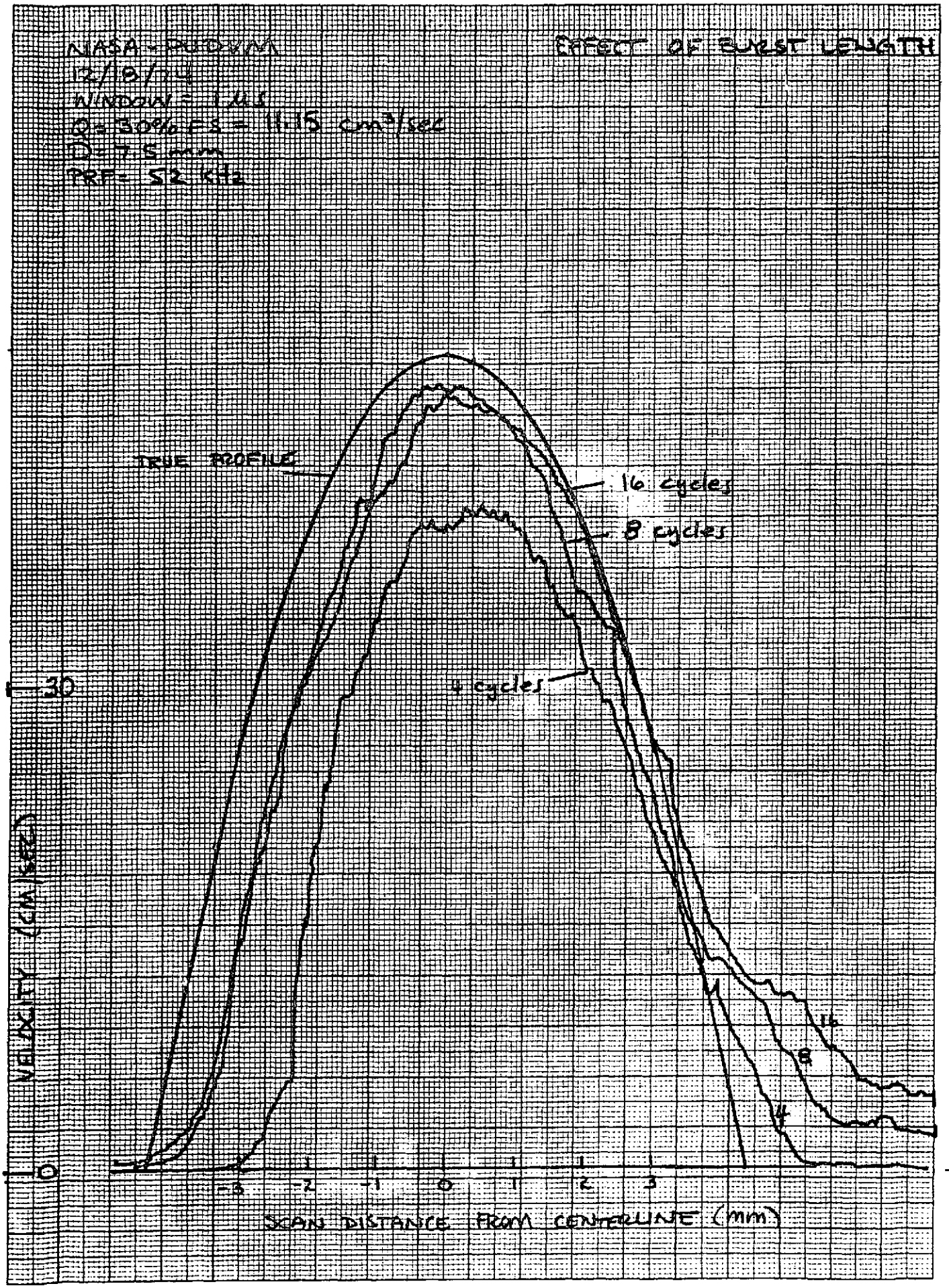

FIGURE 38

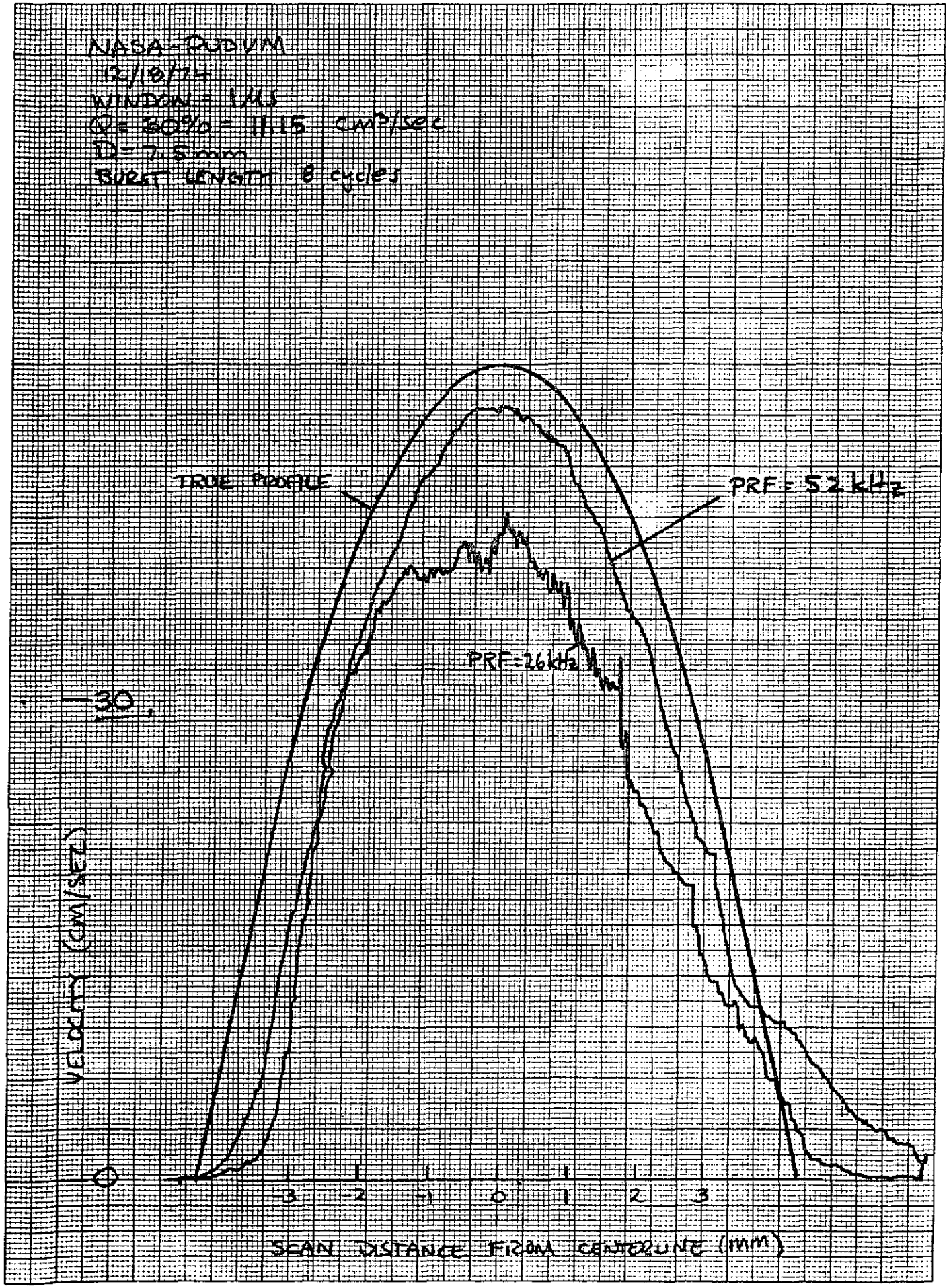

FIGURE 39

X. Standard Test System

A. Objective

The objective of this work was to develop and test a hydraulic flow system that could generate a uniform laminar flow with a linear velocity profile and constant velocity gradient. This system could be used as a standard for evaluating and calibrating pulsed ultrasound flowmeters and transducers. The system was also to be used to determine the characteristics of the sample region. When sampling a linear velocity profile the spectrum of the Doppler audio signal provides a measure of the true spatial distribution of the sample region. In this case, the Doppler frequency is proportional to range and length of the sample region is obtained directly from the band width of the audio spectrum.

B. Design

An almost linear velocity distribtuion can be generated between two concentric cylinders by rotating the outer cylinder at a constant rate and holding the inner cylinder stationary. For this case, the velocity as a function or radius r is given by

$$v(r) = \frac{\omega(1+\frac{h}{r_1})^2}{\frac{h}{r_1}(2+\frac{h}{r_1})} \quad (r - \frac{r_1^2}{r})$$

where r_1 is the radius of the inner cylinder, h the distance between cylinders and ω is the angular velocity of the outer cylinder. Referring to Figure 40; for a transducer location at $r=r_1$ having a beam inclined at an angle α to a radius vector passing through the transducer, the velocity component along the beam at radius r is $V(r)\cos\theta=V_D$ where $\cos\theta=(r_1\sin\alpha)/r$. This is the component of velocity that the PUDVM will sense and the corresponding Doppler frequency is

$$\Delta f = \frac{2foV_D}{C}$$

Radial position r is related to the distance along the beam R and can be determined from the law of cosines. The Doppler velocity then becomes

$$V_D = \frac{\omega r_1 \sin\alpha}{1-\frac{1}{(1+\frac{h}{r_1})^2}} \left[1-\frac{1}{1+(\frac{R}{r_1})^2 + 2(\frac{R}{r_1})\cos\alpha}\right]$$

In order to sense a linear velocity distribution, the Doppler velocity should vary directly as range R. The degree to which V_D approximates a linear function depends on α and the ratio R/r_1. The parameters r_1, h/r_1 and ω only effect the magnitude of V_D. Defining the function $g(\frac{R}{r_1},\alpha)$ as

$$g(\frac{R}{r_1}, \alpha) = \left[1 - \frac{1}{1+(\frac{R}{r_1})^2 + 2(\frac{R}{r_1})\cos\alpha}\right]$$

the normalized velocity distribution as a function of normalized range is given by plotting $g(\frac{R}{r_1}, \alpha)$ vs. R/r_1 for various values of α. This relationship is depicted graphically in Figure 41. Notice that for $\frac{R}{r_1} >$ 0.1 deviations from linearity depend strongly on α. The normalized velocity closely approximates a linear distribution for values of α about 70°. The deviation from linearity can be determined by comparing the actual velocity at any range with the corresponding velocity based on a linear distribution where the linear and true profiles have the same peak velocities. In general, the maximum difference between these two velocities is less than 5% of the peak velocity for $60° < \alpha < 80°$. Hence, to a good approximation, the measured velocity profile will appear linear. The above derivation and conclusions do not account for finite width of the transducer beam and the errors

that may arise. At a given distance from the transducer, a cross section of the beam will sense a band of velocities with an average equal to the value at the center. Although this effect is not expected to introduce significant errors in the velocity estimate, it will cause a frequency spreading in the audio signal. This spreading is minimized for large values of h/r_1 and for samples taken at large R and does not depend strongly on α. For $h/r_1 > .25$ the bandwidth of a sample region of zero length will be less than 5% of the peak Doppler frequency for a transducer with radius $.01\ r_1$.

A schematic of the flow system is shown in Figure 42. The cylinders are made of 1/2" thick aluminum and the outer cylinder is mounted on a turntable which is supported by a thrust bearing. The inner cylinder is stationary and suspended within the outer cylinder by two supports. The turntable is connected to a variable speed dc motor with a rubber belt. A transducer and transducer holder are shown in Figure 43, which also indicates how the transducer is positioned in the flow system. The ultrasound beam lies in a horizontal plane.

C. Results

Only preliminary measurements of velocity profiles and sample volumes have been made using the standard flow system. A detailed summary of the effectiveness of this system for calibrating flowmeters and determining transducer characteristics will be included in the next semiannual report on this project. The working fluid was a water-glycerol solution of viscosity .04 dynes-sec/cm^2 seeded with cellulose particles. The Reynolds number based on the gap width and average velocity in the gap was less than 2000 thereby assuring laminar flow. A velocity profile across part of the gap is shown in Figure 44. The

PUDVM was operated with a burst of 8 cycles (f_o=7.04 MHz) and a gate of 1 μsec. The zero offset on the range axis results from the fact that the ultrasound crystal is recessed about 3 mm from the edge of the inner cylinder. The range is given in mm from the edge of the cylinder. The profile is linear for R < 10 mm but deviates significantly from linear for R > 10 mm. The transducer used for this test had a diameter of about 1.9 mm and the power of the backscattered signal dropped rapidly for R > 10 mm. This could account for the deviation in the profile. Additonal tests will be conducted using blood in the flow system which should give a stronger signal and improved S/N ratio at large R.

To estimate the length of the sample region, the window or receiver gate was positioned within the linear portion of the profile and the frequency spectrum of the audio signal was measured. Since the frequency of the backscattered signal increases linearly with distance from the transducer, the frequency spectrum of the return signal, i.e. the power spectrum of the Doppler signal as a function of frequency, is equivalent to the power of the signal as a function of range. Hence, the plot of the frequency spectrum gives the shape of the sample region along the beam axis. Figure 45 gives frequency spectra of the Doppler signal for various sample gate lengths. Only about 10 db of the audio power spectra are shown. For a gate of 1 μsec the bandwidth of the spectrum is about 725 Hz which corresponds to a sample length of about 3 mm along the beam. As the sample gate is increased from .5 μsec to 4 μsec the bandwidth of the sample region increases from about 700 to 900 Hz. This corresponds to an increase in the length of the sample region of less than .3 mm for each 1 μsec increase in gate time. This estimate of sample length

only includes that portion of the sample region where the power of the Doppler signal is more than about 10% of the peak power of the return signal. The extent to which the effective sample region is broadened by the low power Doppler signals must still be determined.

Additional studies will be made using this linear profile flow system to test the effects of transducer material and backing, gate width, burst length and delay on the length of the sample region.

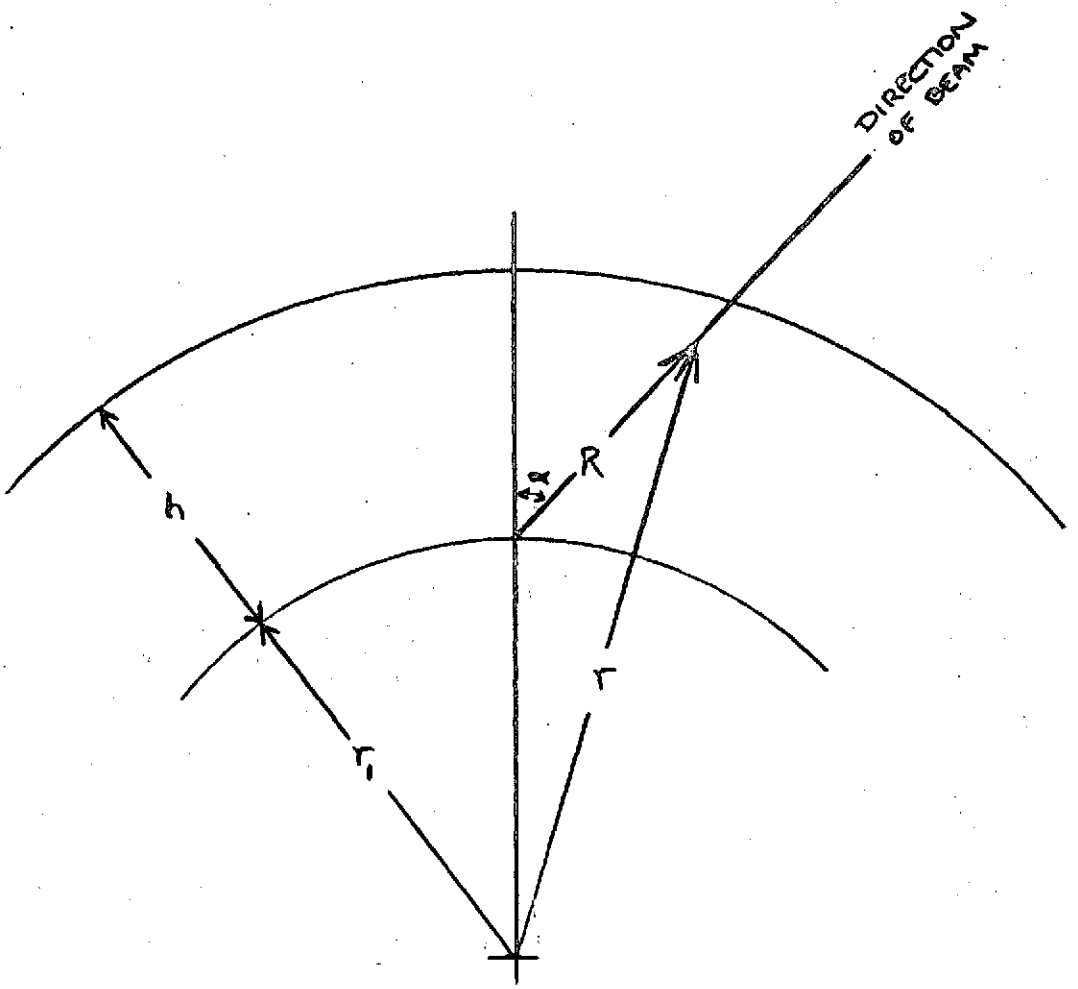

FIGURE 40

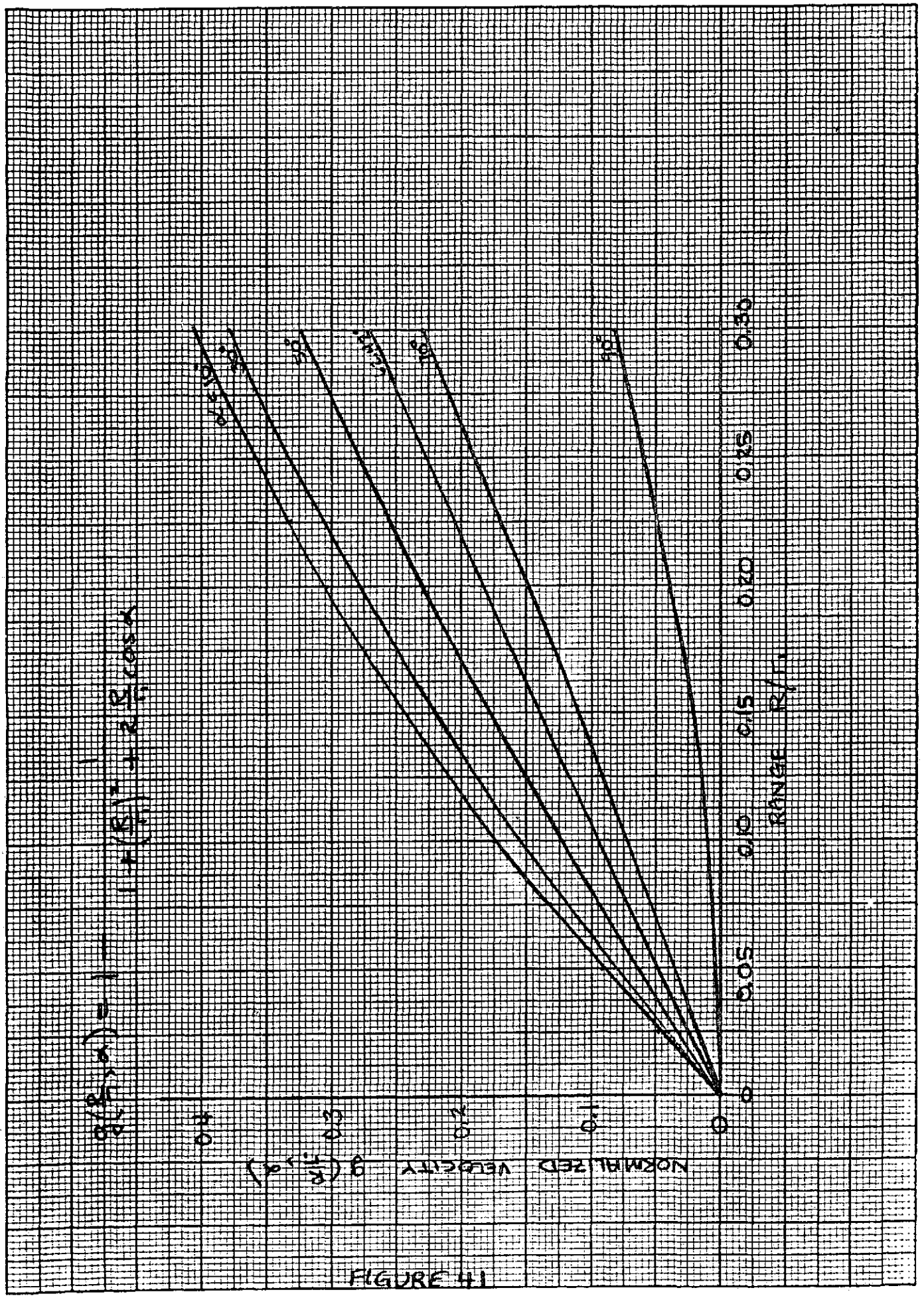

FIGURE 41

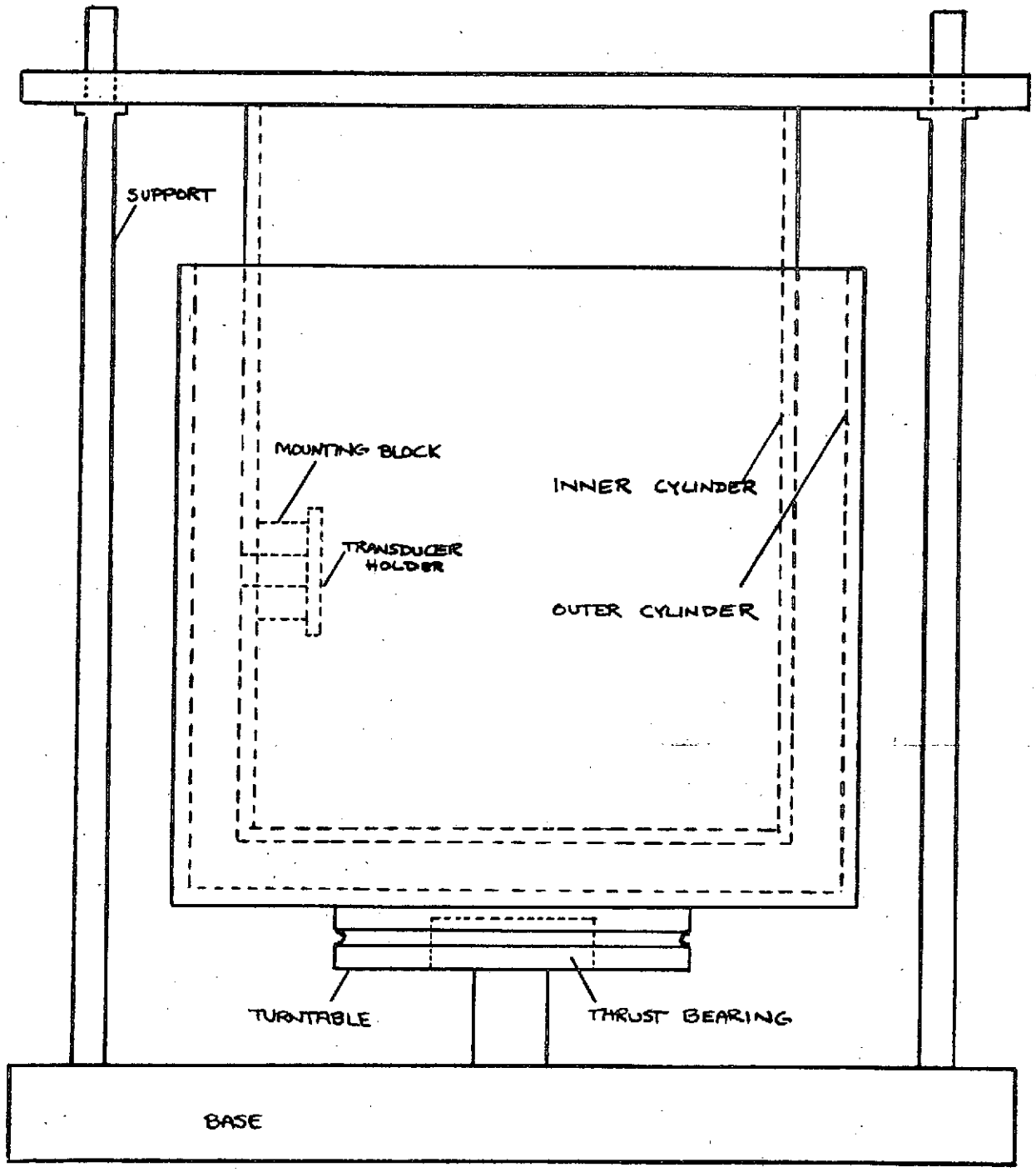
SUPPORT
MOUNTING BLOCK
TRANSDUCER HOLDER
INNER CYLINDER
OUTER CYLINDER
TURNTABLE
THRUST BEARING
BASE

FIGURE 42

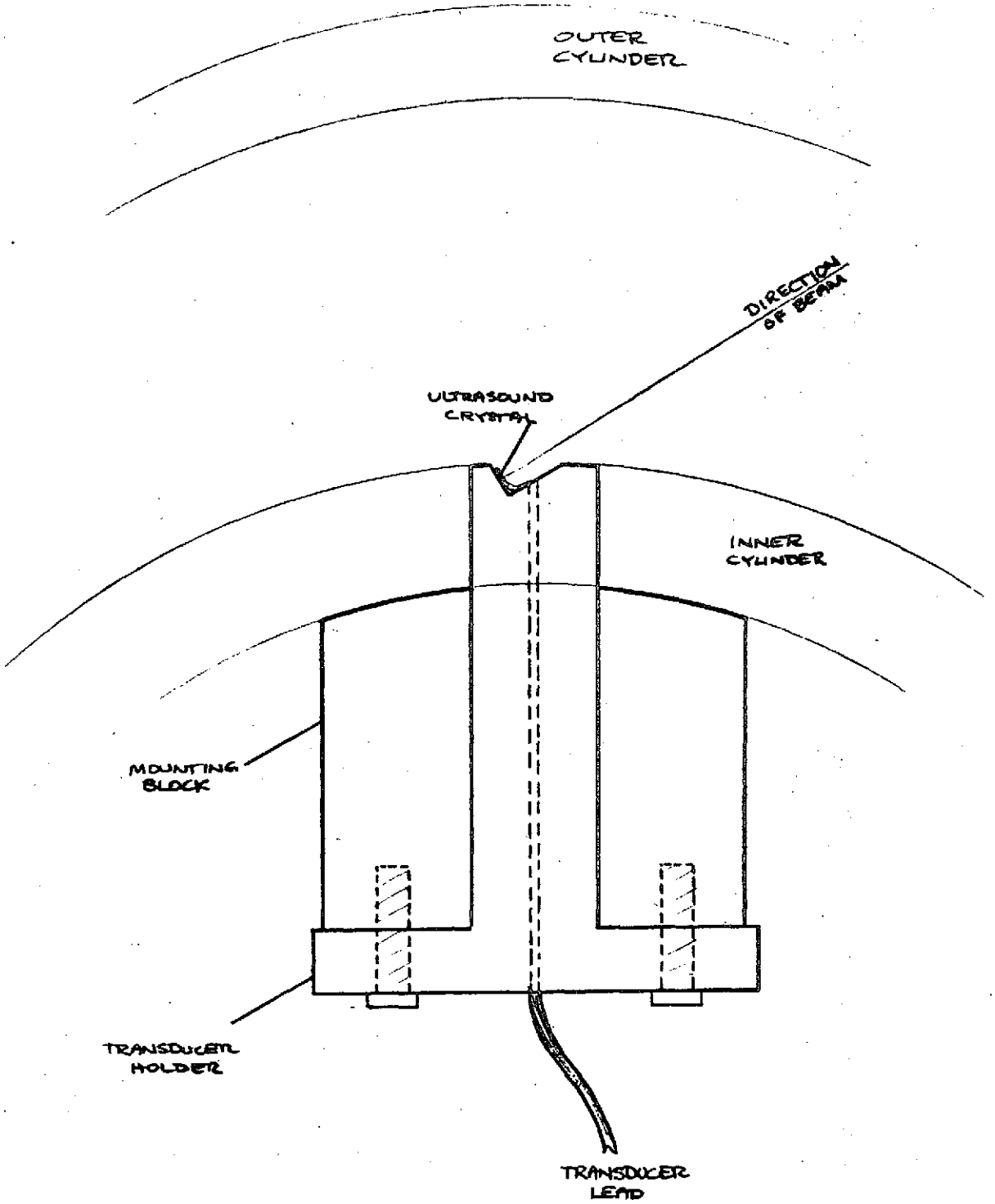
OUTER CYLINDER
DIRECTION OF BEAM
ULTRASOUND CRYSTAL
INNER CYLINDER
MOUNTING BLOCK
TRANSDUCER HOLDER
TRANSDUCER LEAD

FIGURE 43

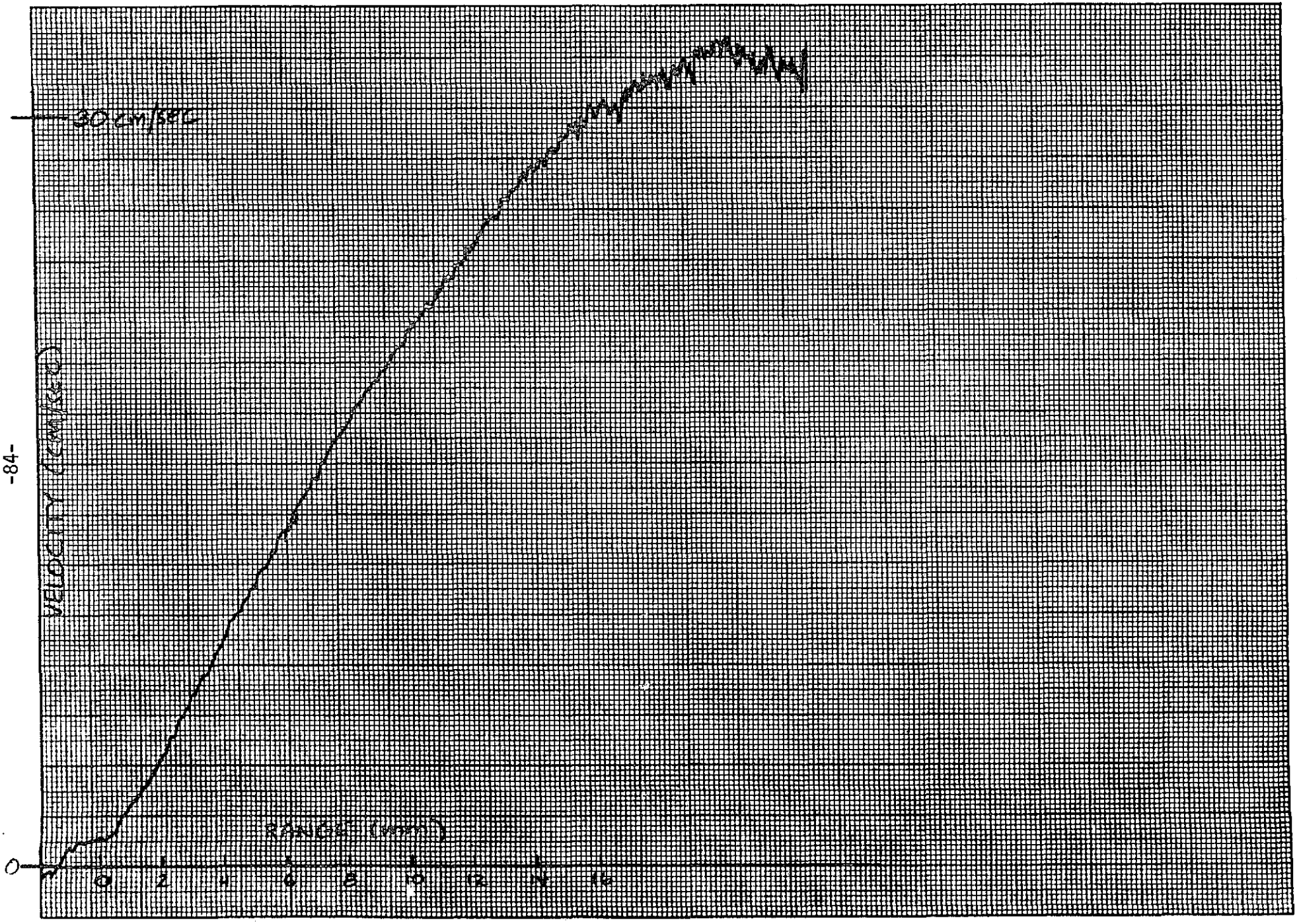

FIGURE 44

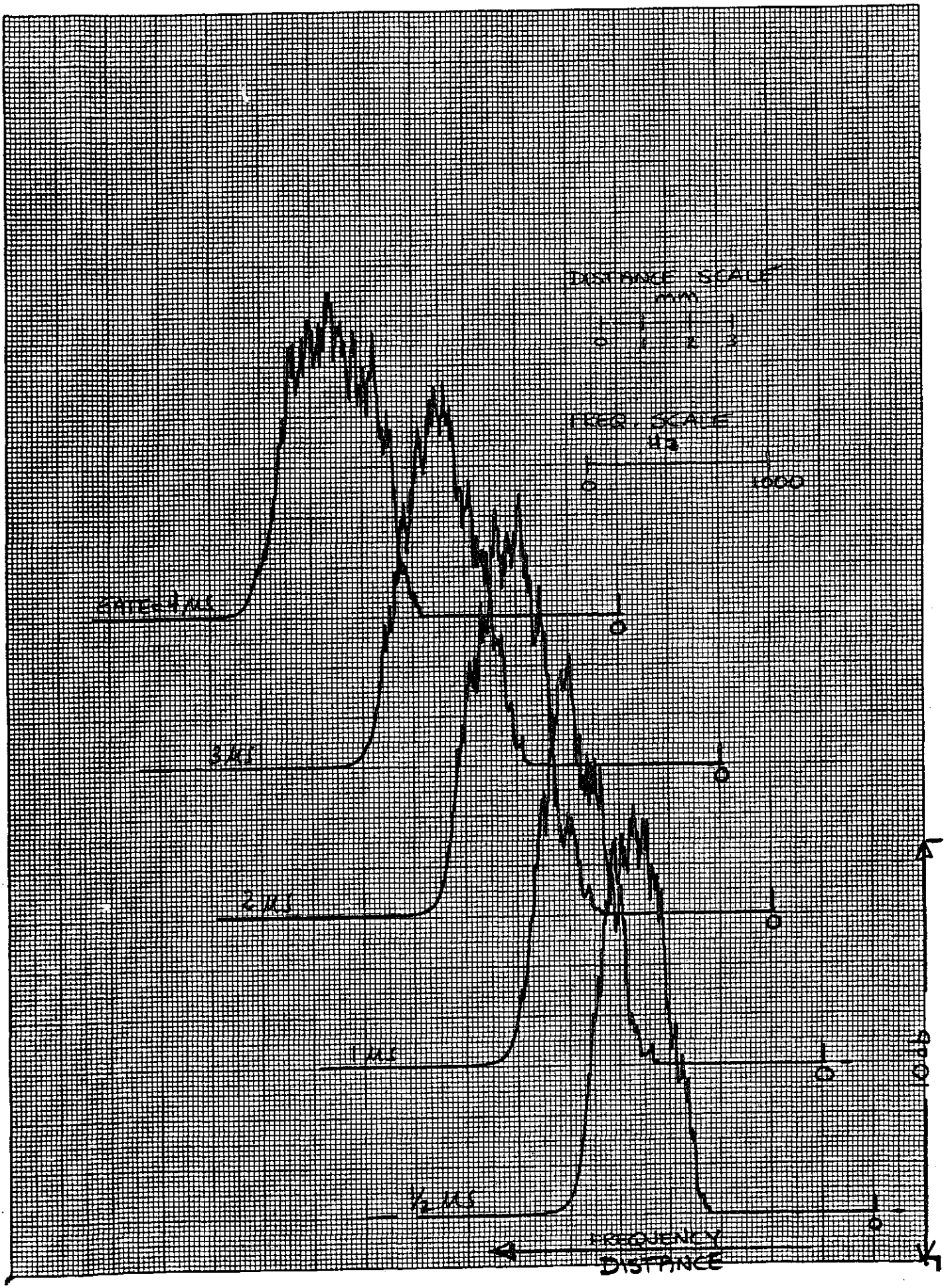

FIGURE 45

BIBLIOGRAPHY

1. Interim Report, "Transcutaneous Measurement of Volume Blood Flows," prepared for NASA-Ames Research Center under NASA Grant NSG-7009, August 1, 1974.

2. Schlichting, H., "Boundary Layer Theory," McGraw-Hill, 1968.

Appendix I

FFT PROGRAM TO ANALYZE ULTRASONIC PULSED DOPPLER AUDIO OUTPUT

The purpose of the program is to perform a frequency analysis on the Doppler shifted audio signal and to thereby provide values indicating the variation of blood velocity with time.

The audio signal is divided into short time intervals and each interval is analyzed using a discrete Fourier transform, the transform is then used to calculate the power spectrum for the interval, i.e. the amount of power in the signal at each frequency. A method is then used to select the frequency "most representative" of the interval and from this frequency a velocity can be caluclated using the relation:

$$V = \frac{c\Delta f}{2fo \cos \alpha}$$

where c represents speed of sound in blood, fo is the ultrasound frequency emitted, α is the angle between the ultrasound source and the direction of blood flow, Δf is the Doppler frequency and V is the velocity. Once the velocity has been obtained for each interval, the time varying velocity can be constructed for a 1 second interval.

Program Structure

Input to the program consists of digital data on tape obtained by digitizing the pulsed Doppler audio signal. At present the analog signal is digitized using a sample rate of 25.6 kHz. This will provide sufficient information to Fourier transform a signal up to 12.8 kHz, much greater than the expected Doppler shift.

The input physical record is 256 words long, each word containing data values in packed format. Thus, each physical record represents 1280 data points.

Program output is a series of microfilm plots of power spectra for each interval analyzed and time varying velocities for each second of time.

Analysis

The audio signal is treated in lengths of one second, and at present is divided into intervals in 1/100th second. The frequency resolution of the Fourier analysis increases with the length of time interval, thus long intervals are desirable. However, with long intervals, time resolution suffers and information about a rapidly varying signal will be lost so that for this consideration short time intervals are preferable. A method is used which attempts to combine these approaches, in the hope of gaining the advantage of both.

The data invervals of 1/100th second are analyzed in pairs, equivalent to a time interval of 1/50th of a second. Subsequent pairs are formed from the last member of the preceding pair and the data interval following it. Thus a frequency resolution of 50 Hz is obtained and the analysis is performed every 1/100th of a second and time resolution is preserved. Each 1/50th of a second interval is transformed using the fast Fourier transform, the square of the transform gives the power at each frequency.

The problem now is to select the frequency considered to best represent the power spectrum. The method used is to calculate an average frequency according to the formula:

$$\bar{f} = \frac{\sum_{i} Pifi}{\sum_{i} Pi}$$

where Pi is the power and fi is the frequency

In order to limit the effect of noise on this computation, it is repeated, using only the portion of the spectrum lying within ± 1.25 kHz. This is in effect a filter or data window.

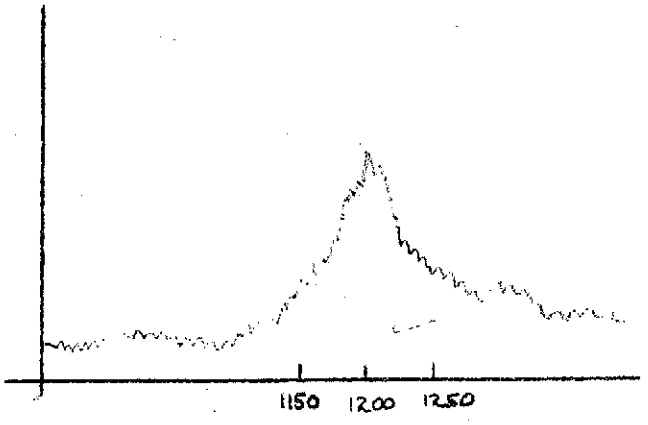

Its effect is to "stretch" the resulting frequencies along the y axis such that peak velocities are high and low velocities near zero.

At present three velocity plots are made using frequency of peak power for each interval, average power and average filtered power.

In addition, there is a printout giving the actual value of the frequency for each interval using these three methods.

APPENDIX II

HEMODYNAMIC PATTERNS IN CORONARY ARTERIES

by

M. K. Wells*
D. C. Winter**
T. C. McCarthy†
A. W. Nelson††

ABSTRACT

A pulsed ultrasound Doppler velocity meter has been used to map the time varying velocity waveforms in the exposed left coronary arteries of anesthetized ponies. Velocity measurements were made without invading the vessels or disturbing the hemodynamic patterns. Typical recordings of velocity waveforms and calculated velocity profiles in the main, descending and circumflex branches are presented. Marked local velocity fluctuations were measured in the major coronary branches and appear to result from longitudinal vibrations of the vessels. In general the coronary flows are characterized by peak Reynolds numbers of 300 to 600 and maximum shear rates of 400 to 600 sec^{-1}.

* Assistant Professor, Department of Mechanical Engineering.
** Graduate Research Assistant, Department of Mechanical Engineering.
† Graduate Research Assistant, Department of Clinical Sciences.
†† Associate Professor, Department of Clinical Sciences.
Colorado State University
Fort Collins, Colorado 80523

HEMODYNAMIC PATTERNS IN CORONARY ARTERIES

INTRODUCTION

The hydrodynamic events of blood flow appear to have a strong influence on the development and distribution of arterial disease. Fry [1]* and Caro et al. [2] have suggested relationships between arterial wall shear stress and the development of atherosclerosis although the exact role of the shearing stress in the disease process (i.e., whether it is a causative or controlling factor in atherogenesis) has not been resolved. The frequent involvement of the left coronary artery and its branches in atherosclerosis necessitates a complete description of the normal hemodynamic patterns in these vessels in order to understand the role of fluid mechanics in atherogenesis. In particular, local blood velocity gradients, especially near the vessel walls, may be most significant in governing the disease process. Indeed, the behavior of the flow near the wall markedly affects the transport of substances across the endothelium and determines the nature of the flow induced mechanical stresses on the vessel wall.

In general, arterial blood flow can be described as nonsteady and laminar although flow disturbances and turbulence might be expected to occur near the entrance to the aorta and in vessels having complex geometry. In addition, blood flow is not necessarily unidirectional. Because of the pulsatile nature of the heart (pump) and the distensibility of the vessels, flow reversal is typically observed in large arteries and may often be accompanied by periods of three dimensional flow. Secondary flows can be generated by centrifugal effects and would be expected in the arch of the

*Numbers in brackets designate References at end of paper.

aorta or near arterial branches. Similarity parameters of interest for studies of arterial hemodynamics are the Reynolds number $Re = UD/\nu$ based on either the peak or the average forward velocity and the Womersley [3] unsteadiness or frequency parameter $\alpha = R(\omega/\nu)^{\frac{1}{2}}$ (U = velocity, $D = 2R$ = vessel diameter, ν = kinematic viscosity and ω = frequency of the flow oscillations). Since the flow is not purely sinusoidal, α represents the ratio of the vessel radius to the thickness of the oscillation boundary layer associated with each harmonic component of the blood flow pulse. Alternatively, taking ω equal to the heart rate or fundamental frequency of the flow oscillations, α^2 can be interpreted as the ratio of the time required for a velocity change to be transported across a vessel by viscous transport to the time of one cardiac cycle. In animals these parameters may vary rapidly and over a wide range depending upon such factors as the physiological condition of the animal or the consequences of surgical preparations. In general, the maximum Reynolds number is less than 10,000 and the unsteadiness parameter less than 25.

Although abundant information is available regarding the fluctuations and distribution of volumetric flows in the cardiovascular system, our understanding of the fluid mechanics of the circulation requires a description of the velocity distribution patterns and local velocity waveforms throughout the arterial system. At present, only two methods have been successfully applied for "point" velocity measurements in the arteries of living animals: hot-film anemometry [4-7] and pulsed ultrasound Doppler techniques [8-10]. To measure blood velocity with an anemometer system a hot-film probe is placed directly into the flow stream either by vessel

puncture or with the aid of a catheter. Velocity profiles are constructed from time varying velocity waveforms obtained at various locations in the lumen cross section as the probe is traversed across a vessel diameter. When the hot-film probe is positioned near the vessel wall, the normal flow pattern in that region is altered and the corresponding velocity waveforms do not represent those of the undistrubed system.

The pulsed ultrasound Doppler velocity meter (PUDVM) provides a less traumatic measurement of blood velocity than a hot-film anemometer since it is possible to monitor velocity waveforms extraluminally or transcutaneously. The PUDVM operates in a radar-like mode which allows measurements to be made at specified ranges within a blood vessel. This differs from continuous wave (CW) ultrasonic velocity detectors which lack range resolution and are used to measure volumetric flow rates. The PUDVM measures the average velocity of blood cells in a small volume within a blood vessel by sensing the change in frequency of ultrasound scattered by the moving particles. Velocity waves from sample volumes located at increments across the vessel lumen are obtained by electronic range gating and velocity profiles at specifid instants of the cardiac cycle can then be constructed. In addition to the fact that this measurement technique is noninvasive in the sense that the blood vessel walls remain intact, it has the additional advantage of not disrupting the normal blood velocity patterns. The pulsed ultrasound flowmeter is suited for measuring velocity distributions in arteries as small as 6 or 7 mm in diameter and has been employed in monitoring blood velocity waveforms in the canine carotid and femoral arteries [10].

METHODS

Pulsed Ultrasound Velocity Meter

The transducers used in this study consist of a small disk of lead titanate zirconate (PZT-5) bonded with epoxy to the inner surface of a polystyrene holder which is fashioned in the form of a half cuff. The circular piezoelectric disk acts as both the emitter and receiver of ultrasound and is mounted such that when the half cuff rests on the surface of a blood vessel the crystal is positioned at an oblique angle to the flow. The cuffs range in size from 3 to 7 mm diameter and contain crystals of 1.5 to 2.5 mm diameter.

The pulsed Doppler velocity detector used in these studies was developed by the NASA Ames Research Center and is based on a design by F. D. McLeod. The directional PUDVM generates pulses of 7-8 MHz ultrasound 4, 8, or 16 cycles in length and at a repetition rate of 13, 26, or 52 kHz. These pulses are used to drive the transducer which directs acoustic waves into the tissue structure and blood vessels. Echoes from these structures and from blood cells are received by the transducer during the interval between pulses. The arrival of the backscattered ultrasound at the transducer is delayed in time by an amount proportional to the distance between the transducer and the scatterer and the frequency of the returning ultrasound is shifted in proportion to the velocity of the blood cells which traverse the ultrasound beam. The velocities of the moving targets are calculated directly from the Doppler formula:

$$V = \frac{\Delta f \; c}{2 \; f_o \; \cos\theta} \qquad (1)$$

where V is the target or particle velocity, Δf the Doppler frequency shift

of the backscattered ultrasound, f_o the frequency of the emitted ultrasound, c the speed of sound in blood or tissue and θ is the angle between the ultrasound beam and the target velocity vector. By time or range gating the return signal, echoes from targets within specific regions of the vessel can be selected for processing. The size of the sample region is determined primarily by the characteristics of the transmitted ultrasound pulse, the transducer radiation pattern, the time over which the return signal is observed and the sensitivity of the signal processor. For the PUDVM and transducers used in these experiments the effective sample region was determined to be about 1 to 1.5 mm in depth while the cross sectional area of the sample region is approximately equal to that of the piezoelectric crystal [11].

The frequency of the backscattered signal received by the transducer during the observation period is compared to the frequency of the original emitted burst in order to determine the Doppler shift or difference frequency Δf. An analog voltage proportional to the Doppler frequency is obtained with the aid of a zero crossing detector and serves as a measure of the average velocity of the scatterers within the sample volume. Processing the signal in this fashion limits the output frequency response of the PUDVM to about 15 Hz, however, the instrument is equally sensitive to velocities in the forward and reverse directions.

Velocity Measurements in Coronary Arteries

A pulsed Doppler velocity meter was used to monitor blood velocity waveforms in the left coronary arteries of 12 ponies of unknown age and history. The ponies ranged in weight from about 125 to 250 kg. Anesthesia

was induced and maintained by an intravenous administration of barbituate and positive pressure ventilation was provided throughout the procedure. The animals were placed in right lateral recumbancy and the chest was entered through a routine left fourth intercostal thoracotomy incision. The lungs were retracted from the operating field and the pericardium opened with a T-shaped incision. The epicardial fat pad was opened immediately over the major branches of the left coronary artery which lie in the coronary groove on the surface of the heart. The main branch of the left coronary artery is short and divides within a few millimeters of its origin at the root of the aorta into an anterior descending branch (LAD) and a circumflex branch. At the bifurcation the LAD branch generally proceeds in a straight line from the main branch whereas the circumflex branch joins at an angle of about 90 degrees. Segments of the left common coronary artery, circumflex branch and descending branch were isolated from the surrounding tissue over lengths of 1 to 2 cm to allow for positioning of the flow transducers. Measurement sites were located on the main, circumflex and descending branches immediately adjacent to their common junction and on the descending branch 2 to 5 cm below the coronary bifurcation. A half cuff was placed on the vessel at the chosen site and secured to the vessel with a strip of umbilical tape 5 mm in width. Care was taken not to distort or partially occlude the vessel in order that the normal hemodynamic patterns would be maintained. Acoustic coupling between the ultrasound transducer and the blood vessel was provided by Aquasonic gel or a small blood clot placed between the piezoelectric crystal and the vessel wall. Time varying velocity waveforms were measured at increments of .5 to .75 mm along

the path of the ultrasound beam between the near and far walls of the vessel. The beam was inclined at an angle of 45 to 60 degrees to the longitudinal axis of the artery and the direction of the velocity vector was assumed to be parallel to this axis. Eight to twelve sequential velocity waveforms were obtained at each range location and a single scan across the vessel would require from 2 to 4 minutes to complete. Velocity data and an electrocardiogram were recorded on a strip chart and on magnetic tape for subsequent computer processing and analysis.

RESULTS

Figure 1 is a computer plot of one cycle of an average centerline velocity waveform obtained in the LAD branch and illustrates the general characteristics of a coronary flow or velocity pulse. The beginning of the cycle coincides with the R-wave of the electrocardiogram which signifies the onset of ventricular contraction. During the first part of the cardiac cycle (systole) intramuscular pressure in the contracting left ventricular wall increases and causes the peripheral coronary arteries, capillaries and veins to close leading to a marked decrease or transient cessation of left coronary artery flow. As the heart muscle relaxes and the hydraulic impedance of the coronary circuit decreases the blood velocity increases rapidly and the maximum flow generally occurs during the latter portion of the heart cycle (diastole). This behavior is evident in the record of Figure 1 which shows the LAD velocity decreasing during systole from an initial value of 115 cm/sec to about 20 cm/sec and then rising again to about 120 cm/sec during diastole. Based on a vessel diameter at peak forward flow of 5 mm the maximum Reynolds number for this example is 1500 and

the Womersley unsteadiness parameter for the heart frequency is about 3.5.

Velocity and flow oscillations in the frequency range of 5 to 10 Hz are often measured during systole and early diastole. It appears that the ventricular contractions generate stress waves that propagate through the heart muscle (myocardium) and cause the coronary arteries to vibrate. These waves are readily observable as they travel across the surface of the heart and their intensities can vary markedly. The presence of this type of wave is seen on the velocity record in Figure 1 and appears to induce an oscillation at about 7 Hz on the mean coronary velocity during late systole. The low amplitude high frequency fluctuations seen on this velocity record (particularly evident during late diastole) are due to statistical variations in the output of the zero crossing detector which is used to convert the Doppler frequency shift to an analog voltage. The fluctuations do not represent flow disturbances or turbulance.

Estimates of the time varying velocity profiles in this same vessel are constructed using the average velocity waveform for each range location and are shown in Figure 2. Profiles are calculated at 18 equally spaced time intervals during the heart cycle and are plotted sequentially with a 10 cm/sec offset between each profile for the sake of clarity. Figure 2 (a) begins at the bottom with the profile for t=o and ends at the top with the profile in the cycle having the greatest average forward velocity. Remaining profiles are given sequentially in Figure 2 (b) beginning with the uppermost curve. The last profile of the heart cycle is at the bottom of Figure 2 (b). In the profile calculations account is made for the transducer orientation and the profiles are plotted as a function of distance

C - 2

from the transducer along a line normal to the vessel axis. The diameter of the flow stream can be estimated from the width of a velocity profile, however, significant errors may be introduced since the profiles are distorted near the walls due to the finite sample volume of the PUDVM. In order to compare relative vessel size among the animals studied, vessel diameters were estimated from the peak forward velocity profile. The distance between the intersections with the zero velocity axis of the lines tangent to the profile at the points of maximum positive and negative slope was taken as the approximate vessel diameter. For the data shown in Figure 2 the lumen diameter calculated on this basis was 5.0 mm while a direct measurement of the vessel yielded a value of about 4 mm. The profiles are relatively symmetric and well developed and resemble profiles for laminar oscillatory flow [3,12]. The profiles are drawn with straight line segments connecting the velocity values at adjacent range locations and sharp dips or peaks in the curves can result from slight variations in heart rate, cardiac output or respiration during the time required to complete the vessel scan.

Figures 3 through 8 illustrate representative velocity waveforms and profiles from the main, descending and circumflex branches of the left coronary artery of a single pony. These data were obtained over a period of about 30 minutes and during this time the pony's heart rate increased from 60 beats/min to about 71 beats/min. Velocity waveforms in the main branch at 7 equal spaced locations from the center of the vessel to the far wall are shown in Figure 3. Again notice the decrease in mean velocity during systole followed by a sustained forward velocity during diastole. In this example an oscillation of 6 Hz is seen superimposed on the velocity

waveforms throughout the heart cycle and is particularly pronounced during systole. Velocity profiles corresponding to these waveforms are given in Figure 4. Successive profiles are off-set vertically by a distance equivalent to a velocity increment of 2 cm/sec. From these records it appears that the time varying velocity measured during systole at a distance of 3.1 mm is slightly elevated compared to the velocities at neighboring range locations. Most probably, this artifact results from a momentary change in cardiac output or arterial pressure or it may be associated with the induced vibration of the vessel.

Velocity patterns from the near wall to the center of the descending branch are shown in Figure 5. Generally, the waves are similar in shape to waves in the main branch although the average velocities are somewhat higher in the LAD because of its smaller diameter. Vessel diameters estimated from the profiles were 6.4 mm for the main branch and 5.9 mm for the descending branch. Profiles for the LAD are plotted in Figure 6.

The characteristic form of velocity waves in the circumflex branch is markedly different from that in the main and LAD branches. Figure 7 illustrates the average velocity waveforms obtained in a scan of the circumflex branch from the near wall to the center of the vessel. Velocity fluctuations resulting from the vibratory motion of the vessel are again present during systole, however, their magnitudes are less than half of the corresponding variations recorded from the main or LAD branch. Furthermore these oscillations do not appear on the velocity waveforms during diastole. With the exception of a transient cessation of the flow at about t=500 msec, the mean forward velocity is about the same in systole

and diastole which is also in contrast to the behavior noted for the other two branches. Velocity profiles for the circumflex branch were constructed from the measured waveforms and are shown plotted in Figure 8. The vessel diameter for this example was estimated from the peak forward profile to be 4.2 mm and was directly measured post-mortem as about 2 mm. Since the length of the PUDVM sample volume is not small compared to the diameter of this circumflex branch, the computed profiles may differ appreciably from the true velocity distributions.

DISCUSSION

The blood velocity waveforms and profiles described above are representative of the results obtained over the entire course of this study. Except for the low frequency systolic fluctuations, the general characteristics of the centerline velocities measured with the PUDVM are similar to phasic flow waves recorded in the coronary arteries of dogs using electromagnetic or continuous wave Doppler flowmeters [13-16]. Reynolds numbers based on the peak centerline velocity normally ranged from about 300 to 600 in the major branches of the left coronary circuit although one flow was observed for which the peak Reynolds number reached 1500 (cf. Fig. 1). The unsteadiness parameter for the heart frequency was usually less than 4 which indicates that profiles corresponding to the mean phasic velocities should be described by well developed boundary layer flows. On the other hand, rapidly fluctuating local flows arising from the longitudinal vibrations of the coronary branches were characterized by α values of 5 to 10 or more and relatively flat velocity profiles would be expected for these

flows. The calculated profiles illustrated above appear to support these predictions. In general, the time varying profiles throughout systole suggest that a plug-like flow occurs during the period of most intense velocity oscillations whereas more fully developed profiles appear later in the flow cycle.

Velocity disturbances which would be indicative of transition or turbulent flow cannot be detected on the velocity records because of the limited frequency response of the PUDVM. Nerem and Seed [17] measured velocities with a hot film anemometer in the ascending aorta of dogs and found that flow disturbances generally occurred for values of $\alpha>6$ whenever the peak Reynolds number exceeded about 150α. Even though the time histories of the coronary and aortic flow pulse are markedly dissimilar only entrance flow exists in either circuit. Furthermore, disturbances created during the ejection of blood from the left ventricle could, under the proper conditions, be transported into the coronary vessels as well as into the aorta. Comparing Nerem's criteria for the existence of flow disturbances with the Reynolds numbers and frequency parameters corresponding to the coronary flows described here leads to the conclusion that velocity disturbances most probably would not be found in the major branches of the left coronary artery.

The most critical question regarding pulsed Doppler velocity measurements is instrument resolution. Since the PUDVM estimates velocity within a finite sample region it is clear that the size of the sample region relative to the vessel dimensions ultimately determines the resolution and accuracy of the measurements. A velocity profile obtained with the PUDVM

is described analytically by a convolution of the sample region with the actual velocity distribution [18]. The measured profile is broadened and flattened by this convolution process and may also be distorted as a result of signal attenuation. In addition, since the PUDVM does not detect zero velocity, the effective size of the sample region changes as it is scanned across a vessel wall thereby introducing an additional boundary error in the velocity estimate. In vessels which are sufficiently large compared to the sample function the measured velocity profile may closely approximate the true distribution. The NASA-PUDVM was used to estimate the velocity profile for fully developed Poiseuille flow (Re = 1500) in a dialysis tube 7.2 cm in diameter. Figure 9 compares the measured and predicted profiles and indicates a slight broadening of the measured profile at the far wall. The ultrasound beam passed through the center of the tube and was inclined at an angle of 60 degrees to the flow axis. The scan diameter estimated from the measured profile is in error by about 10%. The convolution and boundary errors severely limit the accuracy of profiles measured with the PUDVM in vessels with diameters less than about one-fourth the length of the sample function [19]. For the PUDVM used in these studies, calculated velocity profiles are expected to differ significantly in shape from the true profiles in vessels less than 4 to 6 mm in diameter.

Although the PUDVM profiles may be distorted, it is possible to properly account for the boundary error and compute the true time varying velocity gradients at the wall. This calculation requires that one know <u>a priori</u> the actual location of the wall on the estimated profile and this can be obtained, for example, with an ultrasonic pulse-echo imaging system.

Although the correction factor does depend upon the shape of the sample region and the true gradients, the measured profiles, in general, underestimate the velocity gradient at the wall by about one-half. From the coronary profiles obtained in ponies the calculated maximum shear rates were typically 400 to 600^{-1}. In one instance (Fig. 2) the peak shear rate reached about 3000 sec^{-1}. The corresponding wall shear stresses are well below the acute yield stress for endothelial cells of about 380 dynes/cm^2 suggested by Fry [1].

Perhaps the most interesting features of the coronary velocity patterns reported here are the marked fluctuations which regularly occur during systole. Measurements of coronary blood flow in dogs and man using electromagnetic or CW Doppler flowmeters [13-16,20] do not indicate the presence of similar oscillations. Furthermore, the horse is not usually used for studies of cardiovascular mechanics and there is no information in the literature pertaining to either normal or abnormal coronary hemodynamic patterns in this species. As suggested above, these 5 to 10 Hz velocity fluctuations appear to be generated as the artery vibrates along its axis. The velocity signal then represents the superposition of the mean coronary velocity with a locally induced velocity component associated with the motion of the vessel. Relative to the transducer which is fixed to the vessel, the induced flow has the characteristics of a piston-driven oscillating flow in a rigid pipe where the relative velocity at the wall is zero and the maximum velocity fluctuations occur in the center of the vessel. This behavior is readily apparent from the measured velocity waveforms in Figures 3, 5, and 7. Momentarily occluding the vessel

immediately adjacent to the transducer eliminated the induced velocity (and the mean velocity also) as would be expected. In this case, the vessel and blood must execute essentially the same motion in response to the forced oscillation and no relative velocities develop. This situation would be similar to a vibrating fluid-filled tube which is closed at both ends. Other possible explanations for the genesis of these fluctuations such as relative motion between the cuff and the vessel or twisting of the flow cuff and vessel cannot be substantiated from the velocity records or by direct visual observation. One might speculate that the occurrence of these low frequency systolic vibrations is a species dependent phenomena. It could be argued that in the dog, for example, analogous stress waves, if generated, would be less intense and occur at a higher frequency compared to the horse because of the dog's higher heart rate and lower cardiac output. Furthermore, high frequency vibrations would be more rapidly damped and perhaps not easily detected. Preliminary measurements obtained in our laboratory of coronary velocity waves in a conscious intact horse also indicate the presence of local flow fluctuations in the range of 5 to 10 Hz.

CONCLUSION

These results represent a first step toward quantifying the normal hemodynamic patterns in coronary arteries. In the equine species, the measured velocity waveforms are accented by low frequency fluctuations apparently arising from the motion of the myocardial surface. The amplitude of the induced velocity variation appears to depend upon the orientation of the vessel on the heart and may also vary during the cardiac cycle.

The significance of these oscillations relative to the development of coronary artery disease or to the perfusion of the myocardium cannot be evaluated on the basis of these initial observations. It is clear, however, that these unexpected local velocity patterns will greatly influence the stability of the flow and the development of secondary and separated flows and will have an important bearing on the consequences of cyclic hydrodynamic forces.

ACKNOWLEDGEMENT

This work was supported by NSF grant GK41009. We acknowledge the efforts of Dr. R. E. Daigle in developing the computer data reduction program used in these studies and thank Dr. J. F. Fessler, Visiting Professor at Colorado State University and Professor of Large Animal Clinics at Purdue University for his assistance in carrying out the experiments.

REFERENCES

1. Fry, D. L., "Acute Vascular Endothelial Changes Associated with Increased Blood Velocity Gradients," Circulation Research, Vol. 22, 1968, p. 165.

2. Caro, C. G., Fitz-Gerald, J. M., and Schroter, R. C., "Atheroma and Arterial Wall Shear: Observation, Correlation and Proposal of a Shear Dependent Mass Transfer Mechanism for Atherogenesis," Proceedings of the Royal Society of London (B), Vol. 177, 1971, p. 109.

3. Womersley, J. R., "An Elastic Tube Theory of Pulse Transmission and Oscillatory Flow in Mammalian Arteries," Wright Air Development Center, Technical Report TR 56-614, 1957.

4. Ling, S. C., Atabek, H. G., Fry, D. L., Patel, D. J. and Janicki, J. S., "Application of Heated-Film Velocity and Shear Probes to Hemodynamic Studies," Circulation Research, Vol. 23, 1968, p. 789.

5. Seed, W. A., and Wood, N. B., "Development and Evaluation of a Hot-Film Velocity Probe for Cardiovascular Studies," Cardiovascular Research, Vol. 4, 1970, p. 253.

6. Nerem, R. M., Seed, W. A., and Wood, N. B., "An Experimental Study of the Velocity Distribution and Transition to Turbulence in the Aorta," Journal of Fluid Mechanics, Vol. 52, Part 1, 1972, p. 137.

7. Clark, C., and Shultz, D. L., "Velocity Distribution in Aortic Flow," Cardiovascular Research, Vol. 7, 1973, p. 601.

8. Baker, D. W., "Pulsed Ultrasonic Doppler Blood-Flow Sensing," IEEE Transactions on Sonics and Ultrasonics, Vol. SU-17, 1970, p. 170.

9. Peronneau, P., Hinglais, J., Pellet, M., and Léger, F., "Vélocimètre Sanguin par Effet Doppler à Emission Ultrasonore Pulsee," L'Onde Electrique, Vol. 50, 1970, p. 369.

10. Histand, M. B., Miller, C. W., and McLeod, F. D., "Transcutaneous Measurement of Blood Velocity Profiles and Flow," Cardiovascular Research, Vol. 7, 1973, p. 703.

11. Morris, R. L., Histand, M. B., and Miller, C. W., "The Resolution of the Ultrasound Pulsed Doppler for Blood Velocity Measurements," Journal of Biomechanics, Vol. 6, 1973, p. 701.

12. Schlichting, H., Boundary Layer Theory, McGraw-Hill, New York, 1968.

13. Khouri, E. M., Gregg, D. E., and Lowensohn, H. S., "Flow in the Major Branches of the Left Coronary Artery During Experimental Coronary Insufficiency in the Unanesthetized Dog," Circulation Research, Vol. 23, 1968, p. 99.

14. Hepps, S. A., Roe, B. B., and Rutkin, B. B., "Coronary Blood Flow in the Intact Conscious Dog: Studies with Miniature Electromagnetic Flow Transducers," Journal of Thoracic Cardiovascular Surgery, Vol. 46, 1963, p. 783.

15. Elliot, E. C., Khouri, E. M., Snow, J. A., and Gregg, D. E., "Direct Measurement of Coronary Collateral Blood Flow in Conscious Dogs by an Electromagnetic Flowmeter," Circulation Research, Vol. 34, 1974, p. 374.

16. Vatner, S. F., Franklin, D., Van Citters, L., and Braunwald, E., "Effects of Carotid Sinus Nerve Stimulation on the Coronary Circulation of the Conscious Dog," Circulation Research, Vol. 27, 1970, p. 11.

17. Nerem, R. M. and Seed, W. A., "An In Vivo Study of Aortic Flow Disturbances," Cardiovascular Research, Vol. 6, 1972, p. 1.

18. Jorgensen, J. E., and Garbini, J. L., "An Analytical Procedure of Calibration for the Pulsed Ultrasonic Doppler Flow Meter," Journal of Fluids Engineering, Transactions of the ASME, Vol. 96, Series 1, No. 2, 1974, p. 158.

19. Daigle, R. E., McLeod, F. D., Miller, C. W., Histand, M. B., and Wells, M. K., "Transcutaneous Measurement of Volume Blood Flow," Progress Report on NASA Grant NSG-7009 prepared for the NASA-Ames Research Center, 1974.

20. Benchemol, A., Stegall, H. F., and Gartlan, J. L., "New Method to Measure Phasic Coronary Blood Velocity in Man," American Heart Journal, Vol. 81, No. 1, 1971, p. 93.

CAPTIONS

Figure 1. Computer plot of one cycle of the average centerline velocity waveform measured in the descending branch of the left coronary artery of a pony. The beginning of the cycle coincides with the R-wave of the electrocardiogram.

Figure 2. Calculated time varying velocity profiles in the horse LAD coronary artery for 18 equally spaced time intervals during an average heart cycle. (a) The profile for t=0 sec is at the bottom and subsequent profiles are plotted sequentially with a 10 cm/sec offset. The profile in the cycle having the maximum average forward velocity is at the top. (b) Remaining profiles beginning with the uppermost curve. The final profile of the heart cycle is at the bottom.

Figure 3. Velocity waveforms measured in the main branch of the coronary artery from the center of the vessel to the far wall. Near wall to centerline velocities were also mapped. Note the marked 6 Hz fluctuations during the first half of the cycle which may be caused by vibrations of the artery.

Figure 4. Velocity profiles in the main branch constructed from the waveforms given in Figure 3. Profiles are offset by 2 cm/sec for clarity. (a) Profiles from t=0 to the time of peak forward flow. (b) Subsequent profiles from peak forward flow to the end of the heart cycle.

Figure 5. Velocity patterns across the near half of the descending branch of the coronary artery. Corresponding velocity profiles are shown in Figure 6.

Figure 6. (a) and (b). Estimated velocity profiles in the descending branch. The profiles during the early part of the cycle appear flattened compared to the later profiles which are more fully developed.

Figure 7. Average velocity waveforms in the circumflex branch. The centerline velocity oscillations during systole are only about half the magnitude of the corresponding variations measured in the main and descending branches.

Figure 8. (a) and (b). Velocity profiles for the circumflex branch. Due to the limited resolution of the PUDVM profiles calculated in small vessels will be distorted especially near the walls and in regions with high velocity gradients.

Figure 9. Velocity profile measured with the PUDVM compared to the predicted profile for Poiseuille flow in a 7.2 mm diameter tube. The ultrasound beam was inclined at 60 deg to the tube axis.

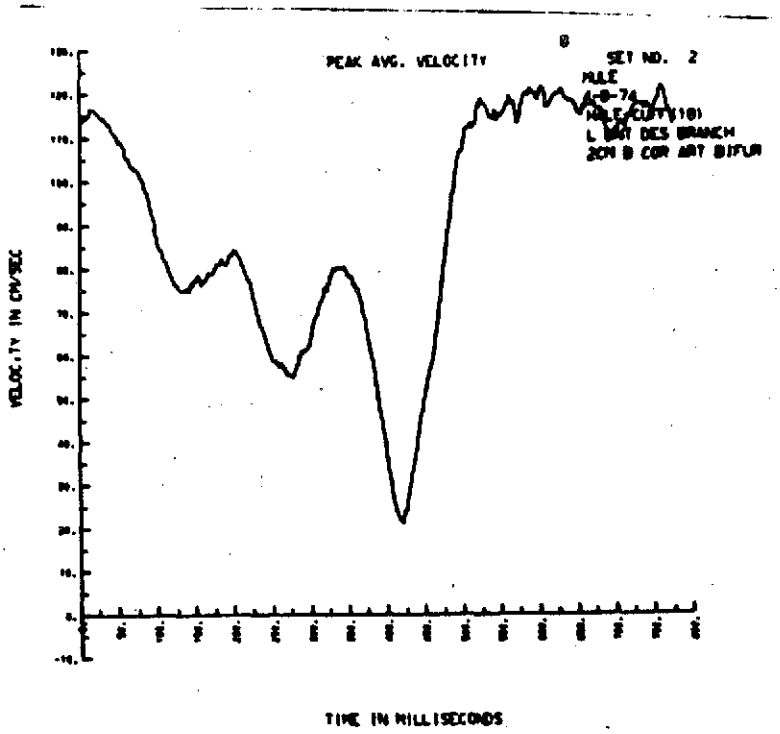

Figure 1.

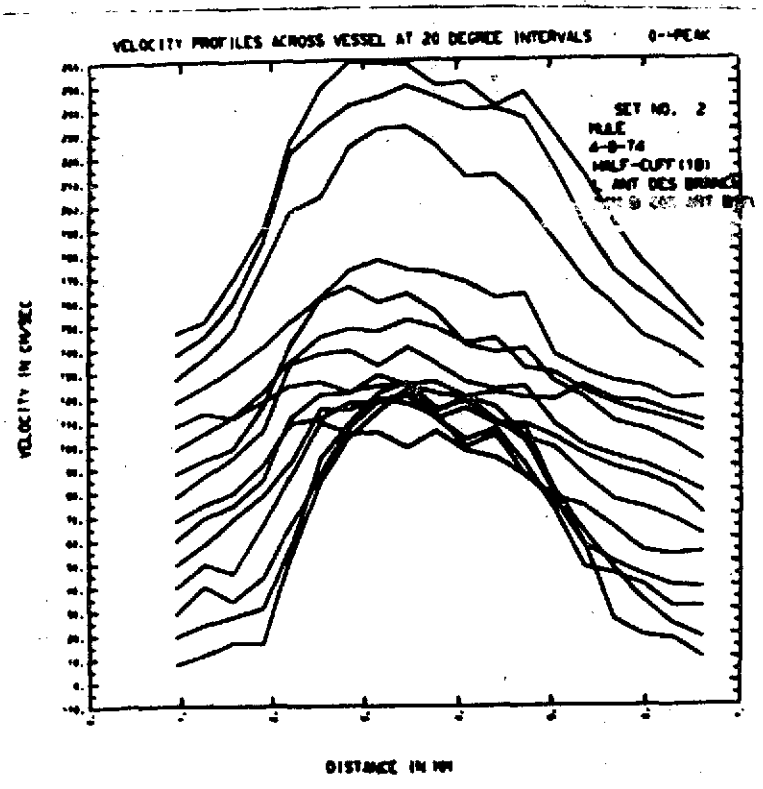

(a)

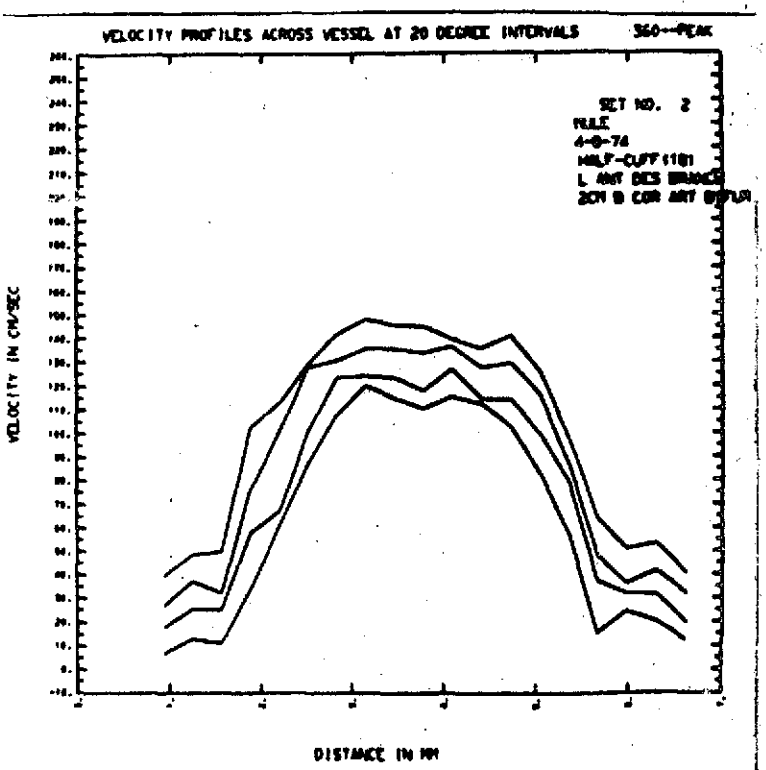

(b)

Figure 2.

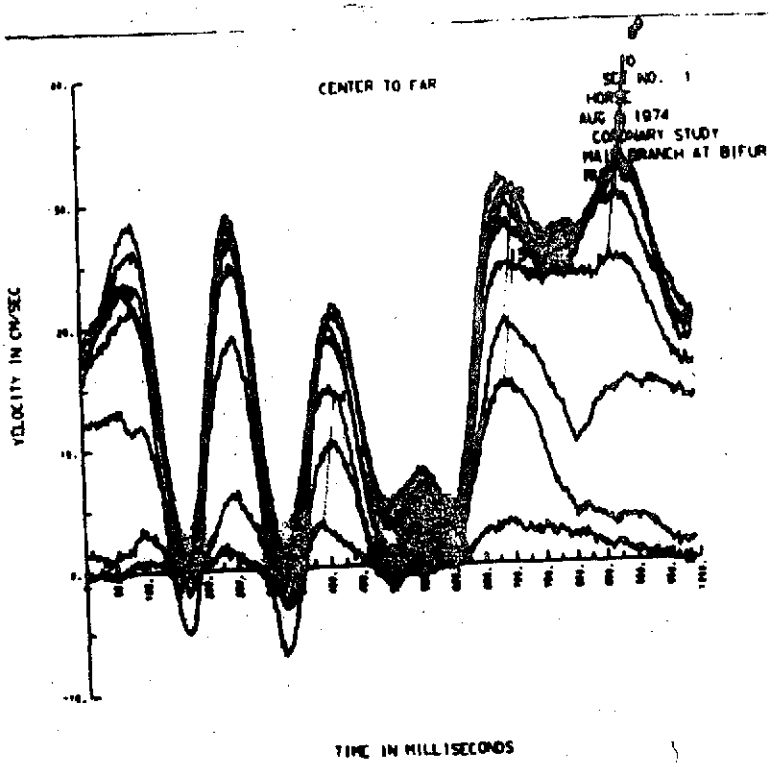

Figure 3.

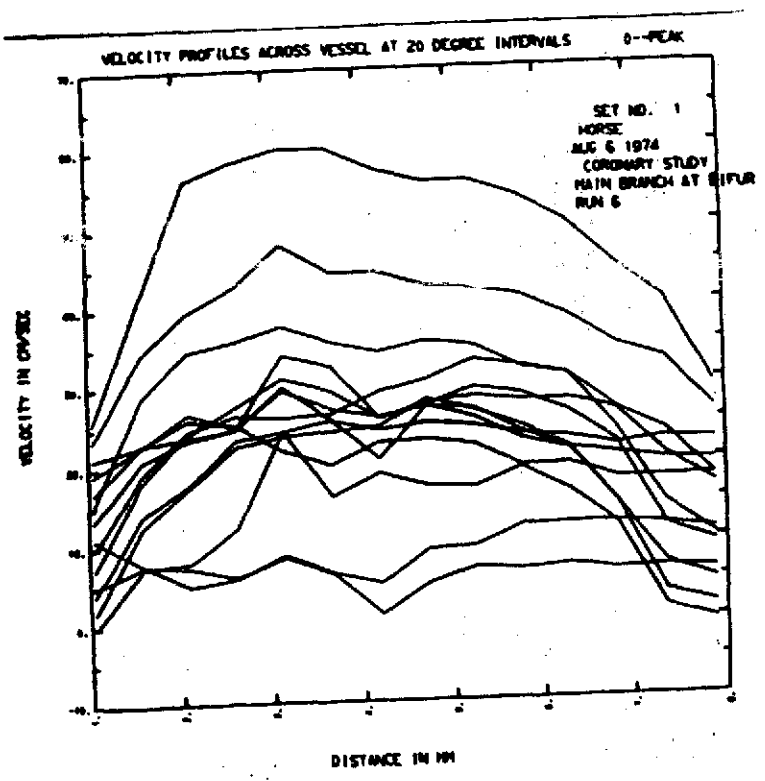

(a)

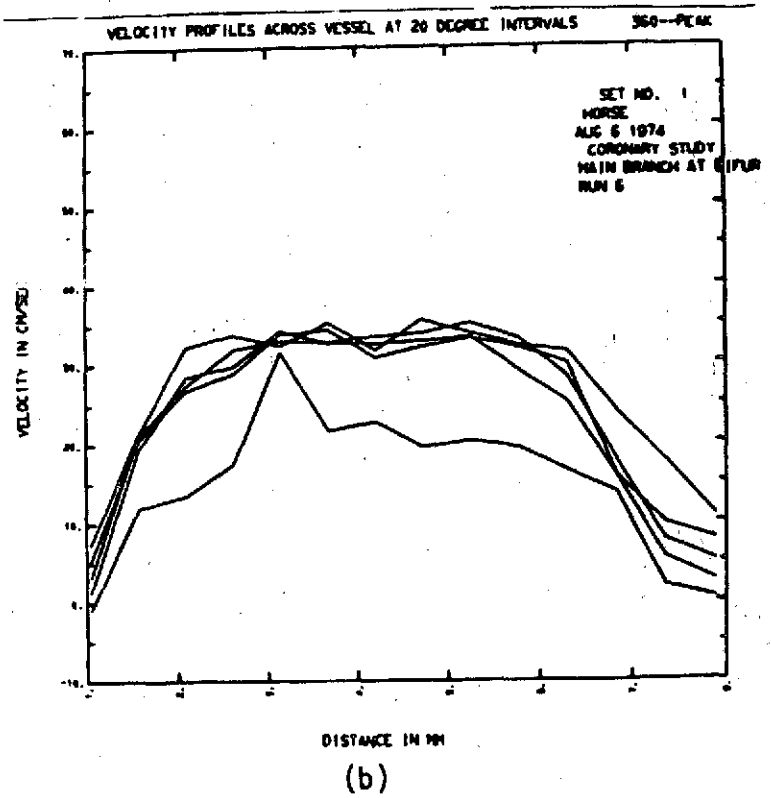

(b)

Figure 4.

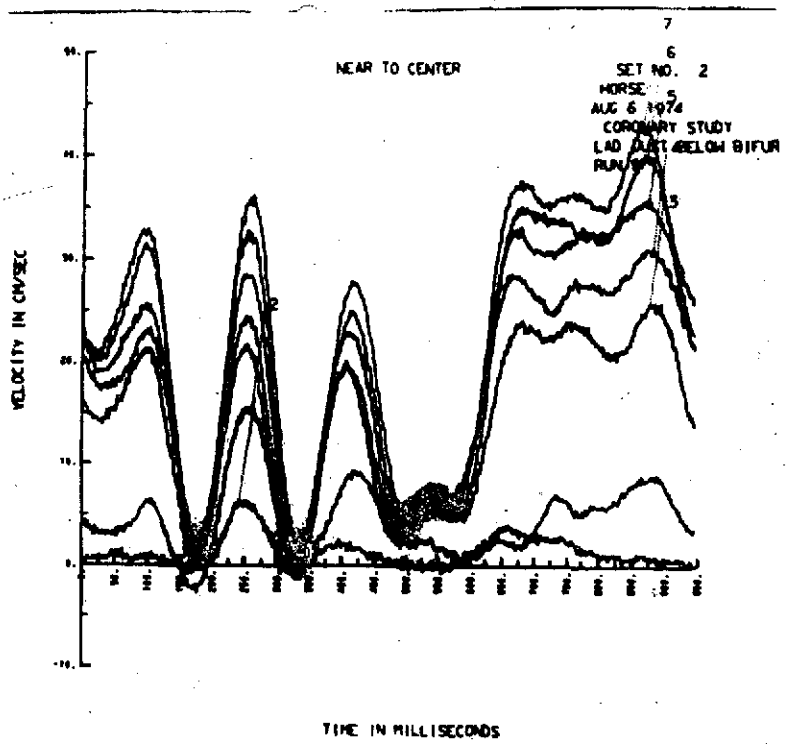

Figure 5.

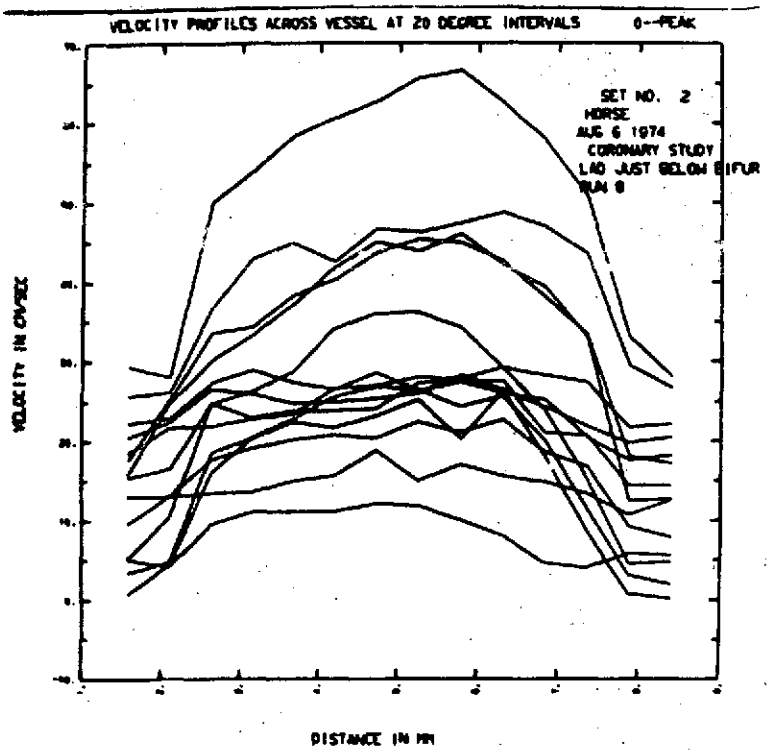

(a)

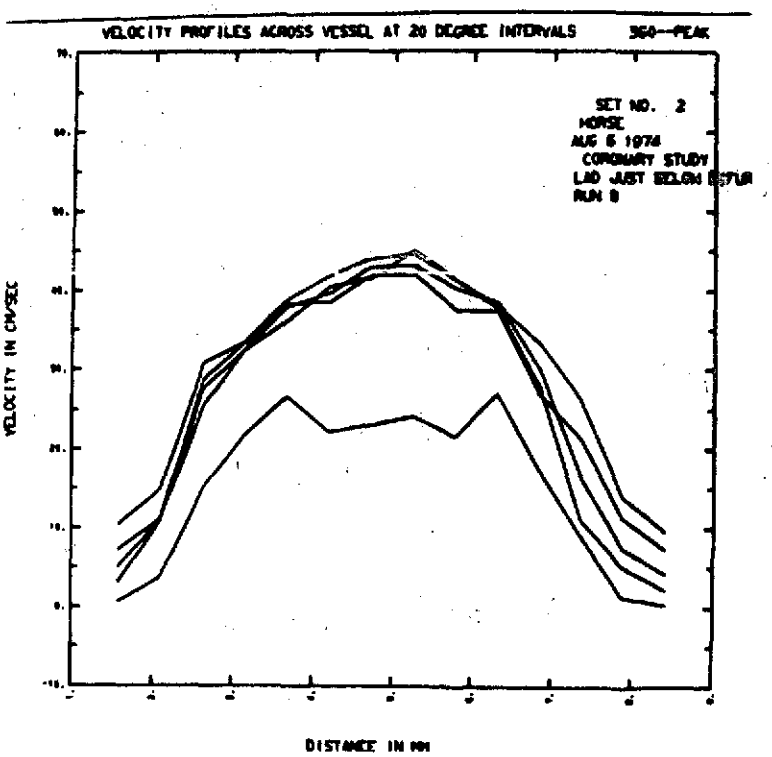

(b)

Figure 6.

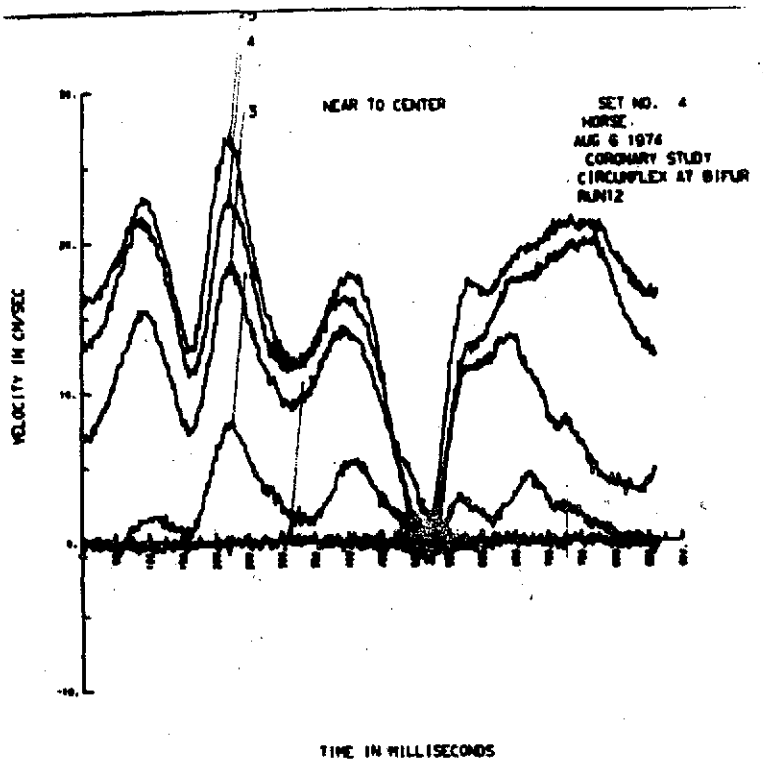

Figure 7.

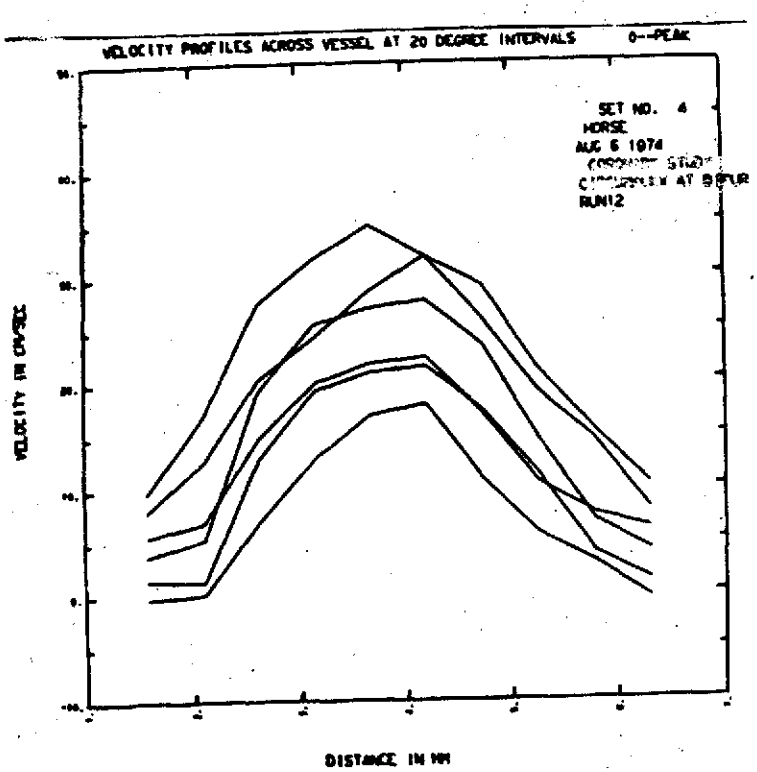

(a)

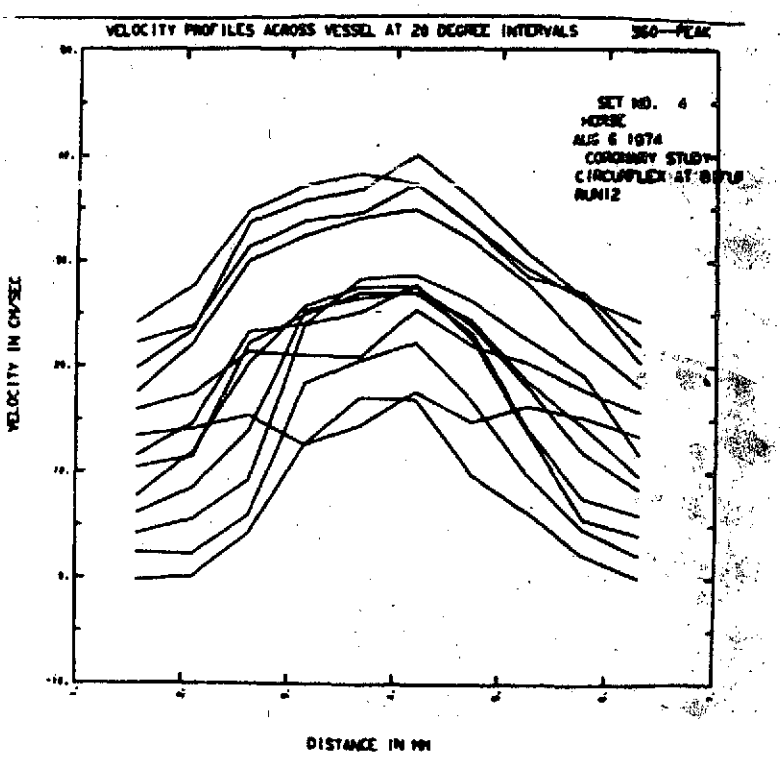

(b)

Figure 8.

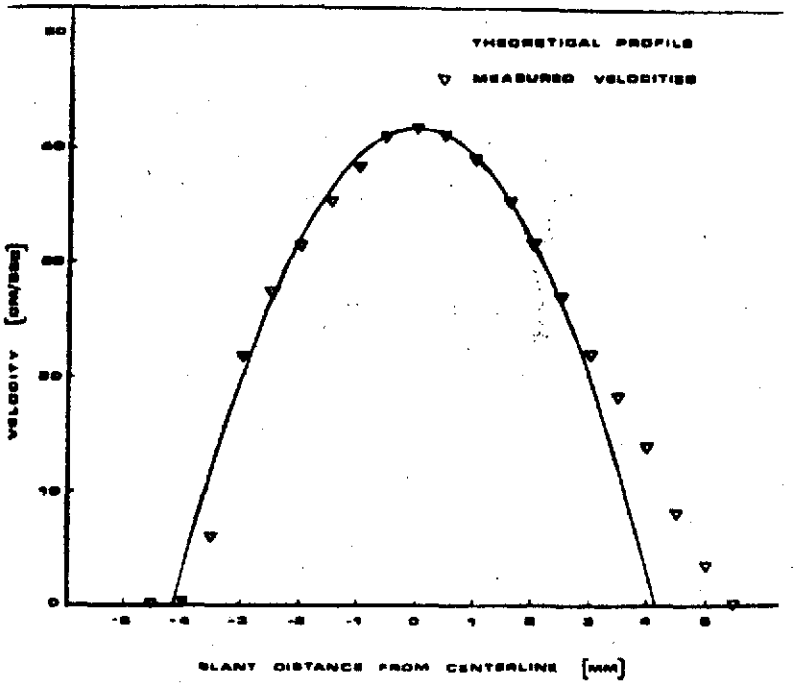
THEORETICAL PROFILE
MEASURED VELOCITIES
VELOCITY [cm/sec]
SLANT DISTANCE FROM CENTERLINE [mm]

Figure 9.